

พฤติกรรม การดูซ้ำ อีออนคอปเปอร์ จากสารละลายด้วย โคลโคซาน-คินเนียวคอมโพสิทที่ถูกเชื่อมโยง



นางสาวศิริพร เอกวรรณกุลศิริ

ศูนย์วิทยทรัพยากร

วิทยานิพนธ์นี้เป็นส่วนหนึ่งของการศึกษาตามหลักสูตรปริญญาวิทยาศาสตรมหาบัณฑิต

สาขาวิชาการจัดการสิ่งแวดล้อม (สหสาขาวิชา)

บัณฑิตวิทยาลัย จุฬาลงกรณ์มหาวิทยาลัย

ปีการศึกษา 2551

ลิขสิทธิ์ของจุฬาลงกรณ์มหาวิทยาลัย

**ADSORPTION BEHAVIOR OF Cu^{2+} FROM AQUEOUS SOLUTION
ON COMPOSITE CROSSLINKED CHITOSAN-CLAY**



Miss Siriporn Akewaranugulsiri

**A Thesis Submitted in Partial Fulfillment of the Requirements
for the Degree of Master of Science Program in Environmental Management
(Interdisciplinary Program)
Graduate School
Chulalongkorn University
Academic Year 2008
Copyright of Chulalongkorn University**

Thesis Title ADSORPTION BEHAVIOR OF Cu^{2+} FROM AQUEOUS
SOLUTION ON COMPOSITE CROSSLINKED CHITOSAN-
CLAY

By Miss Siriporn Akewaranugulsiri

Field of Study Environmental Management

Advisor Associated Professor Nurak Gridanurak, Ph.D.

Co-Advisor Assistant Professor Meng-Wei Wan, Ph.D.

Accepted by the Graduate School, Chulalongkorn University in Partial Fulfillment
of the Requirements for the Master's Degree



..... Dean of the Graduate School
(Associate Professor Pornpote Piumsomboon, Ph.D.)

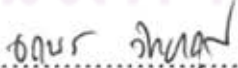
THESIS COMMITTEE


..... Chairman
(Assistant Professor Manaskorn Rachakornkij, Ph.D.)


..... Advisor
(Associate Professor Nurak Gridanurak, Ph.D.)


..... Co-Advisor
(Assistant Professor Meng-Wei Wan, Ph.D.)


..... Examiner
(Associate Professor Jin Anotai, Ph.D.)


..... External Examiner
(Associate Professor Jatuporn Wittayakun, Ph.D.)

ศิริพร เอกวรรณกุลศิริ : พฤติกรรมการดูดซับไอออนคอปเปอร์จากสารละลายด้วย
ไคโตซาน-ดินเหนียวคอมโพสิตที่ถูกเชื่อมโยง (ADSORPTION BEHAVIOR OF
 Cu^{2+} FROM AQUEOUS SOLUTION ON COMPOSITE CROSSLINKED
CHITOSAN-CLAY) อ. ที่ปรึกษาวิทยานิพนธ์หลัก : รศ.ดร.นุรักษ์ กฤษดาบุรุษ,
อ. ที่ปรึกษาวิทยานิพนธ์ร่วม : ศศ.ดร.มอง เวช วัน, 124 หน้า.

เนื่องจากการปนเปื้อนของไอออนของคอปเปอร์ในธรรมชาติส่งผลกระทบต่อคุณภาพ
สิ่งแวดล้อมและสุขภาพของมนุษย์งานวิจัยครั้งนี้จึงได้ทำการทดสอบประสิทธิภาพของไคโตซานที่
ผ่านการปรับปรุงคุณสมบัติแล้วมาใช้ในการบำบัดไอออนของคอปเปอร์ในสารละลายด้วย
กระบวนการดูดซับ เพื่อลดปริมาณการใช้ไคโตซาน ดินเหนียวเบนโทไนท์และคาโอลิไนท์ถูก
นำมาใช้เป็นวัสดุรองรับร่วมกับไคโตซาน ดินเหนียวเบนโทไนท์เป็นวัสดุร่วมกับไคโตซานแสดง
ความสามารถในการดูดซับไอออนของคอปเปอร์ได้มากกว่าการใช้ดินเหนียวคาโอลิไนท์ หลังจากนั้น
นั้นทำการศึกษาผลของสารเชื่อมโยงในการสังเคราะห์ไคโตซาน-เบนโทไนท์คอมโพสิตที่ถูก
เชื่อมโยงพบว่าพันธะเชื่อมโยงที่สร้างด้วยเอธิลีน ไกลคอล ไคโกลซิดิลอีเทอร์ (อีจีดีอี) และ อีพิกลอ
โรไฮดริน (อีซีเอช) สามารถเพิ่มความสามารถในการดูดซับไอออนคอปเปอร์ได้มากขึ้น ซึ่งมากกว่า
การใช้ กลูตาร์อัลดีไฮด์ (จีแอลเอ) โคโยไอโซเทอร์มการดูดซับมีลักษณะตามแลงเมียร์สำหรับตัวดูด
ซับที่ใช้อีจีดีอีและอีซีเอชเป็นสารสร้างพันธะเชื่อมโยง และสอดคล้องกับฟรังก์ลิชเมื่อใช้จีแอลเอ
เป็นสารสร้างพันธะเชื่อมโยง สำหรับจลนศาสตร์การดูดซับของตัวดูดซับทั้งสามสามารถอธิบายได้
ด้วยปฏิกิริยาอันดับสองเทียบกับความเข้มข้นของไอออนของคอปเปอร์ นอกจากนี้แสดงผล
การศึกษาเบื้องต้นของกระบวนการดูดซับแบบต่อเนื่อง และสำหรับพฤติกรรมการดูดซับและการ
คืนสภาพพบว่า ปัจจัยที่มีผลคือ ความเข้มข้นของสารละลายไอออนของคอปเปอร์ ค่าความเป็นกรด-
ด่างของสารละลายไอออนของคอปเปอร์ โดยผลการทดลองทั้งหมดสอดคล้องกับผลการวิเคราะห์
ที่ได้จากคุณลักษณะทางกายภาพด้วยเครื่อง ซิตาร์โพเทนเชียล กล้องจุลทรรศน์แบบส่องกราด
(SEM) วัคการเลี้ยวเบนด้วยรังสีเอกซ์ (XRD) และการดูดซับไนโตรเจน (BET)

สาขาวิชา การจัดการสิ่งแวดล้อม
ปีการศึกษา 2551

ลายมือชื่อนิสิต.....ศิริพร.....เอกวรรณกุลศิริ.....
ลายมือชื่อ อ. ที่ปรึกษาวิทยานิพนธ์หลัก
ลายมือชื่อ อ. ที่ปรึกษาวิทยานิพนธ์ร่วม.....

5087548420 : MAJOR ENVIRONMENTAL MANAGEMENT

KEYWORDS: CHITOSAN / COMPOSITE / CROSSLINK / ADSORPTION ISOTHERM / ADSORPTION KINETIC

SIRIPORN AKEWARANUGULSIRI : ADSORPTION BEHAVIOR OF Cu²⁺ FROM AQUEOUS SOLUTION ON COMPOSITE CROSSLINKED CHITOSAN-CLAY. ADVISOR : ASSOC.PROF.NURAK GRISADANURAK Ph.D., CO-ADVISOR : ASST.PROF.MENG-WEI WAN Ph.D., 124 pp.

Copper ions have been concerned because its contamination caused adverse effects on both environment and human health. A biopolymer, chitosan, is considered to be an effective adsorbent in adsorption processes to remove heavy metal ions. Inexpensive and higher surface area materials, bentonite and kaolinite, were studied as supporting materials for chitosan to reduce the quantity of chitosan. Bentonite exhibited higher adsorption capacity for Cu²⁺ than kaolinite as supporting material. The effect of cross-linking agent for composite crosslinked chitosan-bentonite was investigated, consequently. Composite crosslinked chitosan-bentonite using ethylene glycol diglycidyl ether and epichlorohydrin as crosslinking agents (CCB-EGDE and CCB-ECH beads) improved adsorption capacity and adsorbent strength for Cu²⁺ removal from aqueous solution compared to composite crosslinked chitosan-bentonite using glutaraldehyde as crosslinking agent (CCB-GLA beads). Adsorption isotherm of Cu²⁺ fitted with Langmuir and Freundlich for CCB-EGDE, CCB-ECH beads and CCB-GLA beads, respectively. Adsorption kinetics followed pseudo-second-order kinetic model with respect to Cu²⁺ concentration. Regarding to adsorption-desorption study, the effect of initial Cu²⁺, effect of pH, and continuous adsorption were also preliminarily investigated. Physical characters of adsorbents were characterized by zeta-potential, SEM, XRD, and BET corresponding to adsorption results.

Field of Study: Environmental Management
Academic Year 2008

Student's Signature. *Siriporn Akewaranugulsiri*...
Advisor's Signature..... *Nurak Grisadanurak*.....
Co-Advisor's Signature... *Meng-Wei Wan*.....

ACKNOWLEDGEMENT

The accomplishment of this thesis can not be completed if without the support from these persons. With respect and honesty, I would like to give the thankfulness for the people below:

First of all, I would like to convey the greatest appreciate to my advisor, Assoc. Prof. Dr. Nurak Grisdanurak who gave me a value opportunity and experience in Taiwan. Although we did not talk so much to each other, whenever I got the problems he always helped me with kindness. I really believe that teachers have only goodwill to their students and he is a good exsample. Several times the explanation in my research is quite hard to understand for me but he tried to teach me with patient. He does not give me only the knowledge but he also perform the generosity to everybody and our country. I also can not forget the thankfulness for all professors in Taiwan, Asst. Prof. Dr. Meng-Wei Wan, Asst. Prof. Dr. Chi-Chuan Kan, and Prof. Dr. Chi-Hsiang Liao. All of them are my co-advisors who are very kind when I was in Taiwan. They always asked me about my being there and help me in my research as much as they can. They did not only attend in my research but they also suggest and support my attitude. The most important thing is the experience and the attitude that I can make up during my research proceed.

The sincerely gratitude is also for the thesis committee chairman, Asst. Prof. Dr. Manaskorn Rachakornkij, and the thesis committee members, Assoc. Prof. Dr. Jin Anotai, and Assoc. Prof. Dr. Jatuporn Wittayakun. Thank you for the valuable suggestion, encouragement, and useful detail recommendation. Furthermore, thanks a lot to the National Center of Excellence for Environmental and Hazardous waste Management (NCE-EHWM) for full scholarship that provided the opportunity in master degree for me, the research funding and supporting facilities to complete my research. I also would like to thank Graduate School, Chulalongkorn University for financial support to my research.

Thank you for every encouragement from my parents, my Thai and foreign friends. They supported me for everything with their kindness.

CONTENTS

	page
ABSTRACT (Thai).....	iv
ABSTRACT (English).....	v
ACKNOWLEDGEMENT.....	vi
CONTENTS.....	vii
LIST OF TABLES.....	xii
LIST OF FIGURES.....	xv
LIST OF ABBREVIATIONS.....	xix
LIST OF NOMENCLATURES.....	xxii
CHAPTER	
I INTRODUCTION.....	1
1.1 Introduction.....	1
1.2 Objectives.....	3
1.3 Hypothesis.....	3
1.4 Scope of study.....	3
II THEORETICAL BACKGROUND AND LITERATURE	
REVIEWS.....	5
2.1 Properties and applications of chitosan.....	5
2.2 Clay.....	9
2.2.1 Kaolinite.....	10
2.2.2 Bentonite (Smectice from Volcanic Ash).....	10
2.3 Chitosan intercalated clay.....	13
2.4 Crosslink.....	14
Crosslinked chitosan.....	14

CHAPTER	page
2.5 Adsorption.....	16
2.5.1 Factors affecting adsorption.....	18
2.5.1.1 The percent adsorption.....	18
2.5.1.2 The adsorption capacity.....	18
2.5.2 Adsorption equilibrium.....	19
2.5.2.1 Langmuir adsorption isotherm.....	19
2.5.2.2 Freundlich adsorption isotherm.....	20
2.5.3 Kinetic of adsorption.....	21
2.5.3.1 Pseudo-first-order kinetic model.....	22
2.5.3.2 Pseudo-second-order kinetic model.....	23
2.6 Continuous adsorption.....	24
Mass transfer.....	24
2.7 Zeta-potential.....	25
2.8 X-Ray Diffraction (XRD).....	27
2.9 Brunauer-Emmett-Teller technique (BET).....	29
2.10 Development of chitosan applying for wastewater treatment.....	30
III คูนยวทยทรพยากร METHODODOLOGY.....	33
3.1 Material.....	33
3.1.1 Chitosan.....	33
3.1.2 Crosslinking agents.....	33
3.1.3 CuSO ₄	34
3.1.4 Clay.....	34

CHAPTER	page
3.1.5 Other reagents.....	34
3.1.6 Equipments.....	34
3.2 Experimental procedure.....	35
3.2.1 Preparation of Cu ²⁺ solution.....	35
3.2.2 Preparation of composite chitosan-clay beads.....	35
3.2.3 Preparation of composite crosslinked chitosan-clay beads.....	36
3.2.4 Adsorption study.....	36
3.2.5 Effect of initial Cu ²⁺ concentration.....	37
3.2.6 Effect of pH.....	37
3.2.7 Effect of crosslinking agents.....	37
3.2.8 Desorption study.....	37
3.2.9 Reuse study.....	37
3.2.10 Column adsorption.....	38
3.2.11 Physical characteristics and morphology of adsorbents.....	38
3.3 Analytical methods.....	38
3.4 Mathematical methods.....	39
IV RESULTS AND DISCUSSION.....	40
<u>PHASE I</u> Comparison of kaolinite and bentonite as supporting materials.....	40
4.1 Adsorption capacity of CCK and CCB beads.....	40
4.2 Scanning electron microscopy (SEM) of CCK and CCB Beads.....	43

CHAPTER	page
<u>PHASE II</u> Comparison of the effect of crosslinking agents epichlorohydrin (ECH), ethylene glycol diglycidyl ether (EGDE), and glutaraldehyde (GLA) on composite chitosan-clay properties.....	45
4.3 Adsorption capacity of CCB-EGDE, CCB-ECH, and CCB-GLA beads.....	45
4.4 Adsorption equilibrium.....	47
4.5 Adsorption isotherm.....	48
4.6 Adsorption kinetic.....	50
4.7 Desorption study.....	52
4.8 Reuse study.....	53
4.9 Effect of initial Cu ²⁺ concentration.....	55
4.10 Effect of pH.....	56
4.11 Zeta-potential.....	59
4.12 Column adsorption.....	61
4.13 Morphology.....	63
4.13.1 Scanning electron microscopy (SEM).....	63
4.13.2 X-Ray Diffraction (XRD).....	64
4.13.3 N ₂ adsorption-desorption analysis	66
V CONCLUSION AND RECOMMENDATIONS.....	70
5.1 Conclusion.....	70
5.2 Recommendations.....	71
REFERENCES.....	72
APPENDICES.....	81
Appendix A.....	82

Appendix B.....	118
Appendix C.....	124
BIOGRAPHY.....	124



ศูนย์วิทยทรัพยากร
จุฬาลงกรณ์มหาวิทยาลัย

LIST OF TABLES

Table	page
2.1	Intrinsic properties of chitosan..... 7
2.2	Comparative properties of common silicate clay minerals (Adapted from Brady and Weil, 2996)..... 12
2.3	Results of batch studies for Cu ²⁺ removal using chitosan, modified chitosan, and other materials..... 32
3.1	The physical and chemical properties of crosslinking agents..... 33
3.2	Equipments used in the experiment..... 34
4.1	Adsorption capacity (q_e) of CCK and CCB beads in terms of time and initial Cu ²⁺ concentration..... 42
4.2	Adsorption capacity (q_e) of CCB-EGDE, CCB-ECH, and CCB-GLA beads in terms of time and initial Cu ²⁺ concentration..... 46
4.3	Adsorption isotherm constants and correlation coefficient (R^2) of composite crosslinked chitosan-bentonite..... 49
4.4	Pseudo-first- and pseudo-second-order kinetic constants and correlation coefficient (R^2) for adsorption of Cu ²⁺ on CCB-EGDE, CCB-ECH, and CCB-GLA beads..... 51
4.5	Characteristic of adsorbent beads analyzed by N ₂ adsorption-desorption analysis..... 67
A-1	Final concentration (C , C_e) of Cu ²⁺ using CCK and CCB beads as adsorbents in terms of time and initial Cu ²⁺ concentration..... 82
A-2	Adsorption capacity (q_e) of CCK and CCB beads in terms of time and initial Cu ²⁺ concentration..... 83
A-3	Percent adsorption of CCK and CCB beads in terms of time and initial Cu ²⁺ concentration..... 84

Table	page	
A-4	Final concentration (C , C_e) of Cu^{2+} using CCB-EGDE, CCB-ECH, and CCB-GLA beads as adsorbents in terms of time and initial Cu^{2+} concentration.....	85
A-5	Adsorption capacity (q_e) of CCB-EGDE, CCB-ECH, and CCB-GLA beads in terms of time and initial Cu^{2+} concentration.....	86
A-6	Percent adsorption of CCB-EGDE, CCB-ECH, and CCB-GLA beads in terms of time and initial Cu^{2+} concentration.....	87
A-7	Adsorption isotherm constants and correlation coefficient (R^2) of composite crosslinked chitosan-bentonite.....	88
A-8	Pseudo-first- and pseudo-second-order kinetic constants and correlation coefficient (R^2) for adsorption of Cu^{2+} adsorbed on CCB-EGDE, CCB-ECH, and CCB-GLA beads.....	90
A-9	Percent desorption of Cu^{2+} from CCB-EGDE and CCB-ECH beads using deionized water pH 7 and acid solution pH 1 and pH 3 at equilibrium contact time (240 min).....	93
A-10	Regeneration study of Cu^{2+} on CCB-EGDE and CCB-ECH beads after desorbed in deionized water pH 7 and acid solution pH 1 and pH 3 at equilibrium contact time (240 min).....	94
A-11	Final concentration (C_e) of Cu^{2+} on CCB-EGDE and CCB-ECH beads from effect of pH studied at equilibrium contact time (240 min) and different initial Cu^{2+} concentration.....	95
A-12	Adsorption capacity (q_e) of Cu^{2+} on CCB-EGDE and CCB-ECH beads from effect of pH studied at equilibrium contact time (240 min) and different initial Cu^{2+} concentration.....	95
A-13	Percent adsorption of Cu^{2+} on CCB-EGDE and CCB-ECH beads from effect of pH studied at equilibrium contact time (240 min) and different initial Cu^{2+} concentration.....	96

Table	page	
A-14	Zeta-potential (mV) of adsorbents in the different solution pH values.....	97
A-15	Flow through of Cu^{2+} 500 mg/L on 5 and 10 g of CCB-EGDE beads in packed column.....	98
A-16	Intensity at various 2θ of adsorbents from XRD.....	101
A-17	N_2 adsorption-desorption analysis data of bentonite.....	111
A-18	N_2 adsorption-desorption analysis data of CCB beads.....	112
A-19	N_2 adsorption-desorption analysis data of CCB-ECH beads.....	113
A-20	N_2 adsorption-desorption analysis data of CCB-EGDE beads.....	114
A-21	N_2 adsorption-desorption analysis data of CCB-GLA beads.....	115
A-22	N_2 adsorption-desorption analysis data of chitosan.....	116
A-23	Summary characteristics of adsorbents by N_2 adsorption-desorption analysis analysis.....	117
B-1	pH of Cu^{2+} solution before and after adsorption by adsorbent beads at different contact time.....	119
B-2	pH of Cu^{2+} solution after adsorption by CCB-EGDE beads packed column.....	120

ศูนย์วิทยทรัพยากร
จุฬาลงกรณ์มหาวิทยาลัย

LIST OF FIGURES

Figure		page
2.1	Idealized representation of chitin and chitosan.....	5
2.2	Chemical structure of (a) α -chitosan and (b) β -chitosan.....	6
2.3	Phyllosilicate nomenclature. From Schulze (1989), with permission.....	12
2.4	Intercalation of chitosan into Na ⁺ -montmorillonite (Darder et al., 2003).....	13
2.5	Intercalation of chitosan into Na ⁺ -montmorillonite as a bilayer (Darder et al., 2003).....	13
2.6	Formation of hydrogen bonds between chitosan and montmorillonite (Wang et al., 2005).....	14
2.7	Schematic representation of crosslinked chitosan beads: (a) chitosan-epichlorohydrin (chitosan-ECH), (b) chitosan-glutaraldehyde (chitosan-GLA), and (c) chitosan-ethylene glycol diglycidyl ether (chitosan-EGDE).....	16
2.8	Freundlich isotherm plotting between C_e and q_e presenting n value.....	21
2.9	Breakthrough concentration profiles in fluid at bed outlet which C_b and t_b are concentration and time denote breakthrough point (College of Engineering, University of Rhode Island, 2008).....	25
2.10	Schematic of particle in liquid phase (Cornell University, 2009)....	26
2.11	Point of zero zeta-potential (point of zero charge) (Cornell University, 2009).....	27
2.12	Diffraction of X-rays considered as reflection from a set of lattice planes (Kasai and Kakudo, 2005).....	29
4.1	Adsorption capacity (q_e) of a. CCK and b. CCB beads in terms of time and initial Cu ²⁺ concentration.....	42

Figure	page	
4.2	Formation of hydrogen bond between chitosan and montmorillonite clay (Wang et al., 2005).....	43
4.3	Scanning electron microscopy (SEM) of (a1) kaolinite clay, (a2) CCK beads, (b1) bentonite clay, and (b2) CCB beads.....	44
4.4	Adsorption capacity (q_e) of Cu^{2+} on a. CCB-EGDE, b. CCB-ECH, and c. CCB-GLA beads in terms of time and initial Cu^{2+} concentration.....	47
4.5	Adsorption isotherm of Cu^{2+} on adsorbent beads.....	49
4.6	Linear plots of a. pseudo-first- and b. pseudo-second-order kinetic for Cu^{2+} adsorbed on CCB-EGDE beads.....	51
4.7	Adsorption capacity (q_e) of Cu^{2+} 2000 mg/L on CCB-EGDE and CCB-ECH beads before and after desorption using deionized water pH 7 and acid solution at pH 1 and pH 3.....	53
4.8	CCB-ECH beads (a) and CCB-EGDE (b) after desorption using desorption agent pH 1.....	53
4.9	Adsorption capacity of Cu^{2+} in the first and second time on CCB-EGDE and CCB-ECH beads at initial Cu^{2+} concentration 2000 mg/L.....	55
4.10	Thermodynamic equilibrium diagram of Cu (Ayres, Davis, and Gietka, 1994; Václaviková and Gallios, 2006).....	57
4.11	Speciation diagram for the Cu(II)- H_2O system.....	57
4.12	Effect of pH values on adsorption capacity of CCB-EGDE and CCB-ECH beads for Cu^{2+}	59
4.13	Zeta-potential of bentonite, CCB-EGDE, CCB-ECH, and CCB-GLA beads in the solution at pH 1, 3, and 5.....	60
4.14	Column adsorption in adsorption period 0, 6, 12, 24, 46, and 52 hours ((a) and (b), (c), (d), (e), (f), and (g), respectively).....	61
4.15	Breakthrough curves for Cu^{2+} adsorption of CCB-EGDE beads.....	63

Figure	page
4.16 Scanning electron microscopy (SEM) micrograph of (a) CCB-EGDE, (b) CCB-ECH, and (c) CCB-GLA beads.....	64
4.17 XRD patterns of bentonite, chitosan, CCB beads, CCB-EGDE beads, CCB-ECH beads, and CCB-GLA beads.....	66
4.18 N ₂ adsorption-desorption isotherms of bentonite, CCB beads, and chitosan.....	68
4.19 N ₂ adsorption-desorption isotherms of a. CCB-ECH, b. CCB-EGDE, and c. CCB-GLA beads.....	69
4.20 Different isotherm shapes possible of N ₂ adsorption on solid surface (Nackos, 2006).....	69
A-1 Final concentration (C , C_e) of Cu ²⁺ using a. CCK and b. CCB beads as adsorbents in terms of time and initial Cu ²⁺ concentration.	82
A-2 Adsorption capacity (q_e) of a. CCK and b. CCB beads in terms of time and initial Cu ²⁺ concentration.....	83
A-3 Percent adsorption of a. CCK and b. CCB beads in terms of time and initial Cu ²⁺ concentration.....	84
A-4 Final concentration (C , C_e) of Cu ²⁺ using a. CCK and b. CCB beads as adsorbents in terms of time and initial Cu ²⁺ concentration.	85
A-5 Adsorption capacity (q_e) of a. CCB-EGDE, b. CCB-ECH, and c. CCB-GLA beads in terms of time and initial Cu ²⁺ concentration....	86
A-6 Percent adsorption of a. CCB-EGDE, b. CCB-ECH, and c. CCB-GLA beads in terms of time and initial Cu ²⁺ concentration.....	87
A-7 Adsorption isotherm of Cu ²⁺ adsorbed on a. CCB-EGDE and CCB-ECH beads and b. CCB-GLA beads.....	88
A-8 Linear plots of Langmuir isotherm of Cu ²⁺ adsorbed on a. CCB-EGDE, b. CCB-ECH, and c. CCB-GLA beads.....	89

Figure	page
A-9	Linear plots of Freundlich isotherm of Cu^{2+} adsorbed on a. CCB-EGDE, b. CCB-ECH, and c. CCB-GLA beads..... 89
A-10	Linear plots of pseudo-first-order kinetic adsorption of Cu^{2+} adsorbed on a. CCB-EGDE, b. CCB-ECH, and C. CCB-GLA beads..... 91
A-11	Linear plots of pseudo-second-order kinetic adsorption of Cu^{2+} adsorbed on a. CCB-EGDE, b. CCB-ECH, and C. CCB-GLA beads..... 92
A-12	Percent desorption of Cu^{2+} from a. CCB-EGDE and b. CCB-ECH beads using desorption agents pH 1, 3, and 7..... 93
A-13	Adsorption capacity (q_e) of Cu^{2+} on a. CCB-EGDE and b. CCB-ECH beads from effect of pH studied at equilibrium contact time (240 min) and different initial Cu^{2+} concentration..... 96
A-14	Zeta-potential (mV) of adsorbents in the different solution pH values..... 97
A-15	Scanning electron microscopy (SEM) images of materials used in the experiment..... 100
B-1	Thermodynamic equilibrium diagram of Cu (Ayres, Davis, and Gietka, 1994; Václaviková and Gallios, 2006)..... 118
B-2	Speciation diagram for the Cu(II)- H_2O system (Doyle, and Liu, 2003; Wang, Li, and Sun, 2009)..... 118

LIST OF ABBREVIATIONS

°C	degree Celsius
μ	micron
μm	micrometer
Ø	diameter
Ag	Silver
Al ³⁺	Aluminum (III) ion
As	Arsenic
Au	Gold
BET	Brunauer-Emmett-Teller nitrogen adsorption technique
Bi	Bismuth
Ca	Calcium
Ca ²⁺	Calcium ion
Cd	Cadmium
CEC	Cation exchange capacity
CCB	composite chitosan-bentonite
CCK	composite chitosan-kaolinite
CCB-ECH	composite crosslinked chitosan-bentonite using epichlorohydrin as crosslinking agent
CCB-EGDE	composite crosslinked chitosan-bentonite using ethylene glycol diglycidyl ether as crosslinking agent
CCB-GLA	composite crosslinked chitosan-bentonite using glutaraldehyde as crosslinking agent
cmol	centimole
cm	centimeter
Co	Cobalt
Cr	Chromium
Cr ⁶⁺	Chromium (VI) ion
Cu	Copper
Cu ²⁺	Copper (II) ion

CuSO ₄	Copper sulfate
Cu(OH) ₂	Copper hydroxide
DI	deionized
ECH	Epichlorohydrin
EGDE	Ethylene glycol diglycidyl ether
Fe ²⁺	Iron ion
Fig.	Figure
FTIR	Fourier Transform Infrared Spectroscopy
g	gram
Ga	Gallium
GLA	Glutaraldehyde
H ⁺	Hydrogen ion
HCl	Hydrochloric acid
Hg	Mercury
HSAB	Hard and soft acids and bases
ICP	Inductively Coupled Plasma
ICP-OES	Inductively Coupled Plasma-Optical Emission Spectrometry
JCPDS	Joint Committee on Powder Diffraction Standards
L	liter
Kg	kilogram
M	Clay molecule
m ²	square meter
mg	milligram
Mg ²⁺	Magnesium ion
min	minute
mol	mole
Mn	Manganese
MLP	multilayer perceptron neural network
Mo	Molybdenum
MW	molecular weight
N ₂	Nitrogen
Na	Sodium

Na ⁺	Sodium ion
NaOH	Sodium hydroxide
NH ₂	Amine group
NH ₃ ⁺	Ammonium
Ni	Nickel
nm	nanometer
m	mass
MCLG	Maximum Contaminant Level Goals
mV	millivolt
OH	hydroxyl group
Pd	Palladium
pH _{pzc}	point of zero charge
Pt	Platinum
R	alkyl group
R ²	correlation coefficient
rpm	rounds per minute
SEM	Scanning Electron Microscope
Si ⁴⁺	Silicon ion
SiO ₄	Silicon tetra oxide
USA	United States of America
US\$	Dollar of United States
V	Vanadium, Velocity (cm/min)
W	Tungsten
XRD	X-ray diffraction
Zn	Zinc
Zn ²⁺	Zinc (II) ion

LIST OF NOMENCLATURES

λ	wavelength
θ	angle, degree ($^{\circ}$)
b	Langmuir constant, L/mg
C_0	the initial metal ions concentration, mg/L
C	the final metal ions concentration, mg/L
C_e	the equilibrium concentration of metals ions in solution, mg/L
C_{\max}	the maximum adsorption capacity, mg/g
d	space
d_{001}	interlayer spacing
h	the initial adsorption rate, mg/g min
k_1	the rate constant of the first-order adsorption, 1/min
k_2	the rate constant of adsorption (g/mg min)
K_F	Freundlich equilibrium constant
K_L	Langmuir equilibrium constant, L/g
n	the adsorption intensity
q_e	the amount of metal ions adsorbed, mg/g
q_t	are the adsorption capacities at equilibrium and at time t , min
t	time, min
V	volume of metal ions solution, L
W	weight of the adsorbent used, g

ศูนย์วิจัยทรัพยากร
จุฬาลงกรณ์มหาวิทยาลัย

CHAPTER I

INTRODUCTION

1.1 Introduction

Many heavy metals have been used widely in industrial areas and, without appropriate management; they can be contaminated in environment (Wan et al., 2004) especially in groundwater. The major concerned heavy metals which cause the environmental problems in the present time are arsenic (As), cadmium (Cd), chromium (Cr), cobalt (Co), copper (Cu), manganese (Mn), mercury (Hg), nickel (Ni), and zinc (Zn) (Bhattacharyya and Gupta, 2008b). Among these heavy metals, Cu has been considered because of its toxicity and adverse effects on both environment and human health. Cu can be danger for aquatic organisms even in small concentration. In addition, Cu can accumulate and cause damage in kidney and liver which can lead to death. The important sources of Cu are copper mines. After that Cu has been used in metal cleaning and plating baths, pulp, paper and paper board mills, wood pulp production, and the fertilizer industry, etc. (Nghah, Endud, and Mayanar, 2002; Gupta et al., 2006; Lu and Gibb, 2008.).

Nowadays, there are many remediation technologies for heavy metals which usually based on physical-chemical processes (Jin and Bai, 2002; Wan et al., 2004) including chemical precipitation, ion-exchange, solvent extraction, reverse osmosis, adsorption, etc. All of these technologies are very effective to remove heavy metals. However, they are also have the limitations; for example, some technologies are expensive and complicated to operate, some generate a large amount of sludge (Jin and Bai, 2002; Nghah, Endud, and Mayanar, 2002; Wan et al., 2004; Bhattacharyya and Gupta, 2008b; Chen et al., 2008). Adsorption is another popular method for heavy metal removal from wastewater because it is very effective, economical, versatile, and simple. Furthermore, adsorption provides many advantages such as applicability at very low concentrations, suitability for using batch

and continuous processes, ease of operation, little sludge generation, and possibility of regeneration and reuse (Bhattacharyya and Gupta, 2008b).

Activated carbon and chelation ion-exchange resins are increasingly popular adsorbent in the water and waste industries; however, using these adsorbents are cost-prohibitive processes. Some of the best chelating materials are biopolymer. Therefore, biosorption using biopolymer, chitosan, is recognized as an emerging technique for heavy metals removal from wastewater because the amine groups and hydroxyl groups on the chitosan chain can act as the chelation sites for metal ions (Nghah, Endud, and Mayanar, 2002). Indeed, uses of chitosan are justified by two important advantages: firstly, chitosan has low cost compare with commercial activated carbon because chitosan is derived by deacetylation of chitin which is the second most abundant polysaccharide in the world after cellulose; secondly, chitosan plays a role of chelating agent (Wan et al., 2004; Crini and Badot, 2008).

However, using only chitosan as the adsorbent for heavy metal removal is limited because of its high cost if it was used alone. In order to overcome the high cost of chitosan, the proper and inexpensive material is used as immobilization support for chitosan. Consequently, much lower quantities of chitosan are needed to use in the processes (Wan et al., 2004; Gecol, Ergican, and Miakatsindila, 2005). Among the adsorbents, clays seem to be the cheapest materials. The comparison between the price of clays and chitosan is \$0.04-0.12 kg⁻¹ and \$15.43 kg⁻¹, respectively (Gecol, Ergincan, and Miakatsindila, 2005; Bhattacharyya and Gupta, 2008b).

Although chitosan has the ability to adsorb heavy metal ions, it is soluble in diluted organic acids such as acetic acid and formic acid. This limits the practical application of chitosan as biosorbent. In order to overcome this problem, several methods have been developed to modify raw chitosan either physical or chemical properties. Some crosslinking agents are used to stabilize chitosan in diluted or even concentrated acid solutions and in its resistance to biochemical and microbiological degradation (Nghah, Endud, and Mayanar, 2002; Oshita et al., 2002; Chiou and Li, 2003; Gecol et al., 2006; Chen et al., 2008). The modified bioadsorbents were expected to be used in acidic condition and have more abilities to regenerate for several times.

1.2 Objectives

The main objective of this study is to remove Cu^{2+} from the aqueous solution using modified chitosan. Chitosan is an efficient biosorbent for heavy metals; however, using pure chitosan for heavy metals removal from aqueous solution is cost-prohibitive process and chitosan is easy to dissolve even in a diluted acid solution. Hence, modified chitosan is concerned as an alternative adsorbent. The sub-objectives for this study are as follows:

1. To investigate the efficiency of composite crosslinked and non-crosslinked chitosan-clay to adsorb Cu^{2+} .
2. To develop the biosorbent (composite crosslinked chitosan-clay) and investigate its efficiency for Cu^{2+} removal from aqueous solution.
3. To understand the physical properties of modified clay to Cu^{2+} adsorption. The net charge of adsorbents is measured using zeta-potential. The surface and morphology are investigated by using N_2 adsorption-desorption analysis, XRD (X-ray diffraction) and SEM (Scanning Electron Microscopy).

1.3 Hypothesis

Chemical modified composite chitosan-clay using epichlorohydrin (ECH) as crosslinking agent will improve the strength and the adsorption efficiency more than using ethylene glycol diglycidyl ether (EGDE) and glutaraldehyde (GLA).

1.4 Scope of the study

Cu^{2+} was prepared in the aqueous solution and used as the artificial wastewater. The Cu^{2+} in the aqueous solution was removed by adsorbent, composite non-crosslinked chitosan-clay and composite crosslinked chitosan-clay.

This study was separated into 2 phases. The first phase investigated the adsorption capacity of composite non-crosslinked chitosan-bentonite and kaolinite

at a chitosan:clay ratio of 1:20 by weight to remove Cu^{2+} from aqueous solution. The more effective clay between bentonite and kaolinite based on adsorption capacity was used as a supporting material in the next phase.

The second phase was the adsorbent development using three crosslinking agents, epichlorohydrin (ECH), ethylene glycol diglycidyl ether (EGDE), and glutaraldehyde (GLA) at a chitosan:crosslinking agent mole ratio of 1:1. Three composite crosslinked chitosan-bentonite were investigated to compare the adsorption capacity of Cu^{2+} removal from aqueous solution.

Both phases of studies, the different conditions were set. The initial concentrations of Cu^{2+} was varied to be 100, 500, 1000, and 2000 mg/L. The contact times of adsorption studies introduced by batch experiment was 30, 60, 120, 240, 360, 720, and 1440 min. The Cu^{2+} in aqueous solutions after adsorbed were analyzed by ICP. The data from ICP was determined to understand the adsorption behavior by the models and calculations such as percent adsorption, adsorption capacity, Langmuir and Freundlich adsorption isotherms and pseudo-first-order and pseudo-second-order kinetic models.

Besides adsorption studies, desorption study using desorption agents at pH 1, 3, and 7 was conducted. Then the desorbed adsorbents were used again for adsorption. The pH of initial Cu^{2+} solution was varied to be 1, 2, 3, and 4 to investigate the effect on adsorption capacity and the strength of adsorbent. The net charge of adsorbent in different pH was measured by zeta-potential. Moreover, surface area and morphology of adsorbents were determined using N_2 adsorption-desorption analysis and SEM (Scanning Electron Microscopy). Finally, crystallinity of adsorbent was determined by XRD (X-ray diffraction).

Laboratory experiments were conducted from April 2008 to January 2009 at M504 Laboratory, Taiwan Hot Spring Research Center, Chia Nan University of Pharmacy and Science, Tainan, Taiwan.

CHAPTER II

THEORETICAL BACKGROUND AND LITERATURE REVIEWS

2.1 Properties and applications of chitosan

Chitin and chitosan are the second most abundant natural polymer in the world and mainly exist in crustacean shells (Kumar, 2000; Kasai, 2008; Lu et al., 2008). Because chitosan has been considered to be more beneficial than chitin, a linear polysaccharide of β -(1-4)-2-acetamido-2-deoxy-D-glucopyranose or chitin is deacetylated to be β -(1-4)-2-amino-2-deoxy-D-glucopyranose or chitosan. The ideal structure of chitin and chitosan are depicted in Figure 2.1. (Khor, 2001; Lima and Airoidi, 2004).

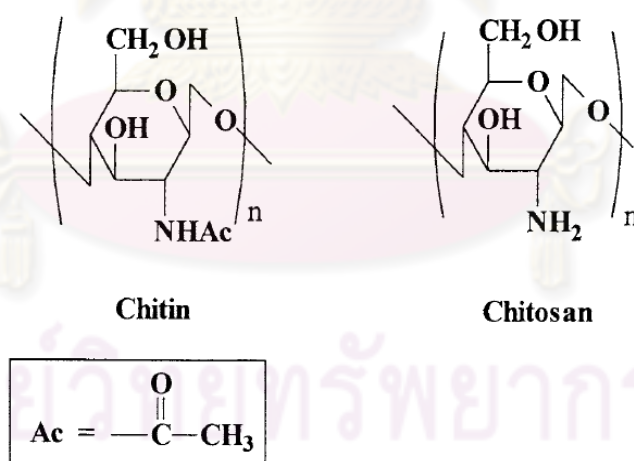


Fig. 2.1 Idealized representation of chitin and chitosan

Natural chitin has three anhydrous crystalline polymorphs, α -chitin (shrimp and crab shells), β -chitin (squid pen), and γ -chitin (stomach cuticles of cephalopoda) (Guibal, 2004), in the native state. The structure of α and β forms differ only in that the piles of chains are arranged alternately antiparallel in α -chitin,

whereas they are all parallel in β -chitin as shown in Fig 2.2. The γ -chitin form has characteristics of both α and β forms, where two chains run in one direction and another chain in the opposite direction; however, it is considered only a variant of the α family, because it has the same properties as the α -chitin. α -chitin is the most abundant and also the most stable thermodynamically, and the β -chitin and γ -chitin forms can be irreversibly converted into the α -form. Chitosan has anhydrous and hydrated forms, with piles chains arranged in an antiparallel fashion (Franca et al., 2008).

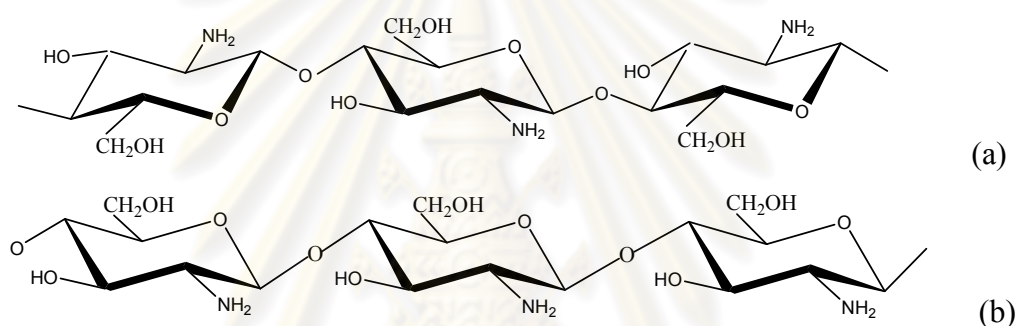


Fig. 2.2 Chemical structure of (a) α -chitosan and (b) β -chitosan

Chitosan has been used in many applications because of its intrinsic properties such as biodegradability, biocompatibility, film-forming ability, and adsorption properties as shown in Table 2.1 (Crini and Badot, 2008).

ศูนย์วิทยทรัพยากร
จุฬาลงกรณ์มหาวิทยาลัย

Table 2.1 Intrinsic properties of chitosan

Physical and chemical properties	<ul style="list-style-type: none"> • Linear aminopolysaccharide with high nitrogen content • Rigid D-glucosamine structure; high crystallinity; hydrophilicity • Capacity to form hydrogen bonds intermolecularly; high viscosity • Weak base; the deprotonated amino group acts a powerful nucleophile (pK_a 6.3) • Insoluble in water and organic solvents; soluble in dilute aqueous acidic solutions • Numerous reactive groups for chemical activation and crosslinking • Forms salts with organic and inorganic acids • Chelating and complexing properties • Ionic conductivity
Biological properties	<ul style="list-style-type: none"> • Biocompatibility <ul style="list-style-type: none"> - Non-toxic - Biodegradable - Adsorbable

Furthermore, chitosan has been used as adsorbent for heavy metal removal because of its excellent adsorption characteristics as such were considered to be due to the following factors (Inoue, Yoshizuka, and Ohto, 1999):

1. The large number of primary amino groups with high activity as adsorption sites.
2. The flexible structure of the polymer chain of chitosan which enables to adopt the suitable configuration for complexation with metal ions.

The main parameter influencing the characteristics of chitosan are its molecular weight (MW) and degree of deacetylation (DD), representing the proportion of deacetylated units. These parameters are determined by the conditions set during preparation (Berger et al., 2004).

Although chitosan has been considered as an effective adsorbent from researches, the application of chitosan in industrial scale is fail. Guibal (2004) explained that this may be caused by several parameters: (a) the cost of the raw material compared to synthetic polymers and resin (about US\$ 10-15), (b) the variability in the characteristics of material (that can rebut industrial user), and (c) the availability of the resource (that is controlled by the demand at the commercial level: the polymer fails at the moment to find an attractive market that would allow expanding the production).

Since chitosan consists a numerous of amino groups ($-\text{NH}_2$), N in amine groups play a role as chelating agent for heavy metal in wastewater (Monteiro and Airoidi, 1999; Kumar, 2000; Crini and Badot, 2008; Lu et al., 2008). The amino groups of chitosan, NH_2 , nitrogen is a donor of electron pairs, although hydroxyl group $-\text{OH}$ can also participate in sorption. The mechanism of combining these reactive groups with ions of heavy metals is much differentiated and can depend on the ion type, pH and also on the main components of the solution (Kaminski et al., 2008). At pH close to neutrality or weak acidity, the free electron doublet on nitrogen maybe bind metal cations; whereas, the protonation of amine groups in acidic solutions gives the polymer a cationic behavior and consequently the potential for attracting metal anions. The different mechanisms of adsorption depend on the composition of the solution and pH because these parameters may affect the protonation of the polymer and the speciation of metal ions (Guibal, 2004).

The considered mechanisms of chitosan are chelation, ion exchange and electrostatic attraction. Chelation is described by the theory of hard and soft acids and bases (HSAB) which describes the ability of ions to interact or enter into coordinate bonding with other ions or with ligands and shows that this depends on the availability of their outermost electrons and empty molecular orbitals. This must be considered on top of any electrostatic effects due to ion-ion, ion-dipole, and ion-higher multipole interactions. The last type of effect is governed primarily by the charge and size of the ion. The first type of effect can be described by means of the softness parameters and Lewis acid/base parameters of the ions. The HSAB concept provides a description of the capacities of ions to prefer ligands of the same kind (soft-soft and hard-hard) to those of different kinds when forming coordinative bonds.

Softness of ions generally goes hand in hand with their polarizability, and hardness with their electrostatic field strength.

Guibal (2004) reviewed the study of Domard who pointed out that chitosan forms a unique complex with copper, whose structure is close to $[\text{CuNH}_2(\text{OH})_2]$ below pH 6.1. Considering the coordination sphere of copper, the fourth site can be occupied by either a water molecule or the OH group in C-3 position.

2.2 Clay

Clay is hydrous aluminosilicates which makes up the colloid fraction ($< 2 \mu$) of soils, sediments, rocks and water (Bhattacharyya and Gupta, 2008b; Gupta and Bhattacharyya, 2008c). And clay may be composed of mixtures of fine grained clay minerals and clay-sized crystals of other minerals such as quartz, carbonate and metal oxides. Generally the term clay is used for material that become plastic when mixed with a small amount of water. In the environment, clay minerals play a role as a natural scavenger of pollutants for metals as water flows over soil or penetrate underground (Bhattacharyya and Gupta, 2008a, 2008b; Gupta and Bhattacharyya, 2008) by taking up cations and anions either through ion exchange or adsorption or both.

Clay minerals are good adsorbents for metal ions from aqueous because of their large specific surface area associated with their small particle sizes, helped by edges and faces of clay particles, their high cation exchange capacity (CEC), chemical and mechanical stability, layered structure, Brönsted and Lewis acidity etc., have made the clays excellent materials for adsorption (Bhattacharyya and Gupta, 2008b; Gupta and Bhattacharyya, 2008; Abillino et al., 2008). Using clay minerals as the adsorbent consists many advantages of being abundant and inexpensive; therefore, they can find application as low-cost (Ayari, Srasra, and Trabelsi-Ayadi, 2005; Abollino et al., 2008), non-secondary pollutant generation, improving efficiency for water treatment with low metal loadings (Arfaoui, Frini-Srasra, and Srasra, 2008; Bhattacharyya and Gupta, 2008c).

The edges and the faces of clay particles can adsorb anions, cations, non-ionic and polar contaminants from natural water. The contaminants can be accumulated on clay particles surface through the processes of ion exchange, coordination, or ion-dipole interactions, H-bonding, van der Waals interactions or hydrophobic bonding (Bhattacharyya and Gupta, 2008a).

Clay minerals are consisted of tetrahedral of SiO_4 and octahedral sheets with Al^{3+} as the octahedral cation (Fig. 2.3) (Sparks, 2003; Bhattacharyya and Gupta, 2008b).

2.2.1 Kaolinite

Kaolinite is one kind of clay minerals in 1:1 Clays (Kaolin-Serpentine Group) as shown in Fig. 2.3. The basic structure of kaolinite consists of a silica tetrahedral sheet bonded to an aluminum octahedral sheet. Layers of kaolinite stack by hydrogen bonding (Sparks, 2003). Kaolinite, $(\text{Si}_4)^{\text{IV}}(\text{Al}_4)^{\text{VI}}\text{O}_{10}(\text{OH})_8$, there is no substitution of Si^{4+} with Al^{3+} in the tetrahedral layer and no substitution of Al^{3+} with other ions (e.g., Mg^{2+} , Zn^{2+} , Fe^{2+} , Ca^{2+} , Na^+ , or K^+). In nature, kaolinite has a small net negative charge arising from broken edges on the clay crystals. The metal adsorption is usually accompanied by the release of hydrogen (H^+) ions from the edge sites of the mineral and also on the flat exposed planes of the silica and the alumina sheets (Bhattacharyya and Gupta, 2008b).

2.2.2 Bentonite (Smectite from Volcanic Ash)

Bentonite (sometimes used incorrectly as synonymous with the term montmorillonite) is a stratigraphically and commercially important rock formed from altered volcanic ash originally deposited in prehistoric lakes, estuaries, or ocean basins. The ash contains glassy material of high Si content necessary for smectite formation. Bentonite beds are most common in Cenozoic and Mesozoic rocks, but also have been found in all Paleozoic systems except Silurian. Much is still unknown about the mechanism of bentonite formation. Marine formation is indicated for

Wyoming bentonite, which is largely Na-saturated, whereas others, presumably fresh-water derived, are Ca-saturated. Other minerals such as apatite, zircon, and biotite found in bentonite beds substantiate their volcanic origin. The survival of apatite indicates that the alteration occurred under conditions of poor drainage and high base content. Bentonites or their derivatives may contribute to the parent materials of many soils, particularly in the western USA (Dixon and Weed., 1989).

The main constituent of bentonite is the clay mineral montmorillonite so the bentonite is defined in 2:1 Clays (Smectite-Saponite Group) as shown in Fig. 2.3. The basic structure of montmorillonite consists of a silica 2 tetrahedral sheets bonded to an aluminum octahedral sheet. The water molecules can present in the interlayer space of montmorillonite, the structure of bentonite. This cause montmorillonite has shrink-swell characteristics. And also other polar molecules can enter between the layers causing the lattice to expand the structure of montmorillonite. Montmorillonite, $(\text{Si}_{7.8}\text{Al}_{0.2})^{\text{IV}}(\text{Al}_{3.4}\text{Mg}_{0.6})^{\text{VI}}\text{O}_{20}(\text{OH})_4$, there is substitution of Si^{4+} by Al^{3+} in the tetrahedral layer and of Al^{3+} by Mg^{2+} in the octahedral layer (Sparks, 2003; Abollino et al., 2008; Bhattacharyya and Gupta, 2008b). The resulting net negative charge is balanced by exchangeable cations adsorbed between the unit layers and around their edges. In montmorillonite, adsorption can occur both at the edge sites, which leads to inner-sphere metal complexes, and at the planar (internal) sites of the clay mineral, which results in outer-sphere metal complexes (Sparks, 2003; Bhattacharyya and Gupta, 2008b). The abundance of montmorillonite, and its low cost are justified to be strong candidate as an adsorbent for the removal of heavy metals from wastewater (Ayari, Srasra, and Trabelsi-Ayadi, 2005).

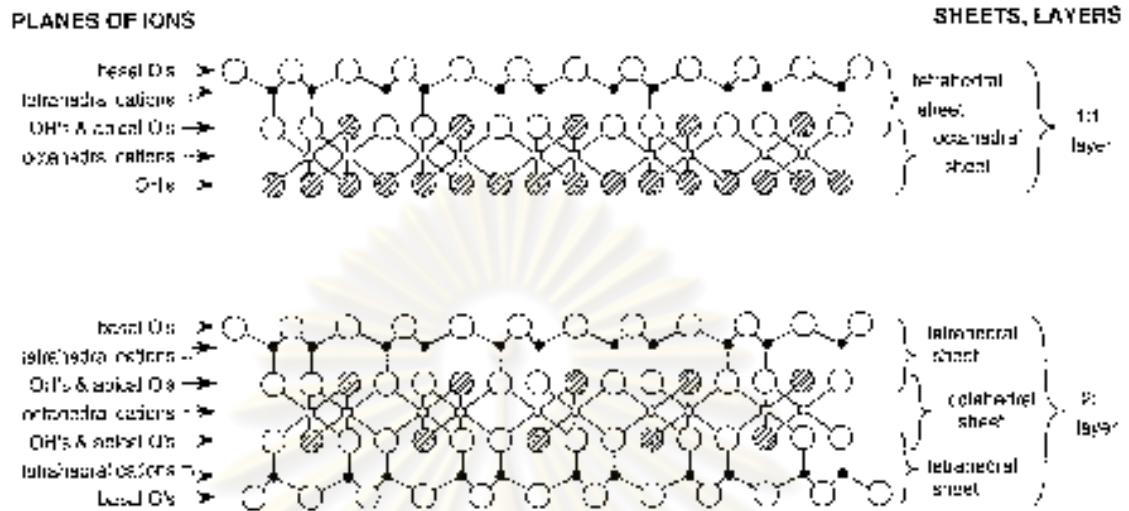


Figure 2.3 Phyllosilicate nomenclature. From Schulze (1989), with permission

The properties of common silicate clay minerals is summarized in Table 2.2 (Jurna, 2001).

Table 2.2 Comparative properties of common silicate clay minerals (Adapted from Brady and Weil, 1996).

Properties	Kaolinite	Montmorillonite
Size (μm)	0.5-5.0	0.01-1.0
Shape	Hexagonal crystals	Flakes
External surface area (m^2/g)	10-30	70-120
Internal surface area (m^2/g)	-	550-650
Plasticity	Low	High
Cohesiveness	Low	High
Swelling capacity	Low	High
Unit-layer charge	0	0.5-0.9
Interlayer spacing (nm)	0.7	1.0-2.0
Bonding	Hydrogen	Van der Waal's bonds (weak attractive force)
Net negative charge (cmol/kg)	2-5	80-120

2.3 Chitosan intercalated clay

The several studies have been investigated the structure of chitosan when it was interacted with clay; for example, Darder and co-workers (2003) investigated the intercalation of the cationic biopolymer chitosan in Na^+ -montmorillonite (Fig. 2.4) which characterized by XRD. Both the studies of Darder et al. (2003) and Tan and co-workers (2008) also presented the figure of intercalation of bilayered chitosan into Na^+ -montmorillonite (Fig. 2.5)

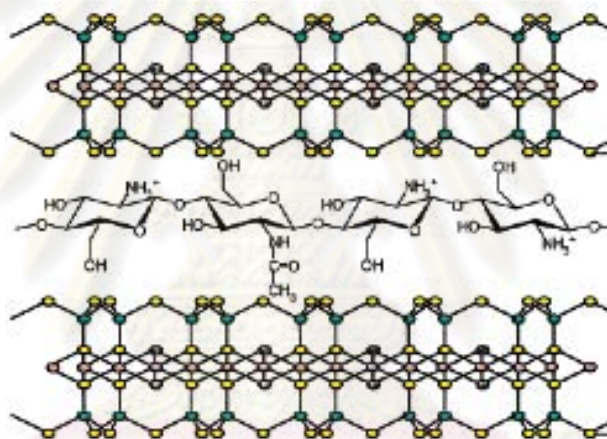


Fig. 2.4 Intercalation of chitosan into Na^+ -montmorillonite (Darder et al., 2003)

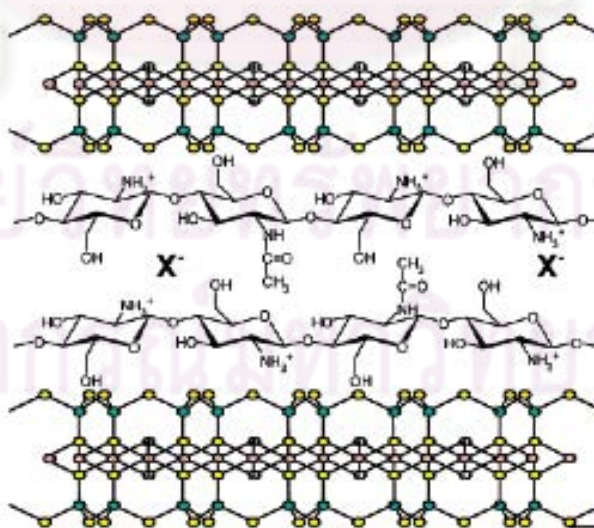


Fig. 2.5 Intercalation of chitosan into Na^+ -montmorillonite as a bilayer (Darder et al., 2003)

The another work introduced the interaction between chitosan and clay using hydrogen bonds performed by Wang et al. (2005) as shown in Fig 2.6.

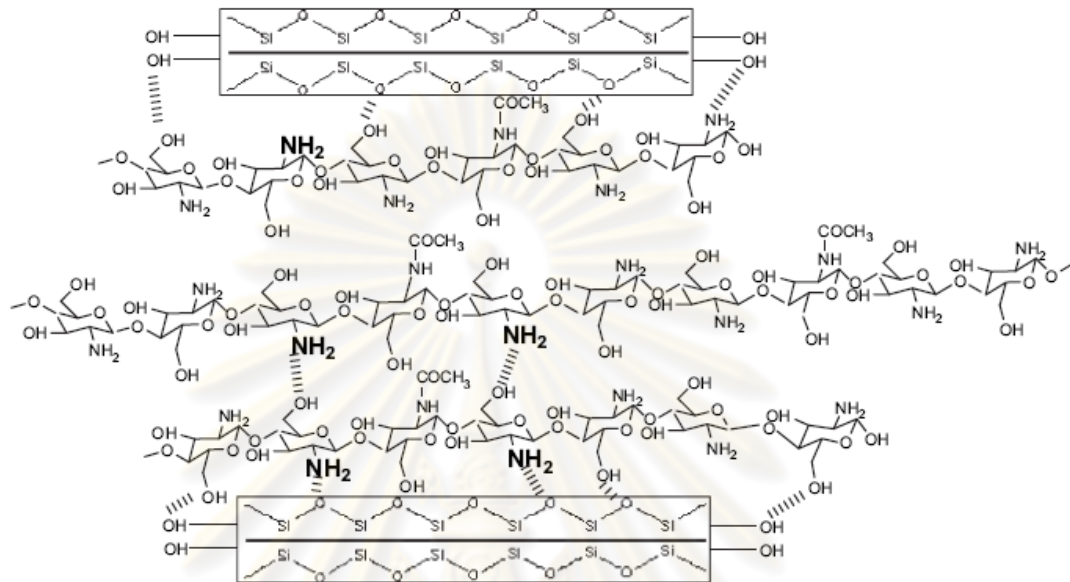


Fig. 2.6 Formation of hydrogen bonds between chitosan and montmorillonite
(Wang et al., 2005)

2.4 Crosslink

Crosslinker are molecules with at least two reactive functional groups that allow the formation of bridges between polymeric chains (Berger et al., 2004).

Crosslinked chitosan

Although chitosan is very useful because of its properties, abundance, non-toxicity, hydrophilicity, biocompatibility, biodegradability, and anti-bacteria, the applications of chitosan are limited by the dissolution ability at pH below 5.5 (Chiou and Li, 2002, 2003; Ngah, Endud, and Mayanar et al., 2002; Vasconcelos, 2008). Chemical modification has been used to stabilize the chitosan in acid solution in the figure of crosslinked chitosan. Moreover, crosslinked chitosan is improved the mechanical resistance and also reinforced the chemical stability of chitosan at drastic pH, which are important features to define a good adsorbent (Crini and Badot, 2008).

In crosslinked chitosan, the polymeric chains are interconnected by crosslinkers, formed by complexation with another polymer (Prashanth and Tharanathan, 2007).

Accordingly, the crosslinked chitosan may be justified by two objectives:

- 1) preventing the dissolving of the polymer when metal sorption is performed in acidic solutions (or when metal desorption occurs in acidic media)
- 2) improving metal sorption properties (increase of sorption capacities or enhancement of sorption selectivity)

The crosslinked chitosan works have been done by the previous work, Chiou and Li (2003) and Ngah and co-worker (2002). Both works compared the efficiency of the chitosan crosslinked by glutaraldehyde (GLA), epichlorohydrin (ECH), and ethylene glycol diglycidyl ether (EGDE).

Glutaraldehyde (GLA) or 1,5-pentanodial ($\text{OHC}-(\text{CH}_2)_3-\text{COH}$) (Beppu et al., 2007) is the crosslinker in dialdehyde group. The GLA reacts with chitosan and crosslinks in inter and intramolecular through the formation of covalent bonds mainly with the amino groups of the polymer, due to the resonance established with adjacent double ethylenic bonds via a Schiff reaction (Berger et al, 2004). However, the main drawback of such reactions is that they are generally considered to be toxic (Crini and Badot, 2008). For example, GLA is known to be neurotoxic, its fate in the human body is not fully understood. Therefore, even if products are purified before administration, the presence of free unreacted dialdehydes in the products could not be completely excluded (Prashanth and Tharanathan, 2007).

Epichlorohydrin (ECH) or 1-chloro-2,3-epoxypropane ($\text{C}_3\text{H}_5\text{ClO}$) and ethylene glycol diglycidyl ether (EGDE) ($\text{C}_8\text{H}_{14}\text{O}_4$) are the crosslinker in epoxide group. The ECH was selected as a convenient base-catalyzed crosslinking agent (Lee, Park, and Kin, 2007). An advantage of ECH is that it does not eliminate the amine function of chitosan. While the EGDE was used to synthesize crosslinked chitosan by Oshita and co-worker (2002) to adsorb some metal ions by two different mechanisms: for Cu (II) and Ag (I), it could adsorb by chelating mechanism, whereas for anionic species existing as oxoanions, such as V, Ga, Mo, W, and Bi, and existing as chloro complexes, such as Hg, Pt, Pd, and Au, by an anion exchange mechanism.

As the result of the interaction between crosslinking agent and chitosan, the ECH crosslinks chitosan molecules by connecting mostly with the $-OH$ group of chitosan whereas GLA and EGDE connecting with more $-NH_2$ group (Chiou and Li, 2003). Therefore, crosslinked chitosan using ECH presented a higher adsorption capacity than GLA and EGDE while GLA and EGDE reduce the major adsorption sites of chitosan (Nghah, Endud, and Mayanar, 2002; Chiou and Li, 2003; Crini and Badot, 2008).

The schematics of crosslinked chitosan using ECH, EGDE, and GLA were presented by Nghah et al. (2002) as shown in Fig. 2.7

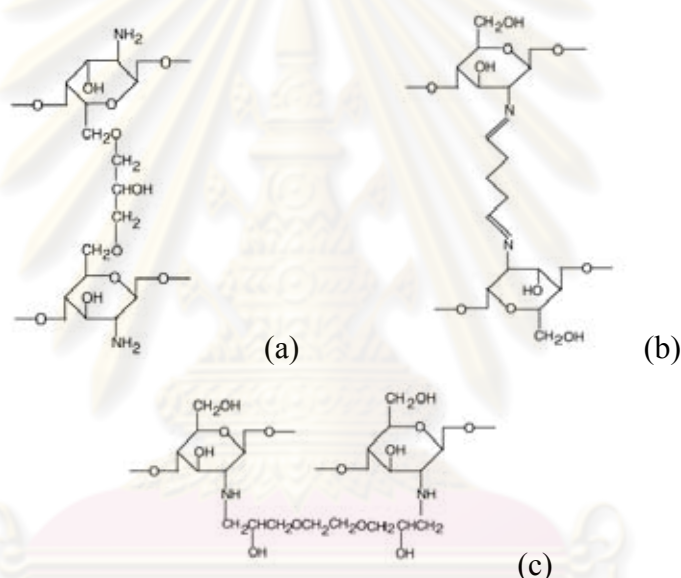


Fig. 2.7 Schematic representation of crosslinked chitosan beads: (a) chitosan-epichlorohydrin (chitosan-ECH), (b) chitosan-glutaraldehyde (chitosan-GLA), and (c) chitosan-ethylene glycol diglycidyl ether (chitosan-EGDE)

2.5 Adsorption

Adsorption is a process as the increase in concentration of a particular component at the surface or interface between two phases (Faust and Aly, 1998). The molecules that bind to the surface are called the adsorbate while the substance that holds the adsorbate is called the absorbent. The process when the molecules bind is called adsorption. Removal of the molecules from the surface is called desorption.

The nature of bonding between adsorbates and surfaces is still subject to some interpretation. It was important to distinguish between two radically different types of adsorption. The chemisorption, where there is a direct chemical bond between the adsorbate and the surface (Masel, 1996). Because chemisorption involves chemical bonding, it often occurs at high temperatures and is usually associated with activation energy. Also, the adsorbed molecules are localized on specific sites and not free to migrate (Faust and Aly, 1998). And the physisorption, where there is no direct bond. Instead the adsorbate is held by physical (i.e., van der Waals) forces (Masel, 1996). These forces, which involve the electrons and nuclei of the system, are electrostatic in origin, and are termed dispersion forces. They are always present regardless of the nature of other interactions, and often account for the major part of the adsorbate-adsorbent potential (Faust and Aly, 1998).

On a more fundamental level, when a molecule is chemisorbed, the electrons are shared between the adsorbate and the surface. As a result, the adsorbate's electronic structure is significantly perturbed. The surface's electronic structure is perturbed to a lesser extent. In contrast, physisorption is governed by polarization (i.e., van der Waals) forces. The surface does not share electrons with the adsorbate. As a result, the electronic structure of the adsorbate is perturbed to a much lesser extent (Masel, 1996).

Physical adsorption can be distinguished from chemisorption according to one or more of the following criteria:

1. Physical adsorption does not involve the sharing or transfer of electrons, and thus always maintains the individuality of interacting species. The interactions are fully reversible, enabling desorption to occur at the same temperature, although the process may be slow because of diffusion effects. Chemisorption involves chemical bonding and is irreversible.
2. Physical adsorption is not site-specific; the adsorbed molecules are free to cover the entire surface. This enables surface area measurements of solid adsorbents. In contrast, chemisorption is site-specific; chemisorbed molecules are fixed at specific sites.

3. The heat of physical adsorption is about 1-10 kcal/mole adsorbed gas while the heat of chemical adsorption is about 20-200 kcal/mole adsorbed gas.

2.5.1 Factors affecting adsorption

1. Surface area and pore structure
2. Particle size
3. Chemistry of the surface
4. Natures of the adsorbate
5. Effect of $[H^+]$
6. Effect of foreign ions
7. Effects of temperature

Many models and calculations are used to describe to investigate and understand about adsorption behaviors. The two parameters which usually used to describe the efficiency of the adsorption are the percent adsorption and the adsorption capacity.

2.5.1.1 The percent adsorption of metal ions on adsorbent is calculated according to:

$$\text{Percent adsorption} = \frac{(C_0 - C)100}{C_0}$$

where C_0 is the initial metal ions concentration (mg/L) and C is the final metal ions concentration (mg/L).

2.5.1.2 The adsorption capacity is calculated for each adsorbent (reported per gram adsorbent), base on the difference of metal ions concentration in aqueous solutions before and after adsorption, the volume of aqueous solution, and the amount of adsorbent used by weight, according to:

$$\text{Adsorption capacity} = \frac{(C_0 - C)V}{W}$$

where C_0 is the initial metal ions concentration (mg/L), C the final metal ions concentration (mg/L), V the volume (L) of metal ions solution, and W is the weight (g) of the adsorbent used.

2.5.2 Adsorption equilibrium

Adsorption from aqueous solutions involves concentration of the solute on the solid surface. As the adsorption process proceeds, the sorbed solute tends to desorb into the solution. Equal amounts of solute eventually are being adsorbed and desorbed simultaneously. Consequently, the rates of adsorption and desorption will attain an equilibrium state called adsorption equilibrium. At equilibrium, no change can be observed in the concentration of the solute on the solid surface or in the bulk solution. The position of equilibrium is characteristic of the entire system, the solute, adsorbent, solvent, temperature, pH, and so on. Adsorbed quantities at equilibrium usually increase with an increase in the solute concentration. The presentation of the amount of solute adsorbed per unit of adsorbent as a function of the equilibrium concentration in bulk solution, at constant temperature, is termed the adsorption isotherm.

Several investigators tried to make the understanding about adsorption behaviors. Up to now, several models have been used for the description of adsorption.

2.5.2.1 Langmuir adsorption isotherm

The basic principles of Langmuir's model or ideal localized monolayer model, are:

- 1) the molecules are adsorbed on definite sites on the surface of the adsorbent;
- 2) Each site can accommodate only one molecule (monolayer);
- 3) The area of each site is a fixed quantity determined solely by the geometry of the surface; and
- 4) The adsorption energy is the same at all sites.

In addition, the adsorbed molecules cannot migrate across the surface or interact with neighboring molecules. The Langmuir equation was originally derived from kinetic consideration. Later, it was derived on the basis of statistical mechanics, thermodynamics, the law of mass action, theory of absolute reaction rates, and the Maxwell-Boltzmann distribution law. The Langmuir adsorption isotherm is expressed as:

$$q_e = \frac{K_L C_e}{1 + b C_e} = \frac{C_{\max} b C_e}{1 + b C_e}$$

where $C_{\max} b = K_L$ and the linearized form of Langmuir equation is represented by

$$\frac{1}{q_e} = \frac{b}{K_L} + \frac{1}{K_L C_e}$$

where q_e is the amount of metal ions adsorbed (mg/g), C_e equilibrium concentration of metals ions in solution (mg/L), K_L the Langmuir equilibrium constant (L/g), and b the Langmuir constant (L/mg).

2.5.2.2 Freundlich adsorption isotherm

The most important multi-site adsorption isotherm for rough surfaces is the Freundlich adsorption isotherm (Masel, 1996). Freundlich isotherm is assumed that the distribution function of adsorption sites are in the exponential form (Rocha et al., 1997). Freundlich equation is expressed as:

$$q_e = K_F C_e^{1/n}$$

The Freundlich equation is an empirical expression that encompasses the heterogeneity of the surface and the exponential distribution of sites and their energies (Faust and Aly, 1998). For linearization of the data, the Freundlich equation is written in logarithmic form.

$$\log q_e = \log K_F + \frac{1}{n} \log c_e$$

where K_F is the Freundlich equilibrium constant which is roughly and indicator of the adsorption capacity and n of the adsorption intensity which can display in the Fig. 2.8.

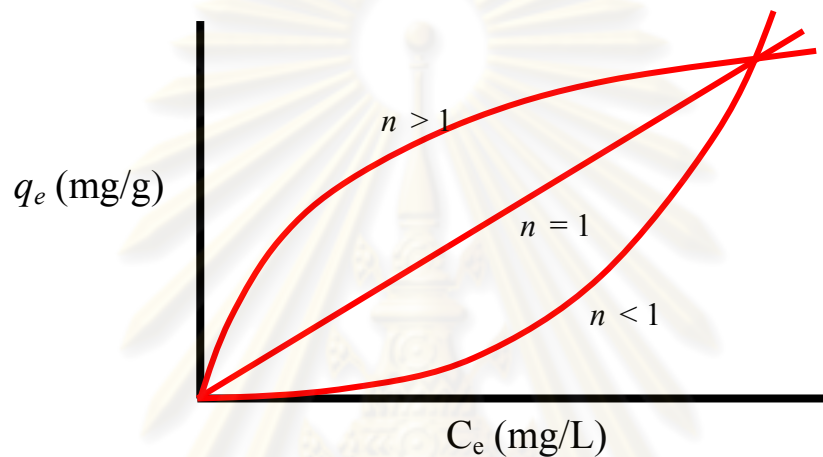


Fig. 2.8 Freundlich isotherm plotting between C_e and q_e presenting n value

2.5.3 Kinetic of adsorption

The understanding about the mechanism of adsorption is very important for the application of adsorbent to remove heavy metal ions. The rate of adsorption for given system is probably the most important factor in adsorption system design, with adsorbate residence time and the reactor dimensions controlled by the system's kinetics (Mckay, 1995; Ho, 2006a).

In the adsorption process, three consecutive steps are involved: (1) the adsorbate species migrate from the bulk liquid phase to the outer surface of adsorbent particle (film diffusion), (2) the adsorbate moves within the micro and macro-pores of adsorbent particles (pore diffusion), and (3) the reaction of adsorbate-adsorbent species takes place on the surface (Tahir and Rauf, 2006). These mechanisms take place with the two-stage process consisting of (a) rapid removal of the adsorbate from the liquid phase through adsorption and (b) much slower uptake continuing till the equilibrium is established (Gupta and Bhattacharyya, 2008). In order to examine the

mechanism controlling the adsorption processes, such as mass transfer and chemical reactions, several kinetic models are used to test experimental data (Ho, 2006a,b) and describe the reaction order of adsorption systems which one is based on solution concentration involving first-order and second-order reversible, first-order and second-order irreversible, and pseudo-first-order and pseudo-second-order and the another one is base on the capacity of the adsorbent including Lagergren's first-order equation, Zeldowitsch's model, and Ho's second-order expression.

The rate of adsorption is described by kinetic model which provides understanding of the time dependence of the concentration of solute in adsorbent and identification of the rate-determining step (Faust and Aly, 1998). The concentration of products does not appear in the rate law because the reaction rate is studied under conditions where the reverse reaction does not contribute to the over all rate. The reaction order rate and rate constant must be determined by experiment. In order to distinguish kinetic equations based on concentration of solution from adsorption capacities of solid, Lagergren's first-order rate equation has been called pseudo-first-order and the second-order rate equation has been called a pseudo-second-order (Ho, 2006a). These two kinetic models include all steps of adsorption such as external film diffusion, adsorption, and internal particle diffusion, so they are pseudo-model (Chang and Juang, 2004).

2.5.3.1 Pseudo-first-order kinetic model

The pseudo-first-order rate equation of Lagergren has been used to describe the adsorption is preceded by diffusion through a boundary (Crini and Badot, 2008).

Lagergren's first-order rate equation is the earliest known one describing the adsorption rate based on the adsorption capacity. It is summarized as follows:

$$\frac{dq_t}{dt} = k_1(q_e - q_t)$$

where q_e and q_t (mg/g) are the adsorption capacities at equilibrium and at time t (min), respectively, and k_1 is the rate constant of the first-order adsorption (1/min).

This equation is integrated with the boundary conditions of $t = 0$ to $t = t$ and $q_t = 0$ to $q_t = q_t$ to yield

$$\log(q_e - q_t) = \log q_e - \frac{k_1}{2.303}t$$

However, in any case using this model does not fit well to the whole range of contact time and is generally applicable over the initial stage of the adsorption processes (Chiou and Li, 2003). The first order process could be applied for the lower surface concentration solid and the second order for higher surface concentrations (Khambhaty et al., 2007).

2.5.3.2 Pseudo-second-order kinetic model

The pseudo-second-order rate expression was used to describe chemisorption involving valency forces through the sharing or exchange of electrons between the adsorbent and adsorbate as covalent forces (Ho, 2006b). The driving force, $(q_e - q_t)$, is proportional to the available fraction of active sites. The kinetic rate equations can be rewritten as follows:

$$\frac{dq_t}{dt} = k_2(q_e - q_t)^2$$

where k_2 is the rate constant of adsorption (g/mg min), q_e the amount of divalent metal ions adsorbed at equilibrium (mg/g), and q_t is the amount of divalent metal ions on the surface of the adsorbent at any time, t (mg/g). After integrating, this equation has a linear form of

$$\frac{t}{q_t} = \frac{1}{k_2 q_e^2} + \frac{1}{q_e}t$$

and

$$h = k_2 q_e^2$$

where h is the initial adsorption rate (mg/g min)

In recent years, the pseudo-second-order rate expression has been widely applied to the adsorption of pollutants from aqueous solutions. The pseudo-second-order equation has the following advantages: it does not have the problem of assigning an effective sorption capacity; the sorption capacity, rate constant of

pseudo-second-order, and the initial sorption rate can all be determined from the equation without knowing any parameter beforehand (Ho, 2006a).

2.6 Continuous adsorption

Metal removal in batch operation generally led to an inefficient utilization of the adsorption capacity of the adsorbent. This is due to the decrease of solute (metal) concentration as the adsorption process continues. Hence, batch type sorption is usually limited to the treatment of small volumes of effluent, whereas fixed bed systems have an advantage over this limitation (Kumar et al., 2004). In continuous operation, the adsorbent is permanently in contact with fresh metal solution and therefore highly efficient utilization of the adsorbent is generally achieved (Bai and Abraham, 2005).

A flow-through system provides a continuous interaction between a solution phase of constant composition and the exchanger phase until equilibrium has been reached. The flow-through method also prevents unwanted loss of exchanger phase that may occur during decantation steps in a batch reaction (DeSutter, Pierzynski, and Baker, 2006).

Continuous adsorption describes the relative concentration profile versus bed height and time as bed becomes saturated. Mass transfer resistance is important and often unsteady state in continuous adsorption.

Mass transfer

Adsorption of solid in solution system involves a mass transfer resistance at the particle surface that may control the adsorption rate. There are many variables involved: geometry of the column, nature of the baffles, type of impeller, speed of rotation (or power input) and solution density all vary with column design. The physical variables include solution density, viscosity and molecular diffusivity of diffusing adsorbate. The size distribution, shape and density of the particles are also

important factors. The adsorption of adsorbate onto chitosan is assumed to occur by 3-step process (Uzun and Güzel, 2004):

- 1) mass transfer of adsorbate from the bulk solution to the adsorbent surface,
- 2) intraparticle diffusion in the bulk solution filled pores,
- 3) adsorption from the bulk solution onto an interior site.

The flow of adsorbate through the adsorbent packed column involves several steps in series, which step dominates the adsorbate transfer process depends on the following factors: adsorbent packed thickness, temperature, and density of solution on the upstream side. For a thicker adsorbent packed column, the adsorbate particle diffusion through the bulk adsorbent film will be the rate-limiting step (Hou and Hughes, 2002).

The description breakthrough concentration profiles in fluid at bed outlet is shown in Fig. 2.9.

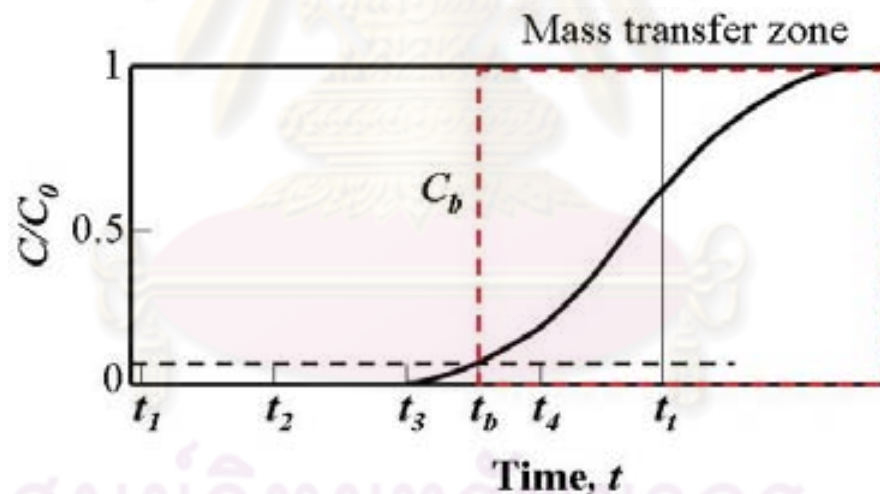


Fig. 2.9 Breakthrough concentration profiles in fluid at bed outlet which C_b and t_b are concentration and time denote breakthrough point (College of Engineering, University of Rhode Island, 2008)

2.7 Zeta-potential

The net surface charge of adsorbent can be determined in term of zeta-potential (Gecol et al., 2006; Hoven, et al., 2007). The development of net charge at

the particle surface affects the distribution of ions in the surrounding interfacial region, resulting in an increased concentration of counter ions (ions of opposite charge to that of the particle) close to the surface. Thus an electrical double layer exists around each particle.

The liquid layer surrounding the particle exists as two parts; an inner region, called the stern layer, where the ions are strongly bound and an outer, diffuse, region where they are less firmly attached as shown in Fig. 2.10. Within the diffuse layer there is a notional boundary inside which the ions and particles form a stable entity. When a particle moves (e.g. due to gravity), ions within the boundary move with it, but called the surface of hydrodynamic shear or slipping plane.

The potential that exists at this boundary is known as the zeta-potential.

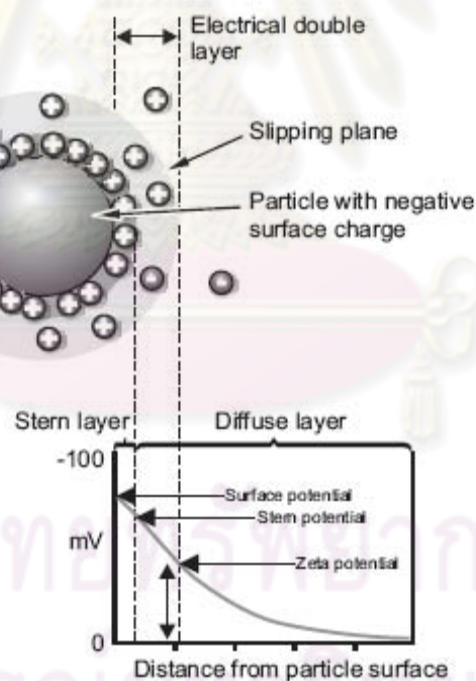


Fig. 2.10 Schematic of particle in liquid phase (Cornell University, 2009)

The magnitude of the zeta-potential gives an indication of the potential stability of the colloidal system. A colloidal system is when one of the three states of matter: gas, liquid and solid, are finely dispersed in one of the others. For this

technique we are interested in the two states of: a solid dispersed in a liquid, and a liquid dispersed in a liquid, i.e. and emulsion.

If all the particles in suspension have a large negative or positive zeta-potential then they will tend to repel each other and there is no tendency to flocculate. However, if the particles have low zeta-potential values then there is no force to prevent the particles coming together and flocculating. The general dividing line between stable and unstable suspensions is generally taken at either +30mV or -30mV are normally considered stable.

The most important factor that affects zeta potential is pH. A zeta-potential value on its own without a quoted pH is a virtually meaningless number.

Imagine a particle in suspension with a negative zeta-potential. If more alkali is added to this suspension then a point will be reached where the negative charge is neutralized. Any further addition of acid can cause a build up of positive charge. Therefore a zeta potential versus pH curve will be positive at low pH and lower or negative at high pH.

The point where the plot passes through zero zeta-potential is called the isoelectric point and is very important from a practical consideration. It is normally the point where the colloidal system is least stable. A typical plot of zeta-potential versus pH is shown below (Cornell University, 2009).

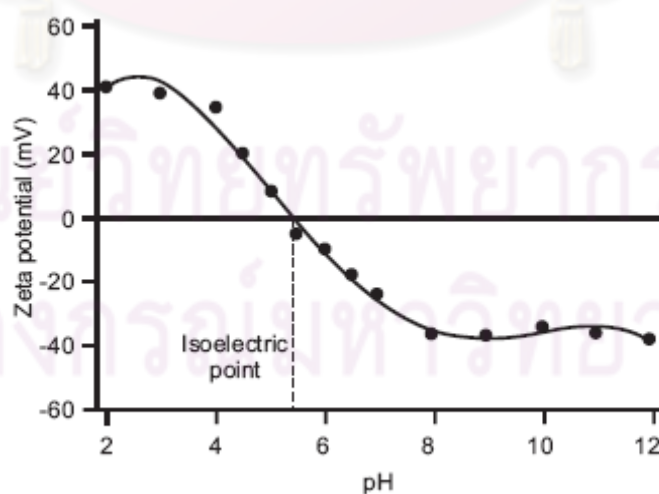


Fig. 2.11 Point of zero zeta-potential (point of zero charge)
(Cornell University, 2009)

2.8 X-Ray Diffraction (XRD)

The point of XRD analysis is that every crystalline substance gives a pattern; the same substance always gives the same pattern; and in a mixture of substances each produces its pattern independently of the others. The XRD pattern of a pure substance is, therefore, like a fingerprint of the substance. The powder diffraction method is thus ideally suited for characterization and identification of polycrystalline phases. The main use of powder diffraction is to identify components in a sample by a search/match procedure. Furthermore, the areas under the peak are related to the amount of each phase present in the sample (Scintag, Inc., 1999). Therefore, X-ray diffraction (XRD) is used to determine the mineralogical composition of the raw material components which the results will be compared with Joint Committee on Powder Diffraction Standards (JCPDS) file standard as well as qualitative and quantitative phase analysis of multiphase mixtures (Nayak and Singh, 2007). Moreover, size distribution for crystallite can be measured by XRD because the widths of the XRD peaks broaden as crystallite size decreases (Eberl, 2002).

The XRD work normally distinguishes between single crystal and polycrystalline or powder application. The single crystal sample is a perfect (all unit cells aligned in a perfect extended pattern) crystal with a cross section of about 0.3 mm. The single crystal diffractometer and associated computer package is used mainly to elucidate the molecular structure of novel compounds, either natural products or man-made molecules. Powder diffraction is mainly used for “fingerprint identification” of various solid materials, e.g. asbestos, quartz (Scintag, Inc., 1999).

The detailed interpretation of the diffraction of X-Rays by crystal can be performed by the Bragg diffraction condition. Fig. 2.12 shows four of a set of parallel crystal lattice planes at which both incident and diffracted (reflected) X-ray beams subtend angles θ . The path difference between waves reflected by the first plane and those reflected by the second plane (and between each successive pair of planes) is $2d \sin \theta$. If the path differences between successive waves are equal to the wavelength of the X-ray used, or some integral multiple of it, there is constructive interference, *i.e.* all waves are in phase, and the reflected beam is very intense. Thus if $2d \sin \theta = \lambda$ an intense diffracted wave is produced in the direction indicated, the

intensity decreasing abruptly with any deviation from the critical value of θ . Note that there is no path difference between waves scattered from different points on the same plane, *i.e.* there will be no difference in phase between waves scattered from point 4 in plane 4, and those from point 4' and 4". The diffractions from the set of planes may therefore be treated as the set of reflections from the point 1, 2, 3, ... on a normal T through the plane (Kasai and Kakudo, 2005).

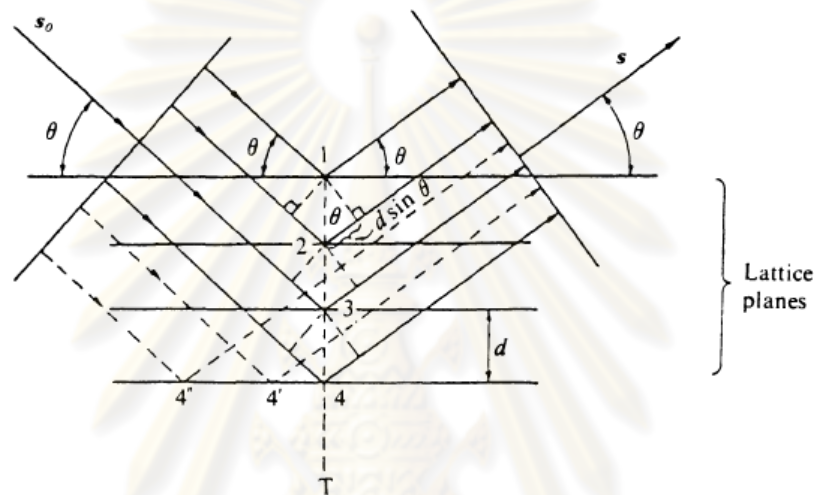


Fig. 2.12 Diffraction of X-rays considered as reflection from a set of lattice planes
(Kasai and Kakudo, 2005)

2.9 Brunauer-Emmett-Teller technique (BET)

BET theory is a rule for the physical adsorption of gas molecules on a solid surface and serves as the basis for an important analysis technique for the measurement of the specific surface area of a material. This theory was presented by Stephen Brunauer, Paul Hugh Emmett, and Edward Teller and published in journal in 1938. The concept of the theory is an extension of Langmuir theory, which is a theory for monolayer molecular adsorption, to multilayer adsorption with the following hypotheses: (a) gas molecules physically adsorb on solid in layer infinitely; (b) there is no interaction between each adsorption layer; and (c) the Langmuir theory can be applied to each layer. BET theory was applied for solid characterization. BET technique is widely used in the laboratories to determine the specific area. Such parameter expresses, the relationship between the total surface of the material and the

weight of the same one is usually expressed in m^2/g . BET technique uses the principle of physical adsorption of inert gas (nitrogen) to vary the relationship between the partial pressure of nitrogen and its vapor pressure to the temperature of liquid nitrogen. This technique can be carried in static or dynamic condition (University of Milan; Eklund and Ochoa, 1994). This technique was applied for N_2 adsorption-desorption analysis.

2.10 Development of chitosan applying for wastewater treatment

The increasing of heavy metals consumption for many applications in presently day leads to the existence of problems that affect both human and environment. Various methods exist for the removal of toxic heavy metals. The efficient methods of heavy metals ions removal from water and waste water are adsorption and chemisorption (Kaminski et al., 2008 and Ngah et al., 2002).

Kaminski, Tomczak, and Jaros (2008) synthesized chitosan beads to remove heavy metal ions from aqueous solution. They estimated sorptivity of chitosan beads and their selectivity towards Cu^{2+} (copper sulfate), Zn^{2+} (zinc sulfate), and Cr^{6+} (potassium dichromate) ions in different concentration range from 20 to 500 mg/l for single ions and their binary and ternary mixtures in aqueous solutions. Then the experimental data were well described by the sorption isotherms and the application of a multilayer perceptron neural network MLP was proposed. As a result, the adsorption capacity of chitosan beads are different for different concentration of aqueous solutions and the sorptivity of chitosan beads depends on the concentration and the composition of the mixture.

Because of using pure chitosan as adsorbent is cost-prohibitive process, the proper and inexpensive material is used to immobilize and support chitosan (Wan et al., 2004; Gecol, Ergican, and Miakatsindila, 2005). As the role of adsorbent, clay is the cheapest materials when compare with others (Gecol, Ergincan, and Miakatsindila, 2005; Bhattacharyya and Gupta, 2008a). There are some literatures studies about modified chitosan. Wan and co-worker (2004) attempted to find a more cost-effective adsorbent material based on chitosan immobilized on sand,

namely, chitosan-coated sand (5% chitosan content). The new material was studied for copper adsorption capacity. Copper recovery from an adsorbent with the possible reuse of the adsorbent material was also evaluated in leaching tests. They found that chitosan-coated sand was a better adsorbent compared to chitosan being used alone and chitosan-coated sand could be useful in creating permeable reactive barrier for the recovery of metals.

Moreover, many literatures investigated the adsorption capacity of adsorbent produced from chitosan/montmorillonite. Tan and co-worker (2007) expected that the chitosan/hydroxyl-aluminum pillared montmorillonite nanocomposites will play multiplex role in wastewater treatment. The nanocomposite was synthesized by incorporating hydroxy-aluminum pillared montmorillonite into chitosan solution prepared by dissolving the chitosan into diluted acetic acid. The ratio of chitosan to the cationic exchange capacity of the montmorillonite was varied. The experiment results indicated that the presence of hydroxyl-aluminum cation was in favor of the chitosan intercalation and the interlayers of montmorillonites was intercalated with the bilayers of chitosan sheets. The nanocomposites can be used in absorption of organic and metal ions from dyeing and finishing effluent.

Although chitosan is a good chelator, its applications were limited by its solubility property in weak acid solution. To improve the strength of chitosan to be used for metal ions and dye removal, Ngah and co-worker (2002) and Chiou and Li (2003) synthesized crosslinked-chitosan using epichlorohydrin (ECH), glutaraldehyde (GLA), and ethylene glycol diglycidyl ether (EGDE) as crosslinking agent to remove metal ions, copper ions, and dye. The crosslinked chitosan can be used to remove copper ions and dye even in strong acid or basic solution and it can be regenerated after desorption. However, the adsorption capacity of crosslinked chitosan were reduced when compared with the adsorption capacity of using only chitosan to remove copper ions, and dye.

Removal of Cu^{2+} using chitosan, modified chitosan, and other materials introduced by batch experiment is presented in Table 2.3

Table 2.3 Results of batch studies for Cu²⁺ removal using chitosan, modified chitosan and other materials

Adsorbent	Form and size	Cu ²⁺ conc. (mg/L)	Contact time (min)	q _e (mg/g)	Reference
Chitosan (Powder, 75-85%DD)	Bead, > 0.5 mm	100	240	25	Wan et al., 2004
		500	240	116	
		1000	240	166	
		2000	240	184	
Sand	> 0.5 mm	100	240	0.20	Wan et al., 2004
		500	240	0.78	
		1000	240	1.39	
Chitosan-coated sand	Bead, > 0.5 mm	2000	240	2.04	Wan et al., 2004
		100	240	1.19	
		500	240	5.9	
Bentonite	Powder, < 2 μm	1000	240	11.19	Mariano, 2008
		2000	240	12.38	
		100	240	1.19	
Kaolinite	Powder, < 2 μm	500	240	5.43	Mariano, 2008
		1000	240	9.02	
		2000	240	11.78	
Chitosan-bentonite	Bead, 0.35-0.7 mm	100	240	0.60	Mariano, 2008
		500	240	0.85	
		1000	240	0.70	
Chitosan-kaolinite	Bead, 0.35-0.7 mm	2000	240	0.67	Mariano, 2008
		100	240	1.20	
		500	240	5.99	
Chitosan (Flake, 57.72%DD)	Bead, < 250 μm	1000	240	10.84	Mariano, 2008
		2000	240	15.92	
		100	240	1.12	
Chitosan-GLA	Bead, < 250 μm	500	240	5.40	Mariano, 2008
		1000	240	8.37	
Chitosan-ECH	Bead, < 250 μm	2000	240	7.54	Mariano, 2008
		5	240	80.71	
Chitosan-EGDE	Bead, < 250 μm	5	240	59.67	Ngh, Endud, and Mayanar, 2002
		5	240	62.47	
Chitosan (Flake, 85%DD)	Flake	5	164	45.62	Ngh, Endud, and Mayanar, 2002
		10	164	20.92	
					Bassai, Prashen, and Sampson, 2000

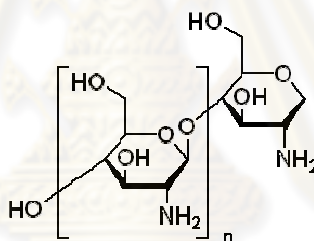
CHAPTER III

METHODOLOGY

3.1 Material

3.1.1 Chitosan

Low molecular weight chitosan ($C_{12}H_{24}N_2O_9$), α -chitosan, produced from crab shell with 75-85% deacetylated was purchased from Sigma Aldrich, Germany.



3.1.2 Crosslinking agents

Physical and chemical properties of crosslinking agents are shown in Table 3.1. Epichlorohydrin (ECH) with a purity 99+%, glutaraldehyde (GLA) solution with a purity 50%, and ethylene glycol diglycidyl ether (EGDE) with a purity 50% were purchased from Sigma Aldrich Germany.

Table 3.1 The physical and chemical properties of crosslinking agents

Crosslinking agent	Chemical formula	Chemical structure	Molecular weight (g/mol)	Density (g/L)
ECH	C_3H_5ClO		92.52	1.183
GLA	$C_5H_8O_2$		100.12	1.110
EGDE	$C_8H_{14}O_4$		174.19	1.151

3.1.3 CuSO₄

Copper sulfate (CuSO₄, MW 159.61 g/mol) was purchased from Merck KGaA, Germany.

3.1.4 Clay

Bentonite (Al₂O₃ · 4SiO₂ · H₂O) and kaolinite (Al₂O₃ · 2SiO₂ · 2H₂O) were purchased from Sigma Aldrich KGaA, Germany.

3.1.5 Other reagents

Sodium hydroxide (NaOH, MW 40.00 g/mol) and hydrochloric acid (HCl) 37% with density 1.19 kg/L were purchased from Merck KGaA, Germany.

3.1.6 Equipments

The equipments used in the experiment are shown in Table 3.2

Table 3.2 Equipments used in the experiment

Equipments	Model	Brand
Hot plate/Stirrer	PC-420D	CORNING
Hot air oven	DV452	CHANNEL
pH meter	Sension 3	HACH
Water bath shaker	BT 350	YIH
Pump	C/K	Masterflow
ICP-OES	Optima 2000DV	PERKIN ELMER
Zeta-potential	Zetasizer nano zs	MALVERN
SEM	S-3000N	HITACHI
XRD	D8	BRUKER
N ₂ adsorption-desorption analysis	GEMINI 2360	MICROMERITICS

3.2 Experimental procedure

3.2.1 Preparation of Cu²⁺ solution

A stock solution of 2000 mg/L of Cu²⁺ was prepared by dissolving 5.0231 g of CuSO₄ in one liter of DI water. This Cu²⁺ was used as the artificial wastewater. It was diluted to be 100, 500, and 1000 mg/L for investigating the appropriate initial concentration of adsorption studies.

3.2.2 Preparation of composite chitosan-clay beads

The method for composite chitosan-clay beads preparation was modified from the procedure described by Wan et al. (2004).

Five grams of chitosan were dissolved in 300 mL of 5% HCl under vigorously stir for two hours. After dissolution, 100 g of clay, bentonite or kaolinite, was added into the solution and stirred for three hours at room temperature, hereafter this solution was called chitosan-clay solution. The chitosan-clay solution was neutralized with 1 N NaOH (pH 13), dropwise until the material was precipitated. Then, it was filtered from the solution, washed by DI water to remove unreacted NaOH, and dried in vacuum oven at 65 °C for 24 hours or until the weight was being constant. After grinding and sieving, the particles were passed through ASTM sieve size #35 and #45, providing bead size of 0.35-0.50 mm. These beads were collected in a plastic bottle and used as adsorbent to investigate the adsorption behavior. Composite chitosan-bentonite and composite chitosan-kaolinite were now assigned as CCB and CCK beads, respectively. The more effective supporting materials, bentonite or kaolinite, was selected from the comparison of adsorption capacity using CCB and CCK beads as adsorbents to remove Cu²⁺ from aqueous solution. The selected clay was used as supporting material to prepare the composite crosslinked chitosan-clay in the second phase.

3.2.3 Preparation of composite crosslinked chitosan-clay beads

Composite crosslinked chitosan-clay beads preparation was modified from the procedure described by Wan et al. (2004), Chiou and Li (2003), and Ngah et al. (2002).

An equimolar 1:1 of Chitosan to EGDE, ECH, and GLA were prepared. 4.578, 1.162, or 2.650 mL of EGDE, ECH, or GLA, respectively was added into the chitosan-clay solution. Then this solution was heated with stirred continuously to 55 °C for three hours for composite chitosan-clay crosslinked with EGDE, 45 °C for two hours for composite chitosan-clay crosslinked with ECH, and 50 °C for six hours for composite chitosan-clay crosslinked with GLA. After that the solution was neutralized with 1 N NaOH dropwise until material was precipitated. The precipitated composite crosslinked chitosan-clay was filtered, washed with DI water to remove unreacted NaOH and crosslinking agents, and dried in vacuum oven at 65 °C for 24 hours or until the weight was being constant. After grinding and sieving, the particles were passed through ASTM sieve size #35 and #45, providing bead size of 0.35-0.50 mm. These beads were collected in a plastic bottle and used as adsorbent to investigate the adsorption behavior. The composite crosslinked chitosan-clays were assigned as CCB-EGDE, CCB-ECH, and CCB-GLA using EGDE, ECH, and GLA as crosslinking agents, respectively.

3.2.4 Adsorption study

2.5 g of adsorbent beads were placed in 100 mL Erlenmeyer flasks which 30 mL of Cu^{2+} solution was added. The continuous mixing was introduced by water bath shaker to agitate the samples at an average static speed of 50 rpm. The contact times were 30, 60, 120, 240, 360, 720, and 1440 min. At the end of each contact time, the solutions were removed from the water bath shaker and filtered through Whatman 40 filter paper. All batch adsorption experiments were carried out at room temperature.

3.2.5 Effect of initial Cu²⁺ concentration

The effect of initial Cu²⁺ concentration on the adsorption capacity of adsorbent was determined by varying the Cu²⁺ concentration to be 100, 500, 1000, and 2000 mg/L in the adsorption experiment with various contact time.

3.2.6 Effect of pH

The effect of pH of Cu²⁺ solution on the adsorption of adsorbent beads was determined by varying the pH of Cu²⁺ solution to be 1, 2, 3, and 4. HCl with concentration of 0.1, 1, and 6 N were used to adjust the pH of the Cu²⁺ solution.

3.2.7 Effect of crosslinking agents

Composite crosslinked chitosan-clay using EGDE, ECH, and GLA as crosslinking agents were investigated for adsorption capacity and the strength of adsorbent. The composite chitosan-clay was crosslinked at a ratio of 1:1 by mole (chitosan:crosslinking agent).

3.2.8 Desorption study

The adsorbed adsorbent beads (composite crosslinked chitosan-clay) from adsorption experiments at equilibrium contact time were placed in 100 mL Erlenmeyer flasks. Desorbing agents, water (pH 7) and diluted HCl solution (pH 3 and 1) were added and agitated in water bath shaker at 50 rpm for two hours. After that, the solutions were removed from the water bath shaker and filtered.

3.2.9 Reuse study

The desorbed composite crosslinked chitosan-clay beads were air-dried for 48 hours. The dried adsorbents were placed in 100 mL Erlenmeyer flasks, 30 mL of Cu²⁺ solution was added and agitated in water bath shaker at 50 rpm until reach

equilibrium contact time. The Cu^{2+} solution at 100, 500, 1000, and 2000 mg/L was used.

3.2.10 Column adsorption

The glass columns ($\text{Ø} = 2$ cm) were used to study the continuous adsorption of Cu^{2+} . The 5 g and 10 g of adsorbent beads were used in column adsorption to compare the effect of external mass transfer. The contact time was chosen at the equilibrium contact time of batch experiment. Then the flow rate for Cu^{2+} solution of 500 mg/L as calculated. Before drainage of Cu^{2+} to the column, the adsorbent in the column was saturated with DI water to reproduce the real case of groundwater. The solutions after adsorption from column were collected every 1 hour and analyzed for Cu^{2+} concentration by ICP-OES. The data from ICP-OES then was plotted between time versus C/C_0 .

3.2.11 Physical characteristics and morphology of adsorbents

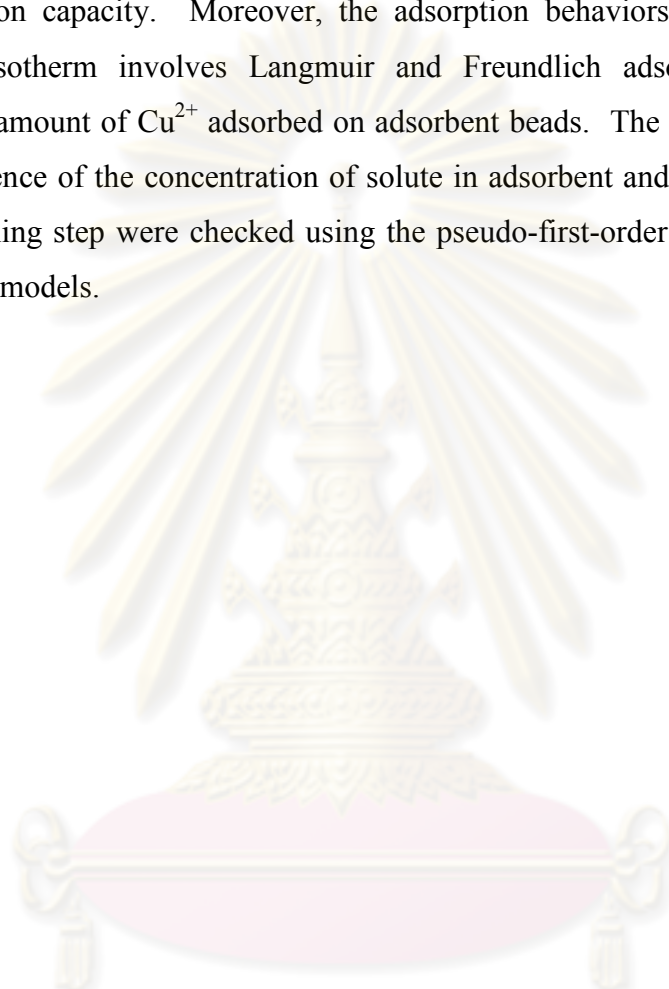
The adsorbent beads using in this study were analyzed. Surface area, crystallinity and morphology were investigated by N_2 adsorption-desorption analysis, powder X-ray diffraction (XRD) and Scanning Electron Microscopy (SEM), respectively, and the net charge of adsorbent beads were investigated by zeta-potential.

3.3 Analytical methods

After sample filtration, Cu^{2+} concentration in the supernatant from the adsorption experiments was diluted and analyzed using Inductively Coupled Plasma-Optical Emission Spectrometry (ICP-OES).

3.4 Mathematical methods

The main parameters for adsorption studies were percent adsorption and adsorption capacity. Moreover, the adsorption behaviors were studied using adsorption isotherm involves Langmuir and Freundlich adsorption isotherm to describe the amount of Cu^{2+} adsorbed on adsorbent beads. The understanding of the time dependence of the concentration of solute in adsorbent and identification of the rate-determining step were checked using the pseudo-first-order and pseudo-second-order kinetic models.



ศูนย์วิทยทรัพยากร
จุฬาลงกรณ์มหาวิทยาลัย

CHAPTER IV

RESULTS AND DISCUSSION

This chapter presents the results of this study which were divided into two phases. The first phase presents the comparison of adsorption capacity of Cu^{2+} when kaolinite and bentonite clay were used as supporting materials. The result showed that adsorption capacity of CCB beads was better than CCK beads for Cu^{2+} adsorption. In the second phase, bentonite was used as a supporting material for crosslinked chitosan. This was to compare the efficiency of adsorbents with different three crosslinking agents. The results showed that adsorption capacities of CCB-EGDE and CCB-ECH beads were somewhat similar whereas CCB-GLA beads gave the least adsorption capacity. The adsorption behaviors and mechanism were determined by adsorption isotherms, Langmuir and Freundlich isotherm, together with adsorption kinetic including pseudo-first- and pseudo-second-order kinetic models. The desorption, regeneration, and effect of pH of CCB-EGDE and CCB-ECH beads were also investigated. For the practical use, a breakthrough curve performed in a continuous flow reactor was studied. Results from material characterizations by SEM, zeta-potential, XRD, and nitrogen adsorption-desorption analysis were used to support the results above.

PHASE I Comparison of kaolinite and bentonite as supporting materials

4.1 Adsorption capacity of CCK and CCB beads

The adsorption capacity (q_e) of Cu^{2+} on CCK and CCB beads is shown in Table 4.1. The result showed that the adsorption capacities of both CCK and CCB beads were almost same when they were used to adsorb Cu^{2+} at 100 mg/L. The difference of adsorption capacity (q_e) was presented lightly when the adsorption was performed in higher Cu^{2+} concentration, 500, 1000, and 2000 mg/L. The

adsorption capacity of CCK and CCB beads for Cu^{2+} at different concentration and contact time is presented in Fig. 4.1.

Properties of kaolinite and bentonite clay were taken in to account for the difference of adsorption capacity. The nature of kaolinite clay which constituted of one layer of Si^{4+} and one layer of Al^{3+} , 1:1 layered clay, presents small negative charge, almost 0 charge/unit cell, thus the structure of kaolinite clay does not support for the substitution of other cation. Whereas bentonite, 2:1 layered clay performed more negative charge, -0.8 charge/unit cell; and it was constructed by weak bond between layers. Hence, it is easy for cation exchange to balance the negative charge between layers and around the edges of bentonite. As a result, bentonite has higher efficiency to adsorb Cu^{2+} (Bhattacharyya and Gupta, 2008a). Another advantage of bentonite over kaolinite is higher surface area. Higher surface area of bentonite (Sparks, 2003; Bhattacharyya and Gupta, 2006) provided space for chitosan and its functional groups, such as amine and hydroxyl groups, for Cu^{2+} to be adsorbed higher than kaolinite.

Accordingly, more net negative charge and surface area of bentonite clay provided the advantages in the case of Cu^{2+} adsorption by itself and it also played a good role of supporting materials for chitosan as shown in the Fig. 4.2 from the study of Wang et al. (2005).

It is not clearly for the difference of adsorption capacity in low concentration of Cu^{2+} (100 mg/L) since the excess functional groups on both CCK and CCB beads were available for the need of Cu^{2+} . Nevertheless, when the Cu^{2+} concentration increased, the functional groups of CCK beads were not enough for Cu^{2+} whereas the remaining of functional groups on CCB beads was still available for Cu^{2+} so it was clear that adsorption capacity of CCB beads for Cu^{2+} in high concentration, 500, 1000, and 2000 mg/L were higher than CCK beads.

Table 4.1 Adsorption capacity (q_e) of CCK and CCB beads in terms of time and initial Cu^{2+} concentration

contact time (min)	100 mg/L		500 mg/L		1000 mg/L		2000 mg/L	
	CCK	CCB	CCK	CCB	CCK	CCB	CCK	CCB
0	0.00	0.00	0.00	0.00	0.00	0.00	0.00	0.00
30	1.02	1.17	4.08	5.03	5.78	8.97	5.80	12.88
60	1.10	1.19	4.10	5.41	6.02	9.30	5.96	13.18
120	1.17	1.19	4.36	5.53	5.79	9.55	6.65	13.98
240	1.19	1.20	4.86	5.73	6.47	10.27	6.05	15.01
360	1.20	1.20	4.87	5.87	6.50	10.42	6.09	14.76
720	1.20	1.20	5.22	5.94	6.67	10.67	6.51	15.21
1440	1.20	1.20	5.31	5.97	6.62	10.84	6.61	15.16

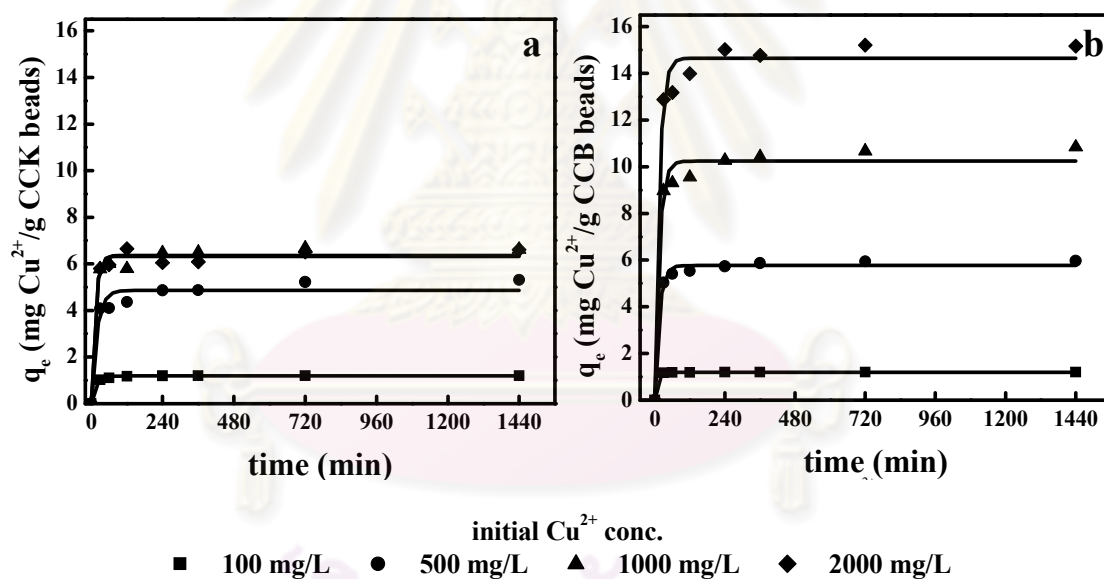


Fig. 4.1 Adsorption capacity (q_e) of a. CCK and b. CCB beads in terms of time and initial Cu^{2+} concentration

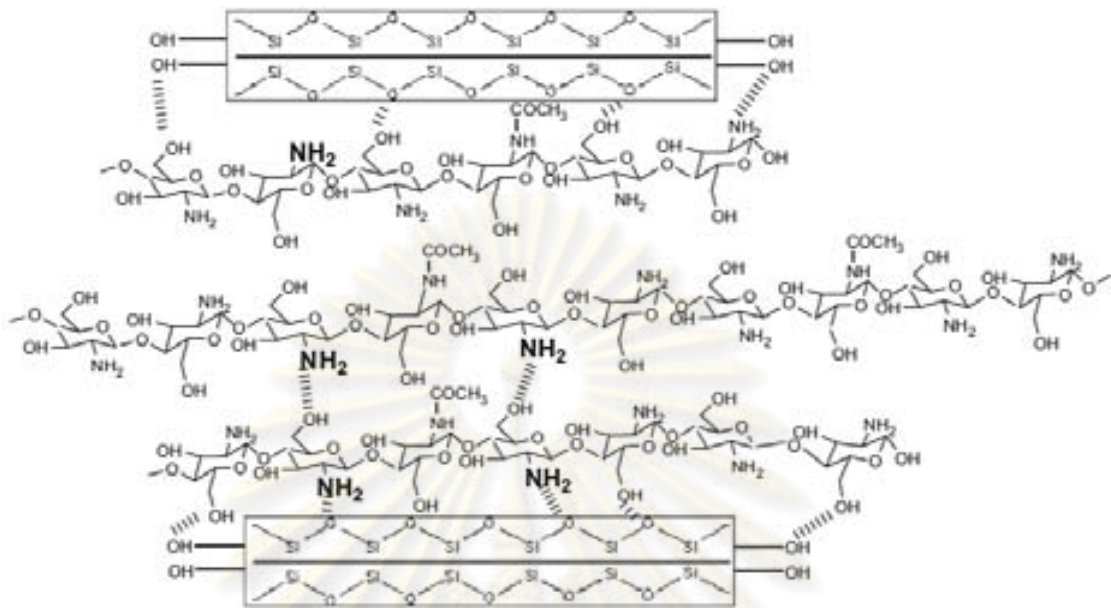


Fig. 4.2 Formation of hydrogen bond between chitosan and montmorillonite clay
(Wang et al., 2005)

4.2 Scanning electron microscopy (SEM) of CCK and CCB beads

The surface morphology of kaolinite, CCK beads, bentonite, and CCB beads was imaged by scanning electron microscope (SEM) (Fig. 4.3). The images from SEM verified that CCK (a2) and CCB (b2) beads were much denser than kaolinite (a1) and bentonite (b1) particle. It is believed that the aggregation structure in composite chitosan-clay is due to the hydroxylated edge-edge interaction of the silicate layers. Since one chitosan unit possesses one amino and two hydroxyl functional groups, these functional groups can form hydrogen bonds with the silicate hydroxylated edge groups, which lead to the strong interaction between matrix and silicate layers (Altinişik, Seki, and Yurdakoç, 2008).

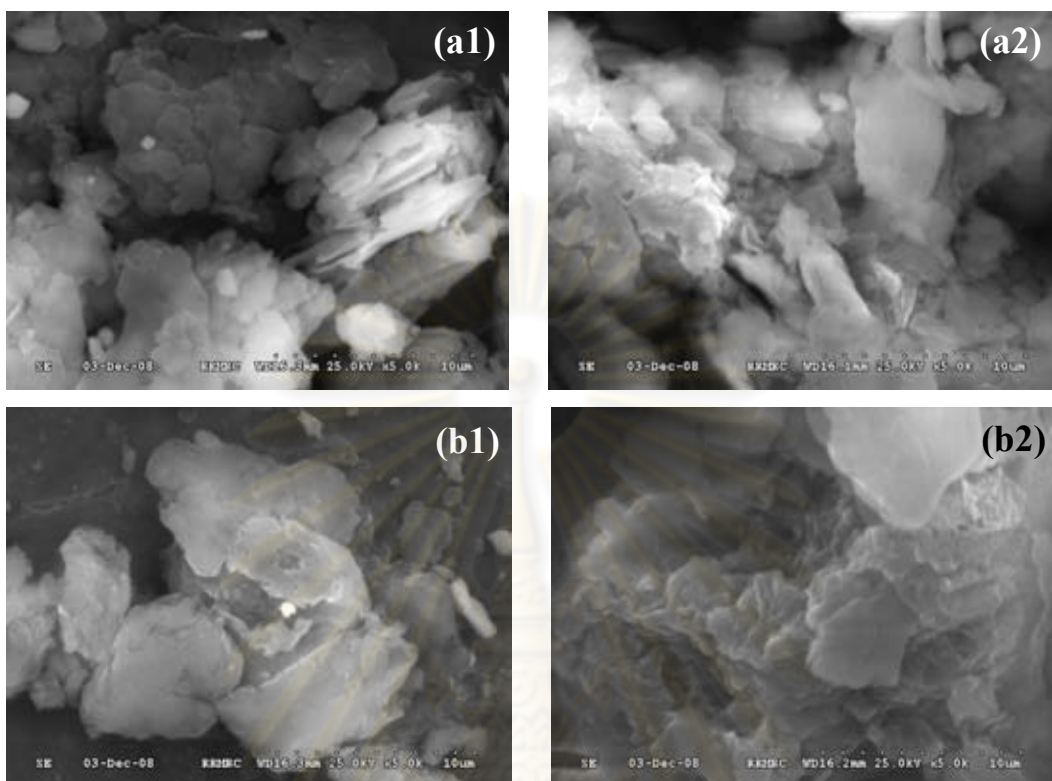


Fig. 4.3 Scanning electron microscopy (SEM) of (a1) kaolinite clay, (a2) CCK beads, (b1) bentonite clay, and (b2) CCB beads

Accordingly, base on adsorption capacities compared between CCK and CCB beads, the bentonite clay was selected to use as supporting material for chitosan in the next phase.

ศูนย์วิทยทรัพยากร
จุฬาลงกรณ์มหาวิทยาลัย

**Phase II Comparison of the effect of crosslinking agents
epichlorohydrin (ECH), ethylene glycol diglycidyl ether
(EGDE), and glutaraldehyde (GLA) on composite chitosan-
clay properties**

**4.3 Adsorption capacity of CCB-EGDE, CCB-ECH, and CCB-GLA
beads**

The adsorption capacity of Cu^{2+} on CCB-EGDE, CCB-ECH, and CCB-GLA beads are presented in Table 4.2 and contact time versus adsorption capacity was plotted in Fig. 4.4. The adsorption capacity of Cu^{2+} is ranked in the following order: CCB-EGDE > CCB-ECH > CCB-GLA, under all Cu^{2+} concentration and contact time. The adsorption capacity using CCB-EGDE were little greater than CCB-ECH whereas the adsorption capacity of CCB-GLA was obviously lower. The explanation of this result might be both of ethylene glycol diglycidyl ether (EGDE) and epichlorohydrin (ECH) are the crosslinking agents in epoxide group where as glutaraldehyde (GLA) is the crosslinking agent in dialdehyde group, as shown in Table 3.1. Epoxide groups after linking with chitosan might contribute more hydroxyl groups, resulting in more hydrogen bonds for the adsorption sites.

The difference of these crosslinking agents are the presence of hydroxyl groups. The hydroxyl groups of chitosan were considered to be the capable functional groups to perform hydrogen bond with the other functional group which was similar to the interaction between chitosan and PVA from the study of Jin and Bai (2002). From this reason, it could be explained that the hydroxyl groups of EGDE > ECH > GLA. Hence, one molecule of EGDE might form hydrogen bonds with chitosan more than ECH and GLA.

Although ECH has less hydroxyl groups than EGDE, it contains free amine groups on chitosan that can interact with Cu^{2+} . As a result, the interaction between hydroxyl groups of EGDE and ECH and amine groups of ECH with Cu^{2+} provided the similar adsorption capacity of Cu^{2+} using CCB-EGDE and CCB-ECH beads as adsorbents.

Using GLA as a crosslinking agent provided less adsorption capacity probably because the properties of adsorbent beads after being modified. Modification of adsorbent beads using GLA had a lower swelling capacities and more hydrophobic character (Guibal, 2004). Thus, CCB-GLA beads showed lower efficiency to remove Cu^{2+} from aqueous solution comparing with CCB-EGDE and CCB-ECH beads. Comparing the adsorption capacity between CCB, CCB-EGDE, and CCB-ECH beads with bentonite, the synthesized adsorbent beads provided adsorption capacity more than bentonite. In addition, the used quantity of chitosan was reduced and the synthesized adsorbents could use in the acid solution.

Table 4.2 Adsorption capacity (q_e) of CCB-EGDE, CCB-ECH, and CCB-GLA beads in terms of time and initial Cu^{2+} concentration

contact time (min)	100 mg/L			500 mg/L			1000 mg/L			2000 mg/L		
	CCB-EGDE	CCB-ECH	CCB-GLA	CCB-EGDE	CCB-ECH	CCB-GLA	CCB-EGDE	CCB-ECH	CCB-GLA	CCB-EGDE	CCB-ECH	CCB-GLA
0	0.00	0.00	0.00	0.00	0.00	0.00	0.00	0.00	0.00	0.00	0.00	0.00
30	1.19	1.18	0.70	5.68	5.54	2.36	10.30	9.89	3.77	15.67	15.26	5.68
60	1.20	1.20	0.78	5.90	5.88	2.47	10.64	10.19	4.05	16.16	15.36	5.90
120	1.20	1.20	0.79	5.95	5.83	2.40	11.31	10.66	3.77	17.14	15.72	5.59
240	1.20	1.20	0.82	5.98	5.98	2.65	11.46	11.08	4.02	17.18	16.36	5.67
360	1.20	1.20	0.83	5.98	5.98	2.66	11.03	11.16	4.45	16.94	16.61	5.84
720	1.20	1.20	0.87	5.99	6.00	2.89	11.37	11.35	4.52	17.41	17.19	6.87
1440	1.20	1.20	0.88	5.98	6.00	3.06	11.72	11.49	4.66	17.59	17.43	7.50

ศูนย์วิทยทรัพยากร
จุฬาลงกรณ์มหาวิทยาลัย

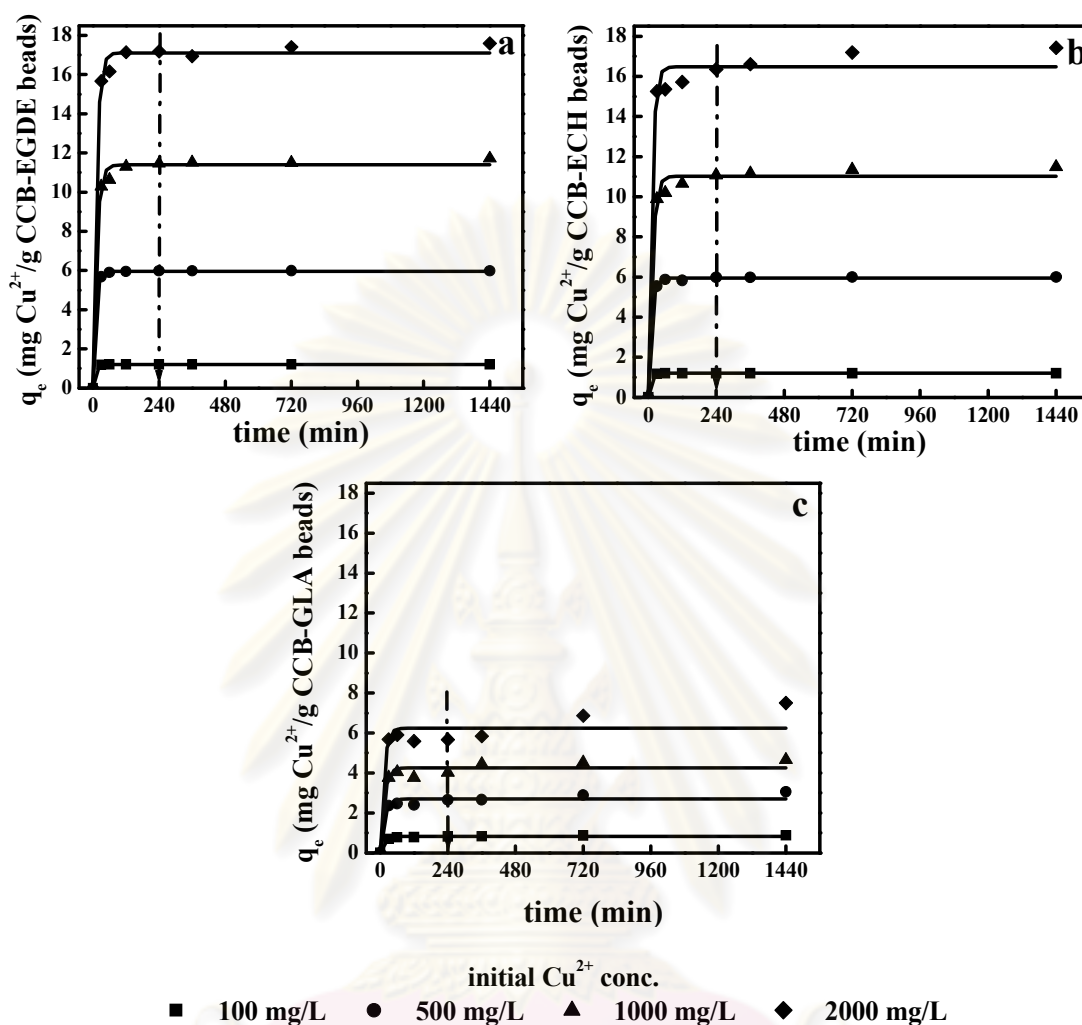


Fig. 4.4 Adsorption capacity (q_e) of Cu^{2+} on a. CCB-EGDE, b. CCB-ECH, and c. CCB-GLA beads in terms of time and initial Cu^{2+} concentration

4.4 Adsorption equilibrium

The adsorption capacity of Cu^{2+} on CCB-EGDE, CCB-ECH, and CCB-GLA beads were exhibited in the same pattern as shown in Fig 4.4. The adsorption capacity of Cu^{2+} on these three adsorbent beads increased sharply until 120 min of contact time for all studied Cu^{2+} concentrations. After 120 min, the adsorption capacity for all Cu^{2+} concentration was stable, referring to the adsorptions have reached equilibrium. However, to ensure that all experimental sets reached equilibrium, 240 min was marked for the batch adsorption before any further investigations.

4.5 Adsorption isotherm

Adsorption behaviors were determined using Langmuir and Freundlich models. The Langmuir isotherm was represented by the following equation and the model was applied for experimental data as shown in Fig. 4.5

$$q_e = \frac{K_L C_e}{1 + bC_e} = \frac{C_{\max} bC_e}{1 + bC_e}$$

where q_e is the equilibrium Cu^{2+} loading on the adsorbent beads, C_e the equilibrium concentration of Cu^{2+} , C_{\max} the ultimate capacity and b is the relative energy (intensity) of adsorption, also known as binding constant (Sankararamakrishnan et al., 2007). The Freundlich isotherm was applied in the equation as shown below and the Freundlich model was applied from experimental data as shown in Fig. 4.6:

$$q_e = K_F C_e^{1/n}$$

where K_F and n are Freundlich coefficients related to adsorption capacity and adsorption intensity of the solid adsorbent, respectively (Gupta and Bhattacharyya, 2008). Each term from Langmuir and Freundlich isotherm model for adsorption of CCB-EGDE, CCB-ECH, and CCB-GLA beads are presented in Table 4.3.

The results showed that adsorption of Cu^{2+} on CCB-EGDE and CCB-ECH beads fitted very well with Langmuir isotherm confirmed with R^2 , 0.996, and 0.998 for CCB-EGDE and CCB-ECH beads, respectively. This indicated a monolayer interaction between the adsorbate and adsorbents. The equilibrium coefficient, b , were 4.299 and 3.799 L/g (Table 4.3) for Cu^{2+} adsorbed on CCB-EGDE and CCB-ECH beads system. The large value showed that at the equilibrium, CCB-EGDE and CCB-ECH beads (solid phase) had spontaneous interactions with Cu^{2+} (aqueous phase) leading to adsorbate-adsorbent complex represented as CCB-EGDE $\cdots\cdots\text{Cu}^{2+}$ and CCB-ECH $\cdots\cdots\text{Cu}^{2+}$, respectively. Under an equilibrium, C_{\max} of Cu^{2+} on both CCB-EGDE and CCB-ECH beads were 10.52 and 11.75 mg Cu^{2+} /g adsorbent beads, respectively.

The adsorption of Cu^{2+} on CCB-GLA beads fitted very well with Freundlich isotherm model with high R^2 , 0.999. The Freundlich coefficient, n , was 1.89 in conformity with the requirement of $n > 1$.

Table 4.3 Adsorption isotherm constants and correlation coefficient (R^2) of composite crosslinked chitosan-bentonite

Adsorbents	Langmuir Isotherm				Freundlich Isotherm		
	R^2	K_L (L/g)	b (L/mg)	C_{\max} (mg/g)	R^2	K_F	n
CCB-EGDE	0.996	45.228	4.299	10.52	0.953	4.150	3.89
CCB-ECH	0.998	44.623	3.799	11.75	0.932	4.311	4.13
CCB-GLA	0.984	0.044	0.011	4.17	0.999	0.152	1.89

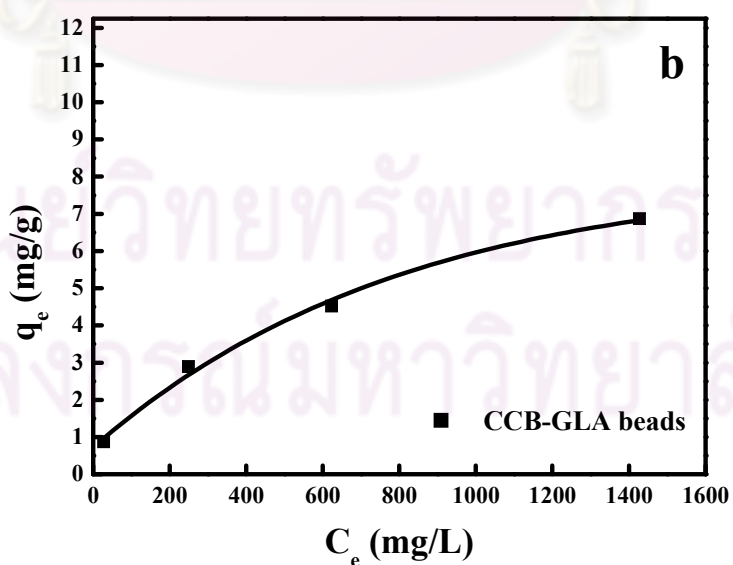
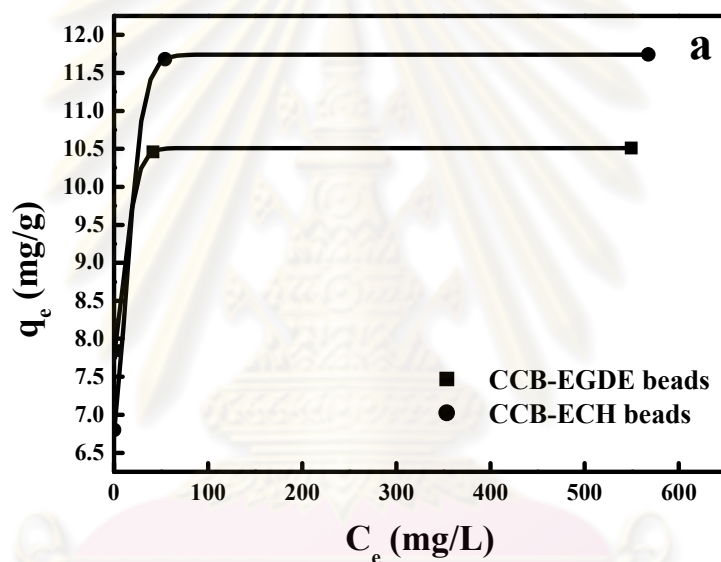


Fig. 4.5 Adsorption isotherm of Cu^{2+} on adsorbent beads

4.6 Adsorption kinetic

The purpose of adsorption kinetic study was to evaluate how well the adsorption behavior before reaching an equilibrium. The rate constant of pseudo-first- and pseudo-second order kinetic model are presented in Table 4.4 and the linear plots of both kinetic models for adsorption of Cu^{2+} on CCB-EGDE, CCB-ECH, and CCB-GLA beads were performed in Appendix A Fig. A-10 for pseudo-first-order kinetic model and Appendix A Fig. A-11 for pseudo-second-order kinetic model. Fig. 4.6 showed the linear plots of pseudo-first-order kinetic model and pseudo-second-order kinetic model for Cu^{2+} adsorbed on CCB-EGDE as an example. The correlation coefficient (R^2) of pseudo-second-order for all adsorbent beads were higher than 0.995. Therefore, the adsorption of Cu^{2+} on CCB-EGDE, CCB-ECH, and CCB-GLA beads were better described by the pseudo-second-order. The comparison between adsorption capacities from the experiment and kinetic model showed that the adsorption capacity from the pseudo-first-order plots was poorly with the experimental adsorption capacity values (Table 4.2). On the other hand, the adsorption capacity values from pseudo-second-order kinetic were agreed with experimental adsorption capacity values. This confirmed that the adsorption of Cu^{2+} on all adsorbent beads was fitted very well with pseudo-second-order kinetic.

Accordingly, the pseudo-second-order adsorption mechanism is predominant and the overall rate of Cu^{2+} adsorption process appears to be controlled by the chemical attachment not mass transport (Chiou and Li, 2003). This adsorption mechanism may involve valency forces through sharing of electrons between Cu^{2+} and adsorbent beads (Ho, 2006; Chen et al., 2008). According to the pseudo-second-order kinetic model, the adsorption rate dq/dt is proportional to the second-order of $(q_e - q_t)$. The presence of high adsorption capacity with short equilibrium time indicates a high degree of affinity between the Cu^{2+} and adsorbent beads, CCB-EGDE, CCB-ECH, and CCB-GLA beads (Chiou and Li, 2002).

Table 4.4 Pseudo-first- and pseudo-second-order kinetic constants and correlation coefficient (R^2) for adsorption of Cu^{2+} on CCB-EGDE, CCB-ECH, and CCB-GLA beads

Adsorbents	Initial Cu^{2+} conc. (mg/L)	Pseudo-first-order kinetic			Pseudo-second-order kinetic		
		R^2	k_1 (L/min)	q_e (mg/g)	R^2	k_2 (g/mg min)	q_e (mg/g)
CCB-EGDE	100	NA	NA	NA	NA	NA	NA
	500	0.910	-0.041	2.208	0.999	0.111	6.020
	1000	0.927	-0.019	3.926	1.000	0.019	11.671
	2000	0.981	-0.048	12.531	0.999	0.016	17.467
CCB-ECH	100	NA	NA	NA	NA	NA	NA
	500	0.778	-0.028	1.941	1.000	0.063	6.034
	1000	0.879	-0.024	5.272	1.000	0.015	11.315
	2000	0.788	-0.023	6.026	0.999	0.014	16.589
CCB-GLA	100	0.880	-0.026	0.403	1.000	0.209	0.838
	500	0.688	-0.016	1.024	0.998	0.052	2.696
	1000	0.595	-0.006	1.415	0.996	0.018	4.463
	2000	0.595	-0.009	1.129	0.999	0.089	5.818

NA: not available

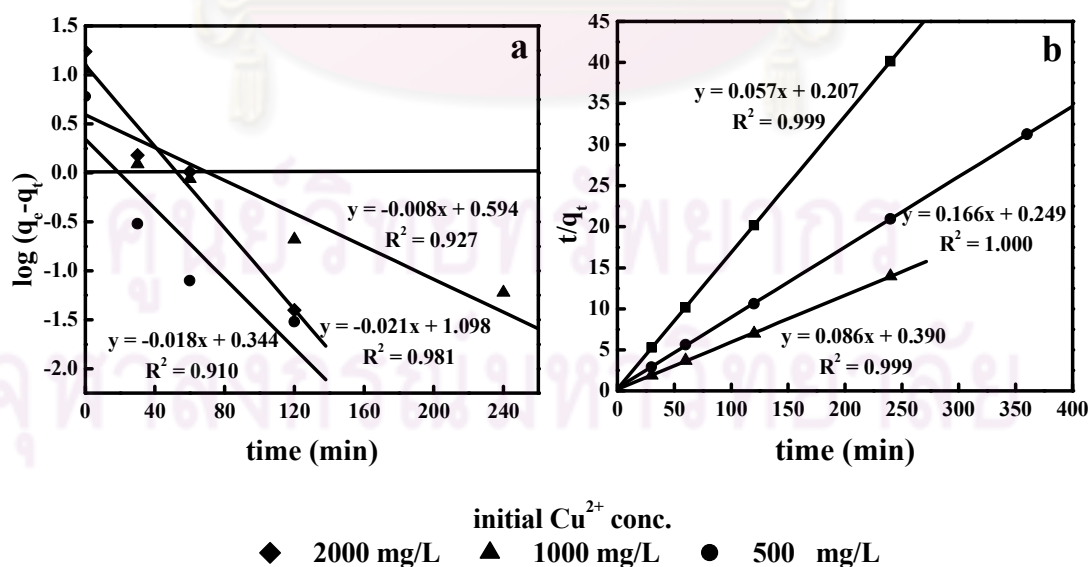


Fig. 4.6 Linear plots of a. pseudo-first- and b. pseudo-second-order kinetic for Cu^{2+} adsorbed on CCB-EGDE beads

4.7 Desorption study

The desorption study could investigate the strength and the efficiency of adsorbent beads to recover Cu^{2+} and adsorbent beads. The desorption agents, deionized water at pH 7, acid solution of pH 1 and pH 3, were used for the different purposes. The desorption in solution pH 3 and pH 7 was performed to reproduce the pH of effluent, investigated the property of CCB-EGDE and CCB-ECH beads to indicate the efficiency to adsorb and do not release Cu^{2+} . The desorption in solution pH 1 was performed to investigate the strength of adsorbent beads that was durability even in strong acid media. After the desorption using the agents pH 3 and 7, Fig. 4.7 showed clearly that almost same amount of Cu^{2+} remain adsorbed on the adsorbent beads while small amount of Cu^{2+} remained on adsorbent beads after desorption with the agent pH 1. In the condition of pH 1, the change of physical structure of adsorbent beads was observed. The CCB-ECH and CCB-EGDE beads were dissolved and some beads were jointed together as shown in Fig. 4.8.

Following the purpose of desorption in reagent pH 3 and 7 which aimed to observe the ability of adsorbent beads to capture Cu^{2+} , both CCB-EGDE and CCB-ECH beads performed effective role as adsorbent to adsorb Cu^{2+} . While desorption in pH 1 could desorb Cu^{2+} from the adsorbent beads but the structure of adsorbent beads still was not strong enough because their structures changed in this pH. Similarly, the study by Chen and co-workers (2008) revealed that crosslinked chitosan was effective as adsorbent at pH 3 and 6 for 4 hours but it was soluble at pH 1.

ศูนย์วิทยทรัพยากร
จุฬาลงกรณ์มหาวิทยาลัย

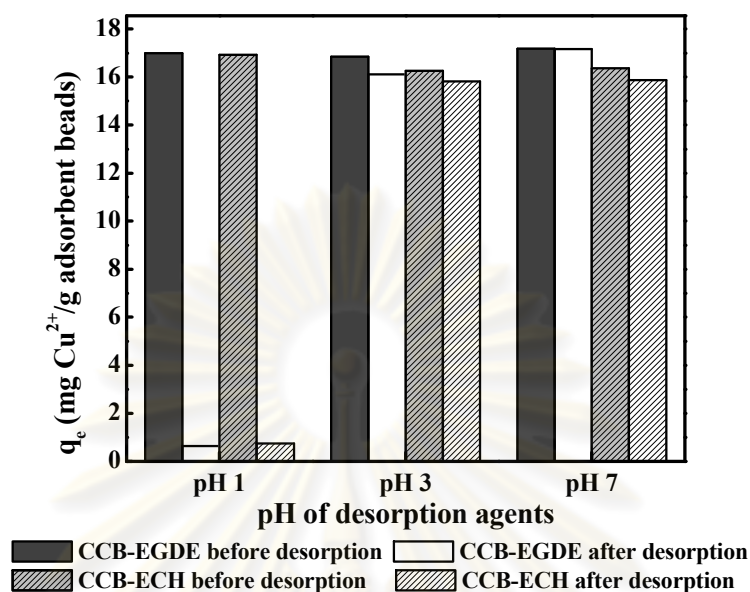


Fig. 4.7 Adsorption capacity (q_e) of Cu^{2+} 2000 mg/L on CCB-EGDE and CCB-ECH beads before and after desorption using deionized water at pH 7 and acid solution at pH 1 and pH 3

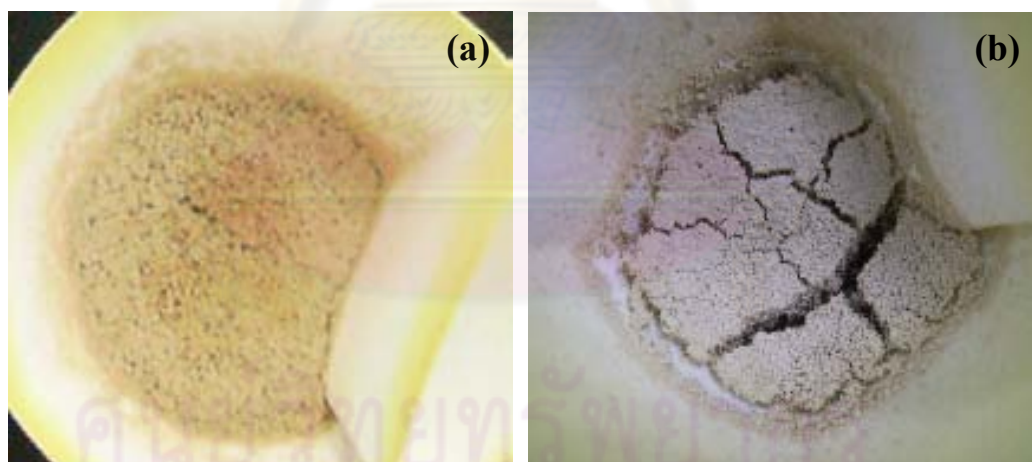


Fig. 4.8 CCB-ECH beads (a) and CCB-EGDE beads (b) after desorption using desorption agent pH 1

4.8 Reuse study

After desorption, the adsorbent beads, CCB-EGDE and CCB-ECH beads, were reused for Cu^{2+} adsorption again. The results are shown in Fig. 4.9 which

the batch adsorption for 240 min, the initial Cu^{2+} concentration of 2000 mg/L was performed. The results showed that the adsorption capacity of the adsorbent beads in the first time were 17.18 and 16.36 mg of Cu^{2+} /g of CCB-EGDE and CCB-ECH beads, respectively. After desorption using reagents pH 1, 3, and 7, these adsorbent beads were used to adsorb Cu^{2+} at concentration 2000 mg/L again (see Fig 4.9). The adsorption capacity in the second time of Cu^{2+} on CCB-EGDE and CCB-ECH beads were 0.00, 5.77, and 6.83 mg/g (adsorbent beads from desorption using reagents pH 1, 3, and 7, respectively) for CCB-EGDE beads and 3.00, 7.99, and 7.75 mg/g as well for CCB-ECH beads. This indicated that CCB-ECH beads exhibited the efficiency for regeneration better than CCB-EGDE beads.

Although using reagent pH 1 gave the greatest adsorption capacity for both CCB-EGDE and CCB-ECH beads, it also destroyed partial structure of adsorbent beads, chitosan was dissolved and jointed together then the forms of effectiveness adsorbent beads might be destroyed as shown in Fig. 4.8, As a result, regeneration using reagent pH 1 provided low adsorption capacity. Using desorption agents pH 3 and pH 7 exhibited low percent desorption; however, the adsorbent beads still could be used for adsorption again but in low adsorption capacity compared with the adsorption in the first time in term of Cu^{2+} compensation on CCB-EGDE and CCB-ECH beads (similar to the study of Vieira and Beppu (2006) that presented the decrease of adsorption capacity from regeneration with low percent desorption). Another possible explanation for the capability for adsorption in the second time of CCB-EGDE and CCB-ECH beads after desorption using reagents pH 3 and 7 was that the adsorbent beads might remain have some available functional groups for Cu^{2+} after the first adsorption or adsorbent beads exhibit some available sites for Cu^{2+} after desorption.

จุฬาลงกรณ์มหาวิทยาลัย

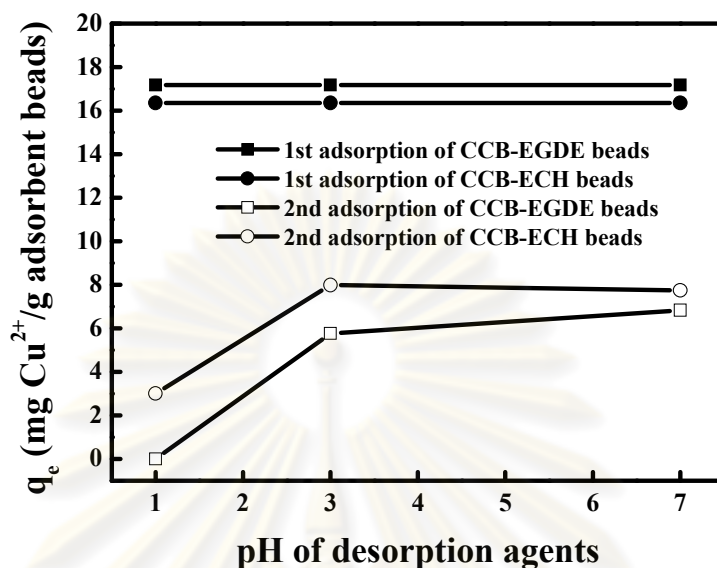


Fig. 4.9 Adsorption capacity of Cu^{2+} in the first and second time on CCB-EGDE and CCB-ECH beads at initial Cu^{2+} concentration 2000 mg/L

4.9 Effect of initial Cu^{2+} concentration

An increase in initial Cu^{2+} concentration led to an increase in the adsorption capacity of Cu^{2+} on adsorbent beads. The adsorption capacity which is shown in Table 4.1 for 240 min (equilibrium contact time) exhibited the milligram of Cu^{2+} per gram of CCB-EGDE, CCB-ECH, and CCB-GLA beads with the initial Cu^{2+} concentration of 100, 500, 1000, and 2000 mg/L as following; Cu^{2+} concentration 100 mg/L was adsorbed by CCB-EGDE, CCB-ECH, and CCB-GLA beads 1.20, 1.20, and 0.82 mg/g, respectively, Cu^{2+} concentration 500 mg/L was adsorbed by CCB-EGDE, CCB-ECH, and CCB-GLA beads 5.98, 5.98, and 2.65 mg/g, respectively, Cu^{2+} concentration 1000 mg/L was adsorbed by CCB-EGDE, CCB-ECH, and CCB-GLA beads 11.46, 11.08, and 4.02 mg/g, respectively, and Cu^{2+} concentration 2000 mg/L was adsorbed by CCB-EGDE, CCB-ECH, and CCB-GLA beads 17.18, 16.36, and 5.67 mg/g, respectively.

At low Cu^{2+} concentration, the ratio of the number of Cu^{2+} ions to the number of available adsorption sites on adsorbent beads was small and consequently, adsorption was independent of initial concentration. Whereas when the concentration of Cu^{2+} increased, the competition between Cu^{2+} for available sites became severe.

As a result, the extent of adsorption came down considerably, but the amount adsorbed per unit mass of the adsorbent had been raised. Similar results had been reported by other studies such as Immobilization of Pb(II), Cd(II) and Ni(II) ions on kaolinite and montmorillonite surfaces from aqueous medium studied by Gupta and Bhattacharyya (2008) or Adsorption behavior of reactive dye in aqueous solution on chemical cross-linked chitosan beads studied by Chiou and Li (2003). These literatures also showed the increase of adsorption capacity of adsorbate on adsorbents with the increase of initial adsorbate concentration.

4.10 Effect of pH

The pH of Cu^{2+} solution was adjusted to be 1, 2, 3, and 4. The Cu^{2+} solution at concentration 500 mg/L was tried to adjusted to pH value of 5 but the precipitation of $\text{Cu}(\text{OH})_2$ occurred because at pH more than around 5.3 under Cu^{2+} concentration 100 mg/L, Cu^{2+} will be precipitated as shown in Fig. 4.10 (Ayres, Davis, and Gietka, 1994; Naoto Takeno, 2005; Václavíková and Gallios, 2006). Therefore, the effect of pH can be studied under pH 1-4. Moreover, the speciation diagram for the Cu(II)- H_2O system (Fig. 4.11) showed that almost all Cu ions were present in the ionic form of Cu^{2+} of pH < 6.0 (Doyle, and Liu, 2003 and Wang, Li, and Sun, 2009). At the initial pH of Cu^{2+} solution, pH 4.81, 4.63, 4.55, and 4.46 for Cu^{2+} concentration 100, 500, 1000, and 2000 mg/L, respectively, Cu^{2+} is the dominated form which can react with adsorbent beads through (1) the electrostatic interaction between the protonated groups of chitosan ($\text{pK}_a = 6.3$ Jin and Bai, 2002; Guibal, 2004) and bentonite clay with Cu^{2+} and (2) the chemical reaction between the adsorbate and the adsorbent (Wang et al., 2007).

จุฬาลงกรณ์มหาวิทยาลัย

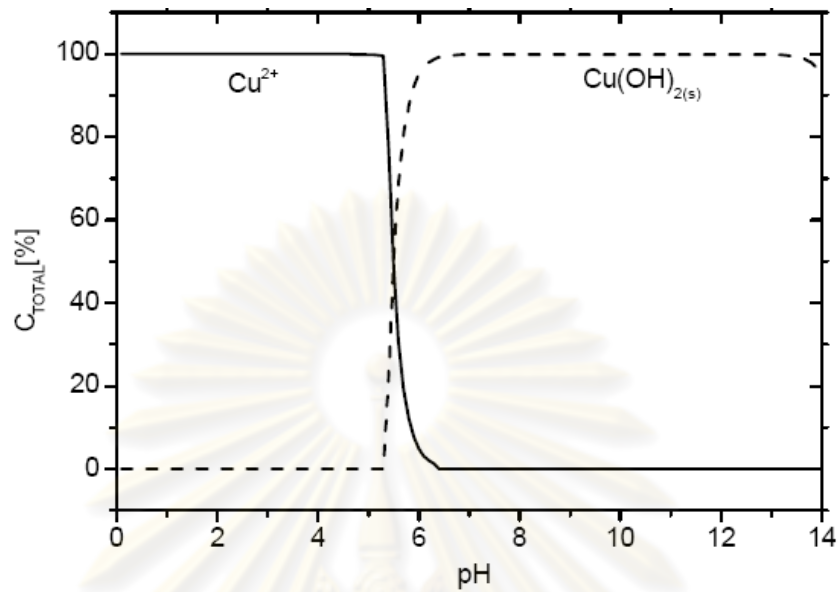


Fig. 4.10 Thermodynamic equilibrium diagram of Cu (Ayres, Davis, and Gietka, 1994; Václavíková and Gallios, 2006)

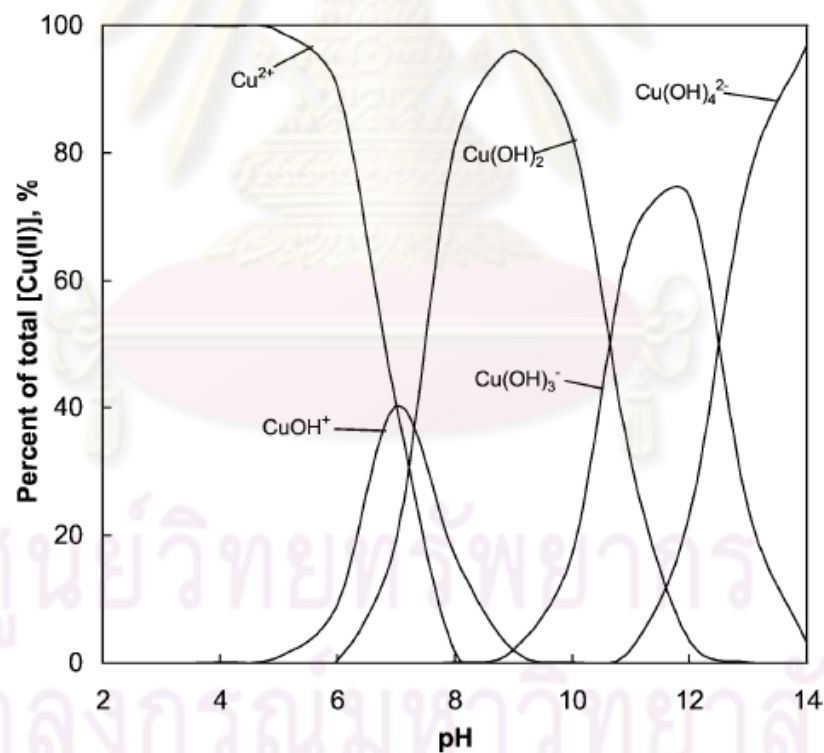


Fig. 4.11 Speciation diagram for the Cu(II)-H₂O system (Doyle and Liu, 2003; Wang, Li, and Sun, 2009)

The pH value of Cu^{2+} solution is important factor which can affect the adsorption capacity as shown in Fig. 4.12. The adsorption of Cu^{2+} at 2000 mg/L

using CCB-EGDE and CCB-ECH beads was compared. The results exhibited adsorption capacity of both CCB-EGDE and CCB-ECH beads for Cu^{2+} that the adsorption capacity increased with increase of pH from 1 to 3 and thereafter the adsorption capacity was quite stable at pH 3 and 4. At low pH condition, more amine groups were protonated followed the equation below and caused the increasing of positive charge of adsorbent beads.



In the case of weak acid solution (pH 3 and pH 4) which the quantities of H^+ were less than the amount of Cu^{2+} , Cu^{2+} still could compete with H^+ to react with NH_2 as shown in the following equation.



This phenomenon is able to occur because the electrical attraction force between the lone pair of electrons from the nitrogen atom and the divalent copper ion (Cu^{2+}) would be stronger than that between the lone pair of electrons from the nitrogen atom and monovalent proton (H^+). This phenomenon sometime was considered as ion exchange mechanism.

In the case of stronger acid solution (pH 1 and pH 2) the quantities of H^+ were much more than Cu^{2+} enhancing the protonation of amine groups of chitosan. Moreover, the Cu^{2+} adsorption to adsorbent beads was also controlled by the transport of Cu^{2+} from the bulk solution to the beads' surface before adsorption can take place. As a result, the transport of Cu^{2+} to the surface sites of R-NH_3^+ could be inhibited. And at very low pH the high electrostatic repulsion force would prevent Cu^{2+} from approaching close enough to the surface for adsorption. Hence, at very low pH condition, the adsorption capacity was reduced as shown in Fig. 4.12 Jin and Bai, 2002).

Accordingly, at low pH condition, the adsorption mechanism could be attributed to two factors. First, protonation of amine groups and the unavailability of amine groups for complexation with Cu^{2+} . Secondly, H^+ ions compete with Cu^{2+} ions to same binding site on the adsorbent (Jin and Bai 2002; Sankararamakrishnan et al., 2007).

Not only the amine groups in chitosan can react with Cu^{2+} but also hydroxyl groups from chitosan, bentonite, and crosslinking agents might react with

Cu^{2+} . The explanation for effect of pH on the clay as adsorbent could be explained by the study of Gupta and Bhattacharyya (2008) which informed that at very low pH, the amount of H^+ exceeds more than Cu^{2+} several times and the H^+ tended to cover on the surface of clay. Furthermore, it is possible that oxygen atoms on clay surface might interact with water in acidic solution forming aqua complexes as shown following



This surface charge interacts repulsively with approaching metal ions and prevents them from reaching the surface. As a result, the adsorption at low pH was reduced.

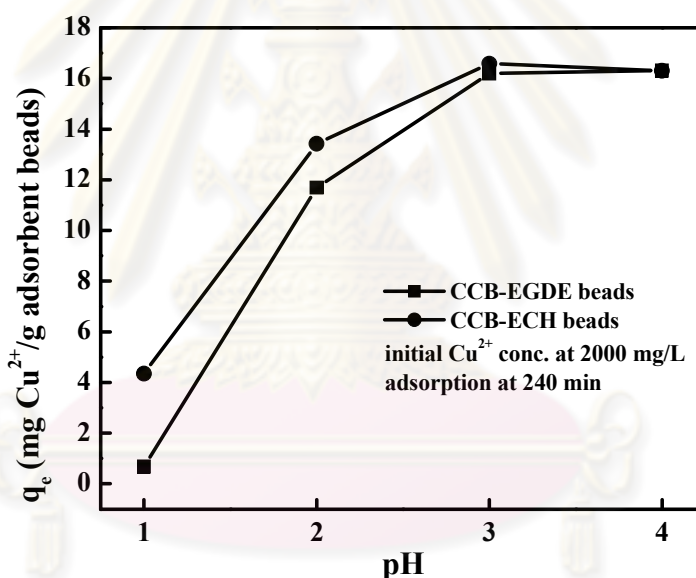


Fig. 4.12 Effect of pH values on adsorption capacity of CCB-EGDE and CCB-ECH beads for Cu^{2+}

4.11 Zeta-potential

The zeta-potential of bentonite, CCB-EGDE, CCB-ECH, and CCB-GLA beads under different solution pH values are showed in Fig. 4.13. The information from zeta-potential explains the net charge of adsorbent beads (Gecol et al., 2006) which can determine the efficiency of adsorbent to react with Cu^{2+} under various of solution pH values. The point of zero zeta-potential (point of zero charge)

of CCB-EGDE, CCB-ECH, and CCB-GLA was presented at pH_{pzc} of 1.8, 2.6, and 3.3, respectively. At point of zero charge, pH_{pzc} of composite crosslinked chitosan-bentonite beads were higher than bentonite. This change confirmed that the modified materials were successful (Gecol et al., 2006).

Naturally, the heavy metal was present in the effluent in a dilute concentration (1-100 mg/L) and at neutral or acidic pH values ($\text{pH} < 7$) (Ayres, Davis, and Gietka, 1994). At pH below 5.3, Cu^{2+} is major specie. Thus, from an electrostatic interaction point of view (Jin and Bai, 2002), the adsorption of Cu^{2+} on CCB-EGDE, CCB-ECH, and CCB-GLA beads can be enhanced at $\text{pH} > 1.8, 2.6,$ and $3.3,$ respectively. Because the adsorbent beads had the negative zeta-potential at $\text{pH} > 3.3,$ they could attract the positively charge of Cu^{2+} . This result supported the adsorption capacity of Cu^{2+} which increased with the increase of Cu^{2+} solution pH values.

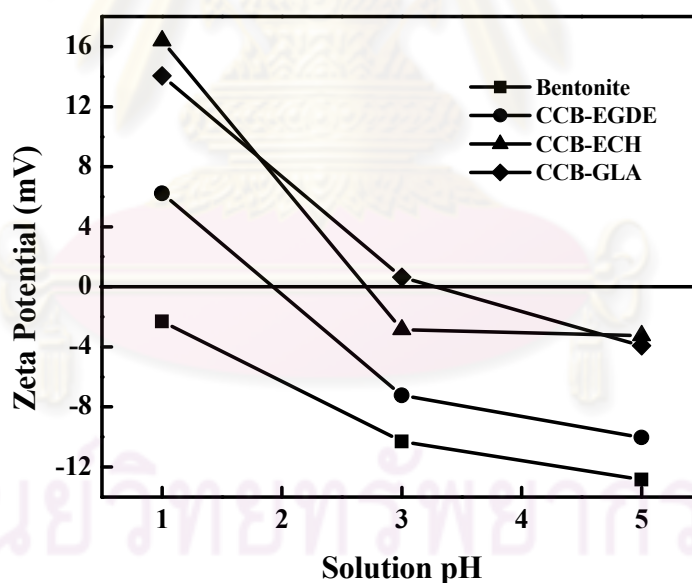


Fig. 4.13 Zeta-potential of bentonite, CCB-EDGE, CCB-ECH, and CCB-GLA beads in the solution at pH 1, 3, and 5

4.12 Column adsorption

One of expected applications for modified biosorbent in this research was to use as a filter to pretreat groundwater. Therefore, the continuous adsorption by breakthrough method was performed (Fig. 4.14). Flow rate using in the test and the result of breakthrough time can be used to scale-up the treatment unit. In order to investigate adsorption excluded mass transfer (internal and external) effect, the same retention tests was presented for the preliminary result. For this study, the effectiveness of column was mentioned from groundwater quality standards for drinking purposes of Cu which has the maximum allowable concentration at 1.5 mg/L (Pollution Control Department, 1978) and the Maximum Contaminant Level Goals (MCLG) for drinking water of Cu is at 1.3 mg/L (United States Environmental Protection Agency, 2006). The C/C_0 value calculated from water quality standard is $0.3\%C_0$. As a result, using 5 g and 10 g CCB-EGDE beads as adsorbent could provide the effectiveness until 34 hours and 40 hours, respectively, under the same retention time as shown in Fig. 4.15.

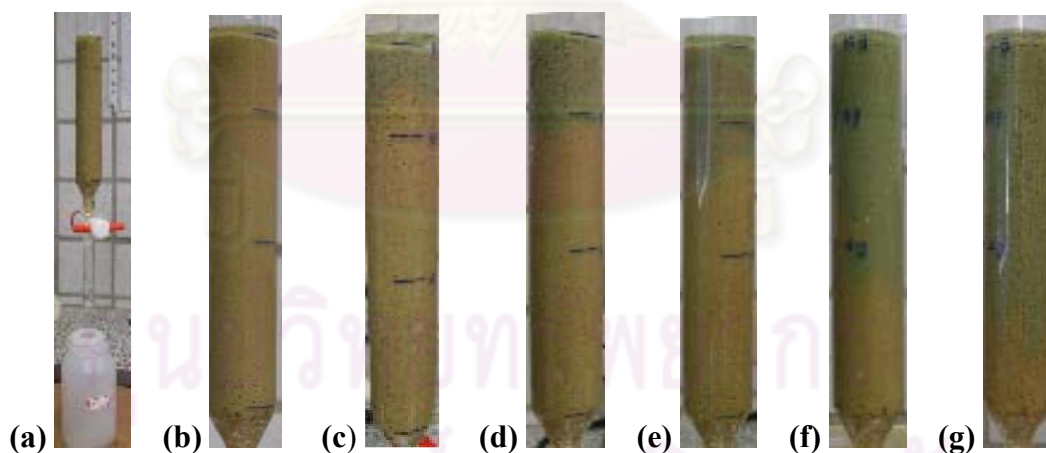


Fig. 4.14 Column adsorption in adsorption period 0, 6, 12, 24, 46, and 52 hours ((a) and (b), (c), (d), (e), (f), (g), respectively)

Consideration from the conditions between continuous adsorption in the first column (5 g CCB-EGDE beads with velocity of Cu^{2+} 0.035 cm/min) and the second column (10 g CCB-ECH beads with velocity of Cu^{2+} 0.07 cm/min), the

adsorption sites and the amount of Cu^{2+} in the second column should be 2 times higher in the first column. Then the ratio between Cu^{2+} and adsorption sites for both columns was same. As a result, the breakthrough curves should be the same pattern. However, the experimental results showed that at 34 hours, the Cu^{2+} from the first column was detected whereas the second column still had the ability to adsorb Cu^{2+} . This meant the second column exhibited the amount of adsorbed Cu^{2+} per unit of adsorbent beads more than the first column. In term of mass transfer, (presented in Fig. 4.15) the wide mass transfer zone means the much of the adsorber goes unused, and the steeper mass transfer zone means that more of the bed is used for separation (College of Engineering, University of Rhode Island, 2008). Accordingly, the unused adsorbent in the first column was more than in the second column and the adsorption in the second column was more than the first column. To learn how much CCB-EGDE beads can exclude the mass transfer, more series of adsorbent mass should be performed for example 4m:4V and 8m:8V until the patterns of breakthrough was stable even the ratio of mass to velocity was changed.

The calculated adsorption capacities from both columns were 21.94 mg/g for the first column (5 g CCB-EGDE beads) and 26.15 mg/g for the second column (10 g CCB-EGDE beads). These adsorption capacities were higher than the adsorption capacity from a batch experiment. The results from this study correlated with the studies of Pattarit (2002) and Seo et. Al. (2008) that showed the adsorption of metals ions using a column was higher than the adsorption capacity of a batch adsorption. Seo and co-worker explained that the metal ions were retained by the adsorbent mainly in the adsorption mechanism of the batch study. In contrast, the column study may have other additional retention mechanism such as surface precipitation along with adsorption.

The more adsorption capacity from column in this study might be because of the surface precipitation of Cu^{2+} . This precipitation might occur because the concentration of Cu^{2+} which flowed through column were constant providing adsorbate/adsorbent ratio in the top area of column more than other part of column. As a result, the top of column contained more amount of Cu^{2+} then the surface precipitation of Cu^{2+} at this area might take place.

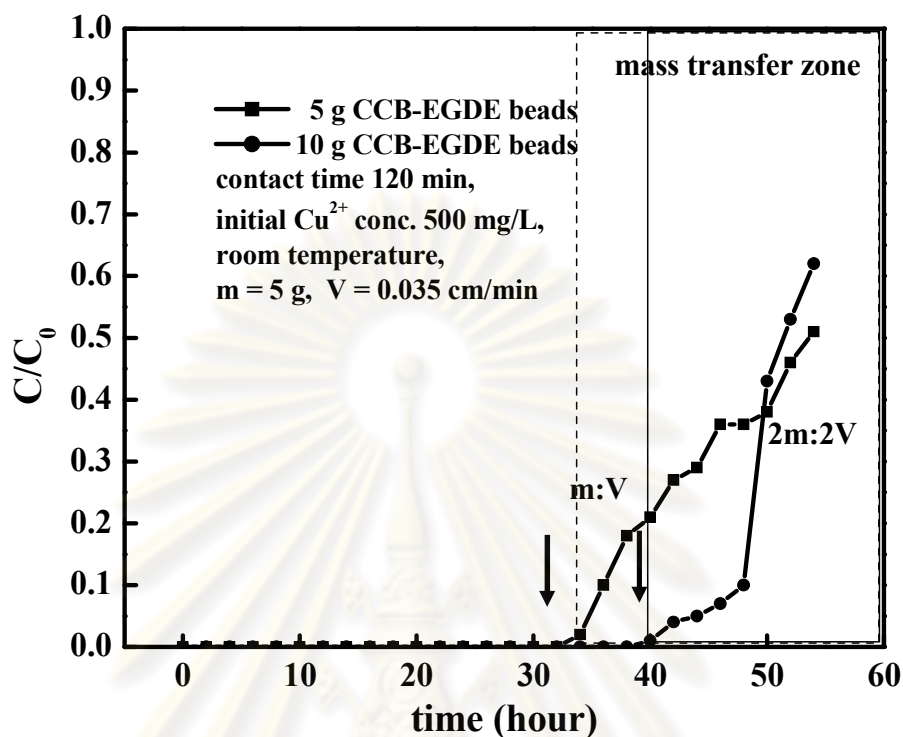


Fig. 4.15 Breakthrough curves for Cu^{2+} adsorption of CCB-EGDE beads

4.13 Morphology

4.13.1 Scanning Electron Microscopy (SEM)

The surface morphology of CCB-EGDE, CCB-ECH, and CCB-GLA beads was imaged by scanning electron microscope (SEM) and presented in Fig. 4.16 (a), (b), and (c), respectively. The results showed that all SEM images from composite crosslinked chitosan-bentonite beads have more aggregation pattern than composite non-crosslinked chitosan-bentonite (Fig. 4.3 b2). The images from SEM verified that CCB-EGDE (a) was much denser and had more coarsely grained than CCB-ECH (b) and CCB-GLA (c) beads. The patterns of crosslinked chitosan of this study agreed with the study of Chen et al. (2008) who synthesized crosslinked chitosan using ECH as crosslinking agent. The SEM of chitosan and ECH crosslinked chitosan prepared from different molar ratios of ECH/chitosan was found

that the surfaces of the crosslinked chitosan prepared with more molar ratios of ECH/chitosan were noted to have much asperity and to be more coarsely grained.

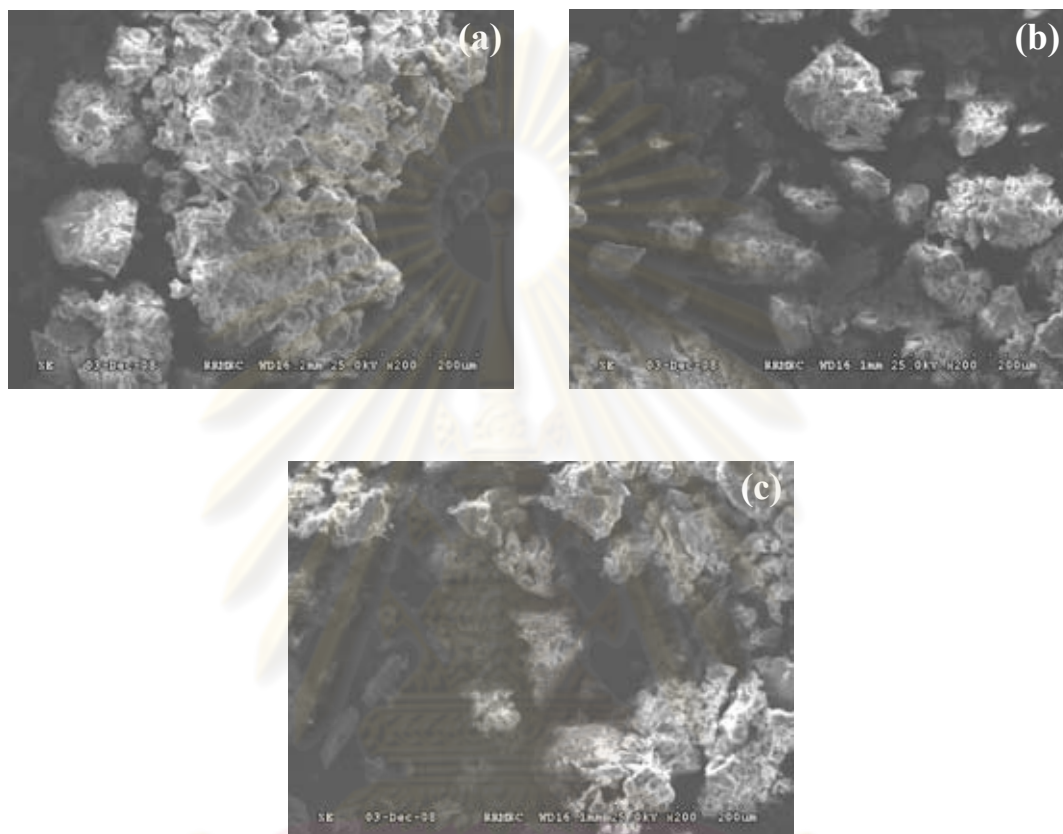


Fig. 4.16 Scanning electron microscopy (SEM) micrograph of (a) CCB-EGDE, (b) CCB-ECH, and (c) CCB-GLA beads

4.13.2 X-Ray Diffraction (XRD)

The Fig. 4.17 shows the XRD patterns of bentonite, chitosan, and composite crosslinked chitosan-bentonite beads. The shifts of XRD peaks were not observed; therefore, 2θ can not used to indicate the intercalation of biopolymer, crosslinked chitosan, as presented by the other researchers. The intercalation of chitosan between layers of clay was studied by Darder and co-worker (2003). They found that after the interaction between chitosan and clay, the XRD patterns showed the decrease of 2θ with the increase of chitosan-clay ratios. Then the change of interlayer spacing (d_{001}) in clay could be detected according to the Bragg equation,

$2d \sin \theta = \lambda$ (Zhao et al., 2004). The difference between Darder's work and this study was the chitosan:clay ratio. The chitosan:clay ratio in this study was 0.025:1 by weight which the amount of chitosan was 5 times less than used in Darder's work. The amount of chitosan might be too low to cause observable intercalations and it might be not clear to note that the interaction between chitosan and bentonite in this work was intercalation except the CCB-GLA which the intercalation might occur because the reducing of 2θ at 6° and 9° was observed. For this study, the possible explanation for change of bentonite crystallinity might be explained in term of change of XRD intensity peak heights.

The XRD intensity of the peak at the 2θ of 6.1° (Fig. 4.17) decreased after bentonite was composited with chitosan and crosslinked chitosan. This indicated that interaction between bentonite with chitosan and crosslinking agents which have the different chemical structures and molecular sizes led to the distortion of intrinsic lattice of bentonite and caused the decrease of crystallinity. The dilution of bentonite with chitosan also might cause the reduction of peak intensity. Furthermore, the distributions for crystallites can be measured by XRD because the widths of the XRD peaks broaden as crystallite size decreases (Eberl, 2002). It meant that after synthesise of composite chitosan and crosslinked chitosan with bentonite, the size of adsorbent crystallites were smaller than original size of bentonite crystal.

ศูนย์วิทยทรัพยากร
จุฬาลงกรณ์มหาวิทยาลัย

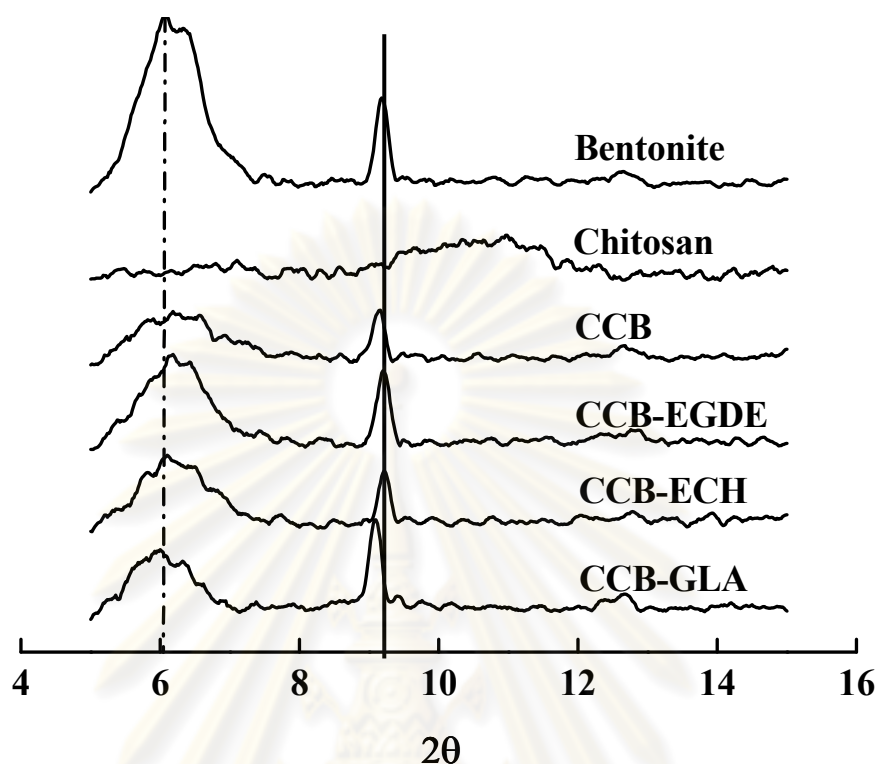


Fig. 4.17 XRD patterns of bentonite, chitosan, CCB beads, CCB-EGDE beads, CCB-ECH beads, and CCB-GLA beads

4.13.3 Nitrogen adsorption-desorption analysis

Informations from nitrogen adsorption-desorption analysis included surface area, pore volume, and average pore diameter of adsorbent beads as presented in Table 4.5. All investigations were performed at liquid nitrogen temperature. The results showed that chitosan exhibited the least surface area ($3.40 \text{ m}^2/\text{g}$) whereas bentonite contained the largest surface area ($94.28 \text{ m}^2/\text{g}$). The combination between bentonite and chitosan, CCB beads, performed the surface area between bentonite and chitosan ($48.81 \text{ m}^2/\text{g}$). The existing of ECH, EGDE, and GLA reduced the surface area of adsorbent beads in order of 38.96 , 20.18 , and $13.45 \text{ m}^2/\text{g}$, respectively. The corresponding relationship between surface area and pore volume was exhibited in the same way. Surface area decreased with the decrease of pore volume. This might be explained by the blocking of chitosan, ECH, EGDE, and GLA in bentonite pore. The similar work was studied by Youji and co-workers (2008). They discussed that the decrease of surface area of activated carbon was reasonably supposed to be the fact

that the effect of nanometer TiO₂ particles on enhancing surface area were fewer than that of its blocking. Moreover, increasing TiO₂ content performed the blocking of pore entrances. The average pore diameter of all adsorbent beads was considered to indicate the porous property. Three pore sizes of particle were classified as following, micropores has diameter less than 2 nm, macropores has diameter larger than 50 nm, and mesopores are between 2 and 50 nm (Nackos, 2006; Vrieling, 2007). From the results in Table 4.5, average pore diameters of all adsorbent beads were between 5 and 10 nm. As a result, these adsorbent beads were mesoporous material. In addition, pore size could be indicated by the plotted isotherm of experimental data from N₂ adsorption and desorption on material surface (see Fig. 4.18 and 4.19). The adsorption-desorption isotherms of N₂ on bentonite, CCB, CCB-ECH, CCB-EGDE, and CCB-GLA beads were type IV (See Fig. 4.20) which are characteristic of mesoporous adsorbent beads. The hysteresis loop was a result from capillary condensation in the mesopores and this isotherm exhibit a limited uptake at high relative pressures (Fletcher, 2008). The N₂ adsorption-desorption isotherm on chitosan showed the type II (Fig. 4.21) which indicated the physical adsorption of gases by non-porous solids but the performance of pore volume and average pore diameter on chitosan surface might noted that chitosan performed mixed micro- and meso-porosity as same as carbons which produced type II isotherms (Fletcher, 2008).

Table 4.5 Characteristic of adsorbent beads analyzed by N₂ adsorption-desorption analysis

Adsorbent beads	Surface area (m²/g)	Pore volume (m³/g)	Average pore diameter (nm)
Bentonite	94.28	0.0113	5.84
CCB	48.81	0.0061	5.02
CCB-ECH	38.96	0.0037	6.21
CCB-EGDE	20.18	0.0002	7.33
CCB-GLA	13.45	<0.0001	8.33
Chitosan	3.40	<0.0001	6.41

The surface area of adsorbents was an important factor to consider for adsorption. The surface area of chitosan was the least among all materials whereas chitosan was suggested as effective biosorbent. Likewise the surface area of composite crosslinked chitosan-bentonite were less than bentonite and composite non-

crosslinked chitosan-bentonite while it inhibited more adsorption capacity for Cu^{2+} . This might be explained by more important role of functional groups of adsorbent which perform chemisorption with Cu^{2+} in aqueous solution instead of physisorption which depends on the surface area of material.

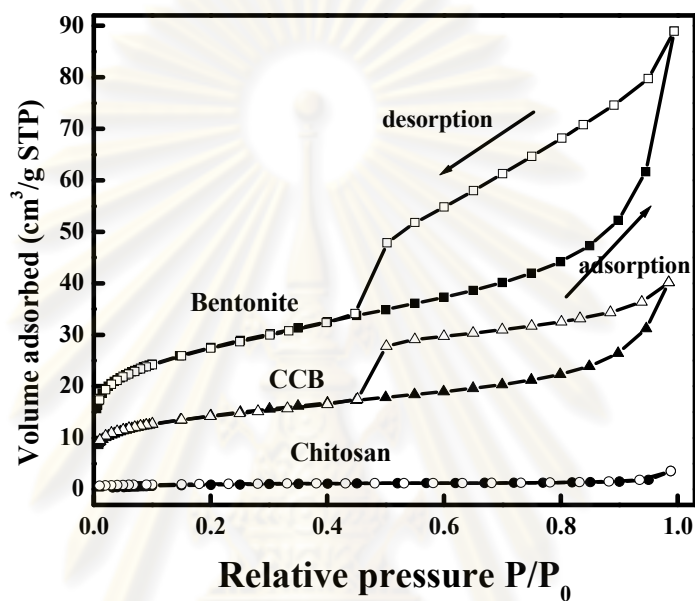
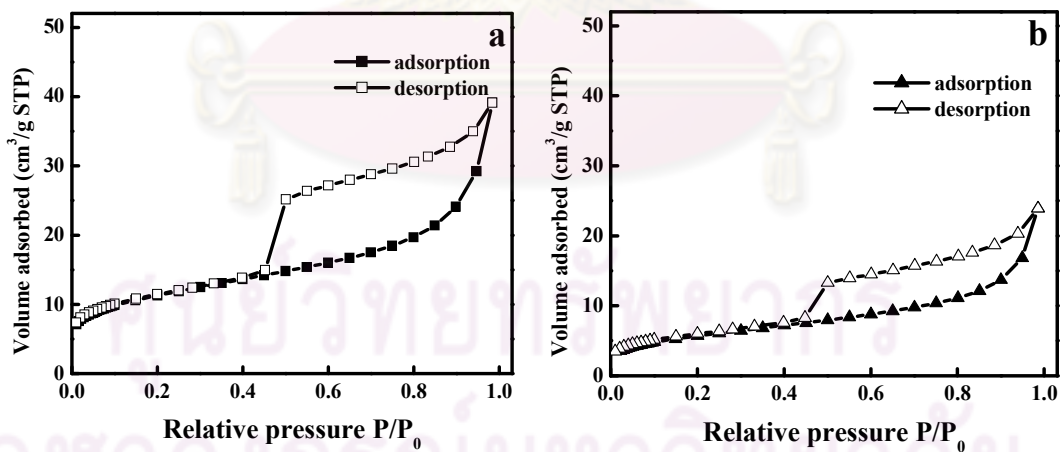


Fig. 4.18 N_2 adsorption-desorption isotherms of bentonite, CCB beads and chitosan



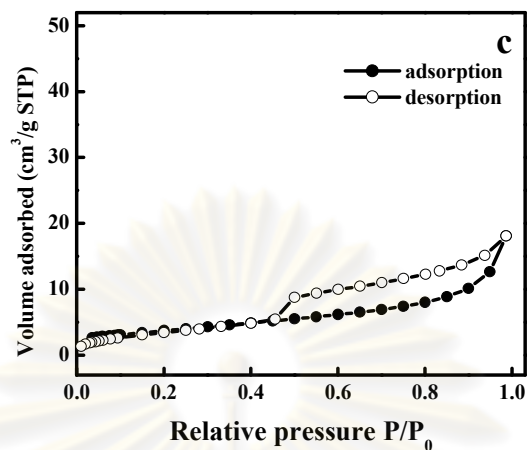


Fig. 4.19 N_2 adsorption-desorption isotherms of a. CCB-ECH, b. CCB-EGDE, and c. CCB-GLA beads

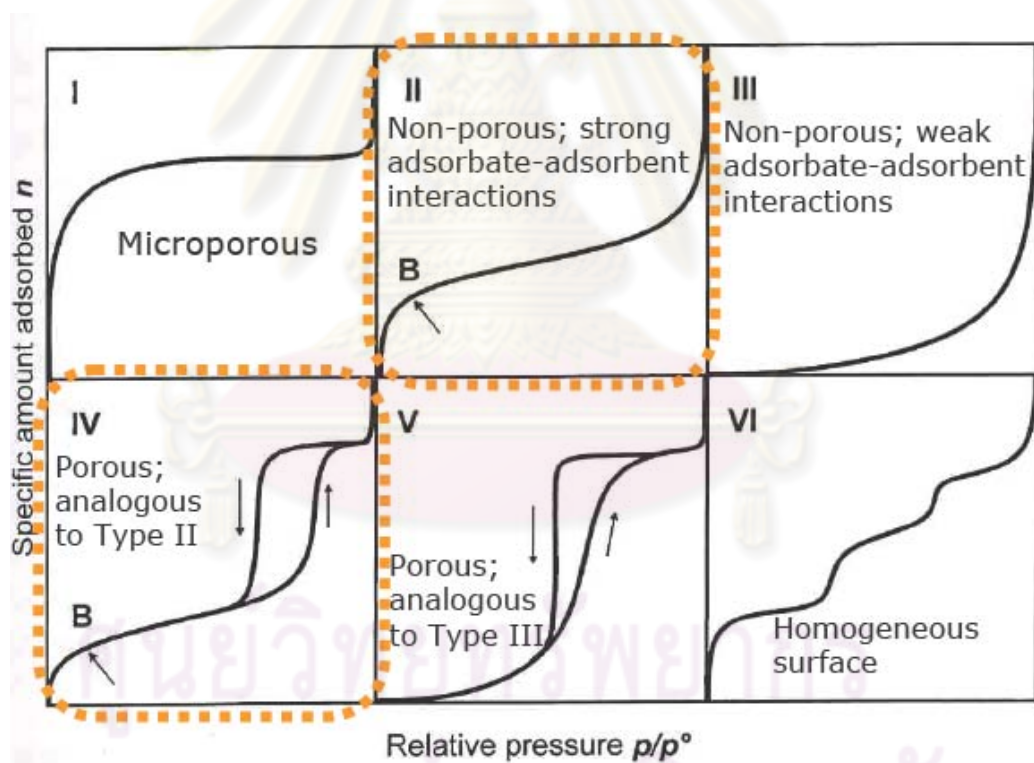


Fig. 4.20 Different isotherm shapes possible of N_2 adsorbed on solid surface (Nackos, 2006)

CHAPTER V

CONCLUSION AND RECOMMENDATIONS

5.1 Conclusion

The synthesized adsorbents using bentonite clay as supporting material presented the efficiency for Cu^{2+} adsorption more than kaolinite effecting by surface area and CEC properties. Then bentonite was selected as supporter for composite crosslinked chitosan-clay.

The adsorption capacity for Cu^{2+} of composite crosslinked chitosan-bentonite presenting in order of CCB-EGDE > CCB-ECH > CCB-GLA beads. This might be noted that more functional groups of EGDE, hydroxyl group, could bond with more chitosan molecules. The adsorption system of these three adsorbents reached the equilibrium at time 120-240 min. Under equilibrium, adsorption isotherm of CCB-EGDE and CCB-ECH beads for Cu^{2+} adsorption was fitted very well with Langmuir isotherm described monolayer coverage on homogeneous surface whereas adsorption using CCB-GLA beads fitted very well with Freundlich isotherm.

The adsorption mechanism before reach equilibrium could be explained by pseudo-second-order kinetic model (confirmed by R^2) with respected to the interaction between Cu^{2+} and adsorbent more than mass transfer.

The crosslinked adsorbents could be used under acidic solution of pH 3, enable to capture Cu^{2+} . In pH 1 solution, the desorption of Cu^{2+} from adsorbents took place with the change of adsorbents beads structure. pH was the important effects on adsorption of Cu^{2+} on all adsorbents, decrease of adsorption capacity of Cu^{2+} respected to the decrease of Cu^{2+} solution pH values. This corresponded with the results from zeta potential analysis which performed more net negative charge with the increase of solution pH supported Cu^{2+} adsorption.

The SEM performed more aggregation of composite crosslinked chitosan-bentonite. Likewise, the results from XRD pattern presented the distortion of bentonite structure after interact with crosslinked and non-crosslinked chitosan.

The surface area and pore volume of composite crosslinked chitosan-bentonite were less than non-crosslinked adsorbents measuring by N₂ adsorption-desorption analysis. These indicated that interaction between functional group of adsorbent, amine and hydroxyl groups, played an important role for adsorption more than surface area or the change of morphology of adsorbent.

Finally, the application of the synthesized biosorbent could be scaled up for wastewater treatment in term of continuous adsorption method which could reduce mass transfer in adsorption system. The further practical experiment should be performed then to scale up for useful application.

5.2 Recommendations

1. The column adsorption in this research was conducted as the initial experiment, many parameters should be also concerned such as porosity of the adsorbent beads in the packed column, the exact density of adsorbent, the regeneration of packed column, etc. The ratio between mass of adsorbent beads and velocity of metal ions solution should be increased to be 4m:4v and 8m:8V to investigate the effect of mass transfer. Then scale up the application of the adsorbent as filter for heavy metal removal from groundwater.
2. In the desorption study, the strong chelating agent such as EDTA can be used to recover the heavy metal to preserve the structure of adsorbent instead of HCl which can dissolve chitosan and reduce the adsorption capacity of adsorbent for heavy metal.
3. The synthesized adsorbent should be used to remove the other concerned heavy metal such as arsenic (As), cadmium (Cd), mercury (Hg), and mixed solution of these heavy metals to investigate the selectivity of this synthesized adsorbent.
4. The adsorption study using synthesized adsorbent should be used to remove heavy metal in the real wastewater as a pilot scale to determine the possibility for the real application.

REFERENCES

English

- Abollino, O., Giacomino, A., Malandrino, M., and Mentasti, E. Interaction of metal ions with montmorillonite and vermiculite. Appl. Clay Sci. 38 (2008): 227-236.
- Alttinişik, A., Seki, Y., and Yurdakoç, K. Preparation and characterization of chitosan/KSF biocomposite film. Polym. Compos. DOI 10.1002 (2008): pc.20651.
- Arfaoui, S., Frini-Srasra, N., and Srasra, E. Modeling of the adsorption of the chromium ion by modified clays. Desalination 222 (2008): 474-481.
- Ayari, F., Srasra, E., and Trabelsi-Ayadi, M. Characterization of bentonitic clays and their use as adsorbent. Desalination 185 (2005): 391-397.
- Ayres, D.M., Davis, A.P., and Gietka, P.M. Removing Heavy Metals from Wastewater [Online]. University of Maryland, Engineering Research Center, 1994. Available from: <http://www.mtech.umd.edu/MTES/docs/PMG%20metal%20precip%20man-1.pdf> [2009, January 26].
- Bassi, R., Prasher, S.O., Simpson, B.K. Removal of selected metal ions from aqueous solutions using chitosan flakes. Sep. Sci. Technol. 35:4 (2000): 547-560.
- Bai, R.S., and Abraham, T.E. Continuous adsorption and recovery of Cr(VI) in different types of reactors. Biotechnol. Prog. 21 (2005): 1692-1699.
- Beppu, M.M., Vieira, R.S., Aimoli, C.G., and Santana, C.C. Crosslinking of chitosan membranes using glutaraldehyde: Effect on permeability and water absorption. J. Membr. Sci. 301 (2007): 126-130.
- Berger, J., Reist, M., Mayer, J.M., Felt, O., Peppas, N.A., and Gurny, R. Structure and interaction in covalently and ionically crosslinked chitosan hydrogels for biomedical applications. Eur. J. Pharm. Biopharm. 57 (2004): 19-34.
- Bhattacharyya, K.G., and Gupta, S.S. Kaolinite and montmorillonite as adsorbents for Fe(III), Co(II) and Ni(II) in aqueous medium. Appl. Clay Sci. 41 (2008a): 1-9.

- Bhattacharyya, K.G., and Gupta, S.S. Adsorption of a few heavy metals on natural and modified kaolinite and montmorillonite: A review. Adv. Colloid Interface Sci. 140 (2008b): 114-131.
- Bhattacharyya, K.G., and Gupta, S.S. Influence of acid activation on adsorption of $i(\text{II})$ and $\text{Cu}(\text{II})$ on kaolinite and montmorillonite: Kinetic and thermodynamic study. Chem. Eng. J. 136 (2008c): 1-13.
- Bhattacharyya, K.G., and Gupta, S.S. Kaolinite, montmorillonite, and their modified derivatives as adsorbents for removal of $\text{Cu}(\text{II})$ from aqueous solution. Sep. Purif. Technol. 50 (2006): 388-397.
- Brady and Weil. The Nature and Properties of Soils. 11 th ed. New Jersey: Prentice Hall, Inc, Simon and Shuster Co., 1996.
- Chang, M.Y. and Juang, R.S. Adsorption of tannic acid, humic acid, and dyes from water using the composite of chitosan and activated clay. J. Colloid Interface Sci. 278 (2004): 18-25.
- Chen, A.H., Liu, S.C., Chen, C.Y., and Chen, C.Y. Comparative adsorption of $\text{Cu}(\text{II})$, $\text{Zn}(\text{II})$, and $\text{Pb}(\text{II})$ ions in aqueous solution on the crosslinked chitosan with epichlorohydrin. J. Harzard. Mater. 154 (2008): 184-191.
- Chiou, M.S., and Li, H.Y. Adsorption behavior of reactive dye in aqueous solution on chemical cross-linked chitosan beads. Chemosphere 50 (2003): 1095-1105.
- Chiou, M.S., and Li, H.Y. Equilibrium and kinetic modeling of adsorption of reactive dye on cross-linked chitosan beads. J. Harzard. Mater. B93 (2002): 233-248.
- College of Engineering. Adsorption (Ch 12)-Mass Transfer to an interface[Online]. University of Rhode Island. Department of Chemical Engineering, 2008. Available from: www.egr.uri.edu/che/course/che349/adsorption.pdf [2009 March 13].
- Cornell University. Zeta Potential Theory[Online]. Cornell University. Available from: www.nbtc.cornell.edu/facilities/downloads/zetasizer%20chapter%2016.pdf [2009, January 29].
- Crini, G., and Badot, P.M. Application of chitosan, a natural aminopolysaccharide, for dye removal from aqueous solutions by adsorption processes using batch studies: A review of recent literature. Prog. Polym. Sci. 33 (2008): 399-447.

- Darder, M., Colilla, M., and Riz-Hitzky, E. Biopolymer-Clay nanocomposite based on chitosan intercalated in montmorillonite. Chem. Mater. 15 (2003): 3774-3780.
- DeSutter, T.M., Pierzynski, G.M., and Baker, L.R. Flow-through and batch methods for determining calcium-magnesium and magnesium-calcium selectivity. Soil Sci. Soc. Am. J. 70 (2006): 550-554.
- Dixon, J.B., and Weed, S.B. Minerals in Soil Environments, 2 nd ed. Wisconsin: Soil Science Society of America, 1989.
- Doyle, F.M., and Liu, Z. The effect of triethylenetetraamine (Trien) on the ion flotation of Cu^{2+} and Ni^{2+} . J. Colloid Interface Sci. 258 (2003): 396-403.
- Eberl, D.D. Determination of illite crystallite thickness distributions using X-ray diffraction and the relation of thickness to crystal growth mechanisms using MudMaster, GALOPER, and associated computer programs. In Teaching Clay Science[Online]. CMS, 2002. Available from: www.clays.org/deuresources/cryssize.doc [2009, January 27].
- Eklund, P.C., and Ochoa, R. New nanophase materials and catalysts from laser pyrolysis. Center for Applied Energy Research 5 (6) (1994).
- Faust, S.D. and Aly, O.M. Chemistry of Water Treatment. 2 nd ed. Florida: CRC Press LLC, 1998.
- Fletcher, A. Porosity and Sorption Behaviour[Online]. Newcastle University, 2008. Available from: www.staff.ncl.ac.uk/a.j.fletcher/adsorption.htm [2009, January 12].
- Franca, E.F., Lins, R.D., Freitas, L.C.G., and Straatsma, T.P. Characterization of chitin and chitosan molecular structure in aqueous solution. J. Chem. Theory Comput. 4 (2008): 2141-2149
- Gecol, H., Ergican, E., and Miakatsindila, P. Biosorbent for tungsten species removal from water: Effects of co-occurring inorganic species. J. Colloid Interface Sci. 292 (2005): 344-353.
- Gecol, H., Miakatsindila, P., Ergican, E., and Hiibel, S.R. Biopolymer coated clay particles for the adsorption of tungsten from water. Desalination 197 (2006): 165-178.

- Guibal, E. Interactions of metal ions with chitosan-based sorbents: a review. Sep. Purif. Technol. 38 (2004): 43-74.
- Gupta, V.K., Rastogi, A., Saini, V.K. and Jain, N. Biosorption of copper(II) from aqueous solutions by *Spirogyra* species. J. Colloid Interface Sci. 296 (2006): 59-63.
- Gupta, S.S., and Bhattacharyya, K.G. Immobilization of Pb(II), Cd(II) and Ni(II) ions on kaolinite and montmorillonite surface from aqueous medium. J. Environ. Manage. 87 (2008): 46-48.
- Hasan, S., Krishnaiah, A., Ghosh, T.K., and Viswanath, D.S. Adsorption of divalent cadmium (Cd(II)) from aqueous solutions onto chitosan-coated perlite beads. Ind. Eng. Chem. Res. 45 (2006): 5066-5077.
- Ho, Y.S. Review of second-order models for adsorption systems. J. Hazard. Mater. B136 (2006a): 681-689.
- Ho, Y.S. Second-order kinetic model for the sorption of cadmium onto tree fern: A comparison of linear and non-linear methods. Water Res. 40 (2006b): 119-125.
- Hou, K., and Hughes, R. The effect of external mass transfer, competitive adsorption and coking on hydrogen permeation through thin Pd/Ag membranes. J. Membr. Sci. 206 (2002): 119-130.
- Hoven, V.P., Tangpasuthadol, V., Angkitpaiboon, Y., Vallapa, N., and Kiatkamjornwong, S. Surface-charged chitosan: Preparation and protein adsorption. Carbohydr. Polym. 68 (2007): 44-53.
- Inoue, K., Yoshizuka, K., and Ohto, K. Adsorptive separation of some metal ions by complexing agent types of chemically modified chitosan. Anal. Chem. Acta. 388 (1999): 209-218.
- Jin, L., and Bai, R. Mechanisms of lead adsorption on chitosan/PVA hydrogels beads. Langmuir 18 (2002): 9765-9770.
- Jurna, N.G. The pedosphere and its dynamics: A systems Approach to Soil Science. Volume 1: Introduction to soil science and soil resources. Alberta: Salman Productions, 2001.
- Kaminski, W., Tomczak, E., and Jaros., K. Interactions of metal ions sorbed on chitosan beads. Desalination 218 (2008): 281-286.

- Kasaai, M.R. A review of several reported procedure to determine the degree of N-acetylation for chitin and chitosan using infrared spectroscopy. Carbohydr. Polym. 71 (2008): 497-508.
- Kasai, N., and Kakudo, M. X-Ray Diffraction by Macromolecules. Japan: Kodansha Ltd. and Springer-Verlag Berlin Heidelberg, 2005.
- Khambhaty, Y., Mody, K., Basha, S., and Jha, B. Pseudo-second-order kinetic models for the sorption of Hg(II) onto dead biomass of marine *Aspergillus niger*: Comparison of linear and non-linear methods. Colloids Surf., A (2007), DOI:10.1016/j.colsurfa.2008.06.017.
- Khor, E. Chitin Fulfilling a Biomaterials Promise. Amsterdam: Elsevier Science, 2001.
- Kumar, K.V., Subanandam, K., Ramamurthi, V., and Sivanesan, S. Solid liquid adsorption for wastewater treatment: Principle design and operation[Online]. Anna University. Department of Chemical Engineering, 2004. Available from: www.eco-web.com/editorial/040201.html [2009, March 13].
- Kumar, M.N.V.R. A review of chitin and chitosan applications. React. Funct. Polym. 46 (2000): 1-27.
- Lee, S.H., Park, S.M. and Kin, Y. Effect of the concentration of sodium acetate (SA) on crosslinking of chitosan fiber by epichlorohydrin (ECH) in a wet spinning system. Carbohydr. Polym. 70 (2007): 53-60.
- Li, Y., Ma, M., and Wang, X. Inactivated properties of activated carbon-supported TiO₂ nanoparticles for bacteria and kinetic study. J. Environ. Sci. 20 (2008): 1527-1533.
- Lima, I.S. and Airoidi, O. A thermodynamic investigation on chitosan-divalent action interactions. Thermochim. Acta 421 (2004): 133-139.
- Lu, J.Z., Duan, X., Wo, Q., and Lian, K. Chelating efficiency and thermal, mechanical and decay resistance performances of chitosan copper complex in wood-polymer composites. Bioresour. Technol. 99 (2008): 5906-5914.
- Lu, S., and Gibb, S.W. Copper removal from wastewater using spent-grain as biosorbent. Bioresour. Technol. 99 (2008): 1509-1517.
- Masel, R.I. Principles of adsorption and reaction of solid surfaces. New York: John Wiley & Sons, INC. 1996.

- Mariano, A.F.V. Adsorption of copper (Cu²⁺) ions from aqueous solution by non-crosslinked and crosslinked chitosan-coated bentonite beads. Master's Thesis, Department of Civil Engineering College of Engineering University of the Philippines. 2008.
- Mckay, G. Use of Adsorbents for the Removal of Pollutants from Wastewaters. Florida: CRC Press, 1995.
- Monteiro, J.O.A.C., and Airoidi, C. Some thermodynamic data on copper-chitin and copper-chitosan biopolymer interactions. J. Colloid Interface Sci. 212 (1999): 212-219.
- Nackos A. Adsorption, Surface Area, and Porosity[Online]. College of Engineering and Technology. Brigham Young University, 2006. Available from: www.et.byu.edu/groups/catlabweb/Presentations/GroupPresentations/AdsorptionandSurfaceArea-Aron.pdf. [2009, February 16].
- Nayak, P.S., and Singh, B.K. Instrumental characterization of clay by XRF, XRD and FTIR. Bull. Mater. Sci. 30 (2007): 235-237.
- Ngah, W.S.W., Endud, C.S., and Mayanar, R. Removal of copper(II) ions from aqueous solution onto chitosan and cross-linked chitosan beads. React. Funct. Polym. 50 (2002): 181-190.
- Oshita, K., Oshima, M., Gao, Y.H., Lee, K.H., and Motomizu, S. Adsorption behavior of mercury and precious metals on cross-linked chitosan and the removal of ultratrace amounts of mercury in concentrated hydrochloric acid by a column treatment with corss-linked chitosan. Anal. Sci. 18 (2002): 1121-1125.
- Pollution Control Department (PCD). Water Quality Standards[Online]. Ministry of Natural Resources and Environment. Ministry of Industry, 1978. Available from: www.pcd.go.th/info_serv/en_reg_std_water01.html [2009, January 27].
- Pattarit K. Removal of lead by silica gel produced from kaolin and its immobilized thiol group. Master's Thesis, Department of Chemistry Faculty of Science Khon Khean University. 2002.
- Prashanth, K.V.H., and Tharanathan, R.N. Crosslinked chitosan – preparation and characterization. Carbohydr. Polym. 70 (2007): 53-60.

- Rocha, M.S.D., Iha, K., Faleiros, A.C., Corat, E.J., and Suárez-Iha, M.E.V. Freundlich's isotherm extended by statistical mechanics. J. Colloid Interface Sci. 185 (1997): 493-496.
- Sankararamakrishnan, N., Sharma, A.K., and Sanghi, R. Novel chitosan derivative for the removal of cadmium in the presence of cyanide from electroplating wastewater. J. Hazard. Mater. 148 (2007): 353-359.
- Scintag, Inc. Chapter 7: Basics of X-ray Diffraction[Online]. CA. U.S.A., 1999. Available from: <http://epswww.unm.edu/xrd/xrdbasics.pdf>. [2009, February, 1].
- Seo, D.C., Yu, K., Delaune, R.D. Comparison of monometal and multimetal adsorption in Mississippi River alluvial wetland sediment: Batch and column experiments. Chemosphere 73 (2008): 1757-1764.
- Sparks, D.L. Environmental Soil Chemistry. 2 nd ed. New York: Academic Press, 2003.
- Tahir, S.S and Rauf, N. Removal of cationic dye from aqueous solutions by adsorption onto bentonite clay. Chemosphere 63 (2006): 1842-1848.
- Takeo, N. Atlas of Eh-pH Diagrams: Intercomparison of thermodynamic databases [Online]. National Institute of Advanced Industrial Science and Technology. Research Center for Deep Geological Environments, 2005. Available from: <http://www.gsj.jp/GDB/openfile/files/no0419/openfile419e.pdf> [2009, January 26].
- Tan, W., Zhang, Y., Szeto, Y.S., and Liao, L. A novel method to prepare chitosan/montmorillonite nanocomposites in the presence of hydroxyl-aluminum oligomeric cations. Compos. Sci. Technol. 68 (2008): 2917-2921.
- Uzun, İ., and Güzel, F. External mass transfer studies during the adsorptions of some dyestuffs and p-nitrophenol onto chitosan from aqueous solution. Turk. J. Chem. 28 (2004): 731-740.
- United States Environmental Protection Agency. Ground water & Drinking water: Consumer Factsheet on: Copper[Online]. National Primary Drinking Water Regulations, 2006. Available from: www.epa.gov/OGWDW/contaminants/dw_contmfs/copper.html [2009, January 27].

- University of Milan. BET Technique[Online]. University of Milan. Dept. of Physical Chemistry and Electrochemistry. Available from: www.dcfce.unimi.it/bet%20globali_inglese.htm [2009, February 1].
- Václavíková, M. and Gallios, G.P. Removal of cadmium, zinc, lead and copper by sorption on leaching residue from nickel production. Acta Montanistica Slovaca 11 (2006): 393-396.
- Vasconcelos, H.L., Camargo, T.P., Goncalves, N.S., Neves, A., Lavanjeira, M.C.M., and Fávere, V.T. Chitosan crosslinked with a metal complexing agent: Synthesis, characterization and copper (II) ions adsorption. React. Funct. Polym. 68 (2008):572-579.
- Vieira, R.S., and Beppu, M.M. Mercury ion recovery using natural and crosslinked chitosan membranes. Adsorption 11 (2005): 731-736.
- Vrielink, L. BET: a Practical Approach[Online]. Faculty of Science and Technology, IMPACT. University of Twente Enschede the Netherlands, 2007. Available from: <http://cpm.tnw.utwente.nl/people/Vrielink/Techniques/BET%20presentatie%202008-final.pps>. [2009, February 1].
- Wan, M.W., Petrisor, I.G., Lai, H.T., Kim, D., and Yen, T.F. Copper adsorption through chitosan immobilized on sand to demonstrate the feasibility for in situ soil decontamination. Carbohydr. Polym. 55 (2004): 249-254.
- Wang, S.F., Shen, L., Tong, Y.J., Chen, L., Phang, I.Y., Lim, P.Q., and Liu, T.X. Biopolymer chitosan/montmorillonite nanocomposites: Preparation and characterization. Polym. Degrad. Stab. 90 (2005): 123-131.
- Wang, X.S., Li, Z.Z., and Sun, C. A comparative study of removal of Cu(II) from aqueous solution by locally low-cost materials: marine macroalgae and agricultural by-products. Desalination 235 (2009): 146-159.
- Yang, H., Sathitsuksanoh, N., Lu, Y., and Tatarchuk, B. Mass transfer study of H₂S removal from reformats with microfiber entrapped ZnO/SiO₂ sorbents for fuel cell application (II)[Online]. Auburn University. Center for Microfibrous Materials Manufacturing (CM³) Chemical Engineering Department, 2005. Available from: www.eng.auburn.edu/center/microfibrous/pubs/aiche/9.pdf [2009, January 27].

Youji, L., Mingyuan, M., Ziaohu, W., and Ziaohua, W. Inactivated properties of activated carbon-supported TiO₂ nanoparticles for bacteria and kinetic study.

J. Environ. Sci. 20 (2008): 1527-1533.

Zhao, Z., Yu, Wenzue, Liu, Y., Zhang, J., and Shao, Z. Isothermal crystallization

behaviors of nylon-6 and nylon-6/montmorillonite nanocomposite. Mater.

Lett. 58 (2004): 802-806.



ศูนย์วิทยทรัพยากร
จุฬาลงกรณ์มหาวิทยาลัย



APPENDICES

ศูนย์วิทยทรัพยากร
จุฬาลงกรณ์มหาวิทยาลัย

Appendix A

Table A-1 Final concentration (C , C_e) of Cu^{2+} using CCK and CCB beads as adsorbents in terms of time and initial Cu^{2+} concentration

contact time (min)	100 mg/L		500 mg/L		1000 mg/L		2000 mg/L	
	CCK	CCB	CCK	CCB	CCK	CCB	CCK	CCB
0	100.00	100.00	500.00	500.00	1000.00	1000.00	2000.00	2000.00
30	15.40	2.44	159.93	80.67	518.57	252.23	1516.60	926.60
60	8.14	0.93	158.63	49.27	498.63	224.63	1503.40	902.00
120	2.74	0.72	136.27	39.05	517.40	204.43	1445.60	834.93
240	1.17	0.06	94.92	22.48	461.03	144.03	1495.47	748.93
360	0.29	0.09	94.48	10.43	458.33	131.47	1492.40	770.87
720	0.00	0.06	65.07	4.93	444.40	110.47	1457.33	732.87
1440	0.00	0.03	57.70	2.25	448.70	96.67	1449.53	736.60

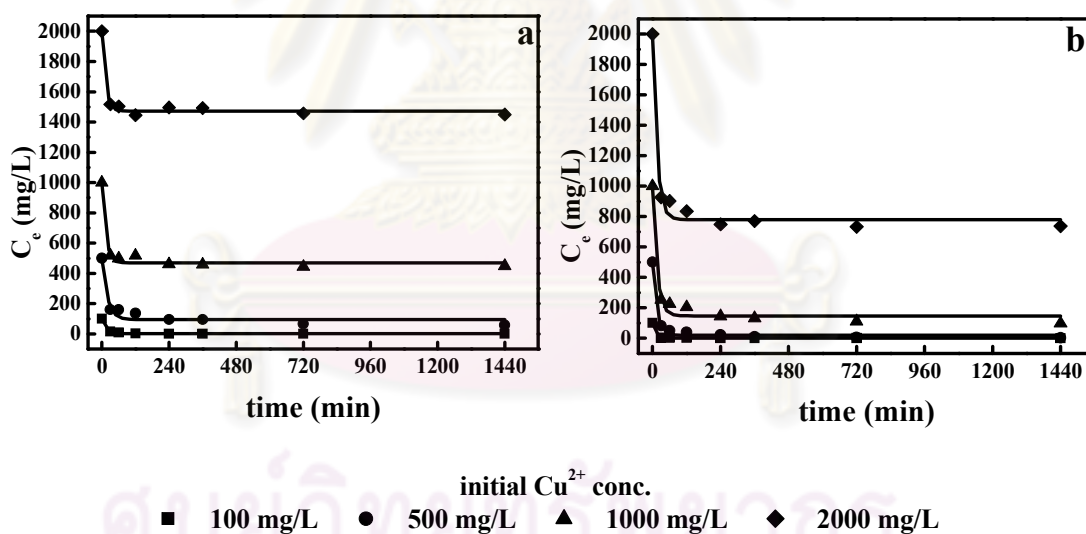


Fig. A-1 Final concentration (C , C_e) of Cu^{2+} using a. CCK and b. CCB beads as adsorbents in terms of time and initial Cu^{2+} concentration

Table A-2 Adsorption capacity (q_e) of CCK and CCB beads in terms of time and initial Cu^{2+} concentration

contact time (min)	100 mg/L		500 mg/L		1000 mg/L		2000 mg/L	
	CCK	CCB	CCK	CCB	CCK	CCB	CCK	CCB
0	0.00	0.00	0.00	0.00	0.00	0.00	0.00	0.00
30	1.02	1.17	4.08	5.03	5.78	8.97	5.80	12.88
60	1.10	1.19	4.10	5.41	6.02	9.30	5.96	13.18
120	1.17	1.19	4.36	5.53	5.79	9.55	6.65	13.98
240	1.19	1.20	4.86	5.73	6.47	10.27	6.05	15.01
360	1.20	1.20	4.87	5.87	6.50	10.42	6.09	14.76
720	1.20	1.20	5.22	5.94	6.67	10.67	6.51	15.21
1440	1.20	1.20	5.31	5.97	6.62	10.84	6.61	15.16

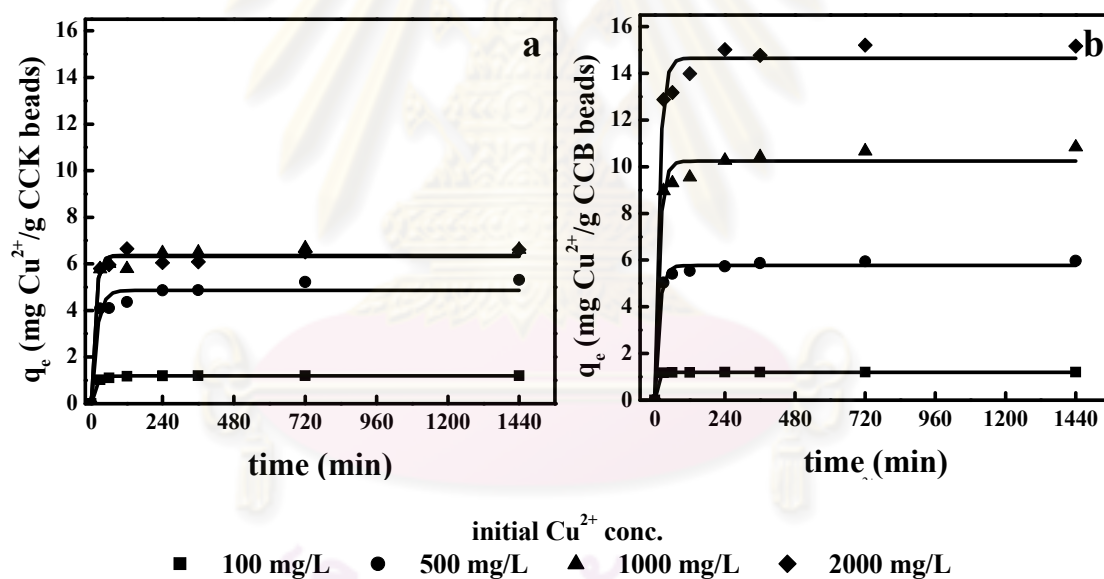


Fig. A-2 Adsorption capacity (q_e) of a. CCK and b. CCB beads in terms of time and initial Cu^{2+} concentration

Table A-3 Percent adsorption of CCK and CCB beads in terms of time and initial Cu^{2+} concentration

contact time (min)	100 mg/L		500 mg/L		1000 mg/L		2000 mg/L	
	CCK	CCB	CCK	CCB	CCK	CCB	CCK	CCB
0	0.00	0.00	0.00	0.00	0.00	0.00	0.00	0.00
30	84.60	97.56	68.01	83.87	48.14	74.78	24.17	53.67
60	91.86	99.07	68.27	90.15	50.14	77.54	24.83	54.90
120	97.26	99.28	72.75	92.19	48.26	79.56	27.72	58.25
240	98.83	99.94	81.02	95.50	53.90	85.60	25.23	62.55
360	99.71	99.91	81.10	97.91	54.17	86.85	25.38	61.49
720	100.00	99.94	86.99	99.01	55.56	88.95	27.13	63.36
1440	100.00	99.97	88.46	99.55	55.13	90.33	27.52	63.17

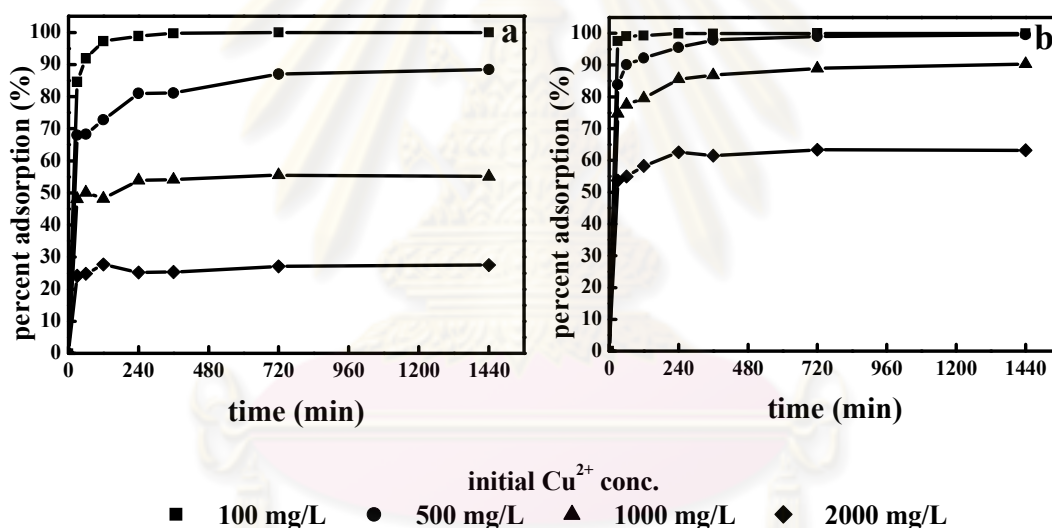


Fig. A-3 Percent adsorption of a. CCK and b. CCB beads in terms of time and initial Cu^{2+} concentration

Table A-4 Final concentration (C , C_e) of Cu^{2+} using CCB-EGDE, CCB-ECH and CCB-GLA beads as adsorbents in terms of time and initial Cu^{2+} concentration

contact time (min)	100 mg/L			500 mg/L			1000 mg/L			2000 mg/L		
	CCB-EGDE	CCB-ECH	CCB-GLA	CCB-EGDE	CCB-ECH	CCB-GLA	CCB-EGDE	CCB-ECH	CCB-GLA	CCB-EGDE	CCB-ECH	CCB-GLA
0	100.00	100.00	100.00	500.00	500.00	500.00	1000.00	1000.00	1000.00	2000.00	2000.00	2000.00
30	0.68	1.77	41.64	27.05	38.13	303.17	141.33	175.72	686.17	693.80	728.27	1526.40
60	0.27	0.27	35.20	8.13	10.19	294.47	113.03	150.57	662.67	652.93	719.60	1508.20
120	0.05	0.06	34.43	3.77	14.54	300.33	57.20	112.02	685.83	571.80	690.00	1534.20
240	0.05	0.04	31.28	1.53	1.43	279.40	45.33	77.03	665.17	567.93	633.93	1527.33
360	0.05	0.04	30.77	2.03	1.62	278.00	40.20	69.60	629.50	587.87	615.87	1513.33
720	0.03	0.03	27.71	0.68	0.36	259.43	41.50	54.48	623.50	549.40	567.53	1427.80
1440	0.06	0.03	26.94	1.40	0.26	245.07	23.13	42.32	612.00	534.40	547.80	1375.33

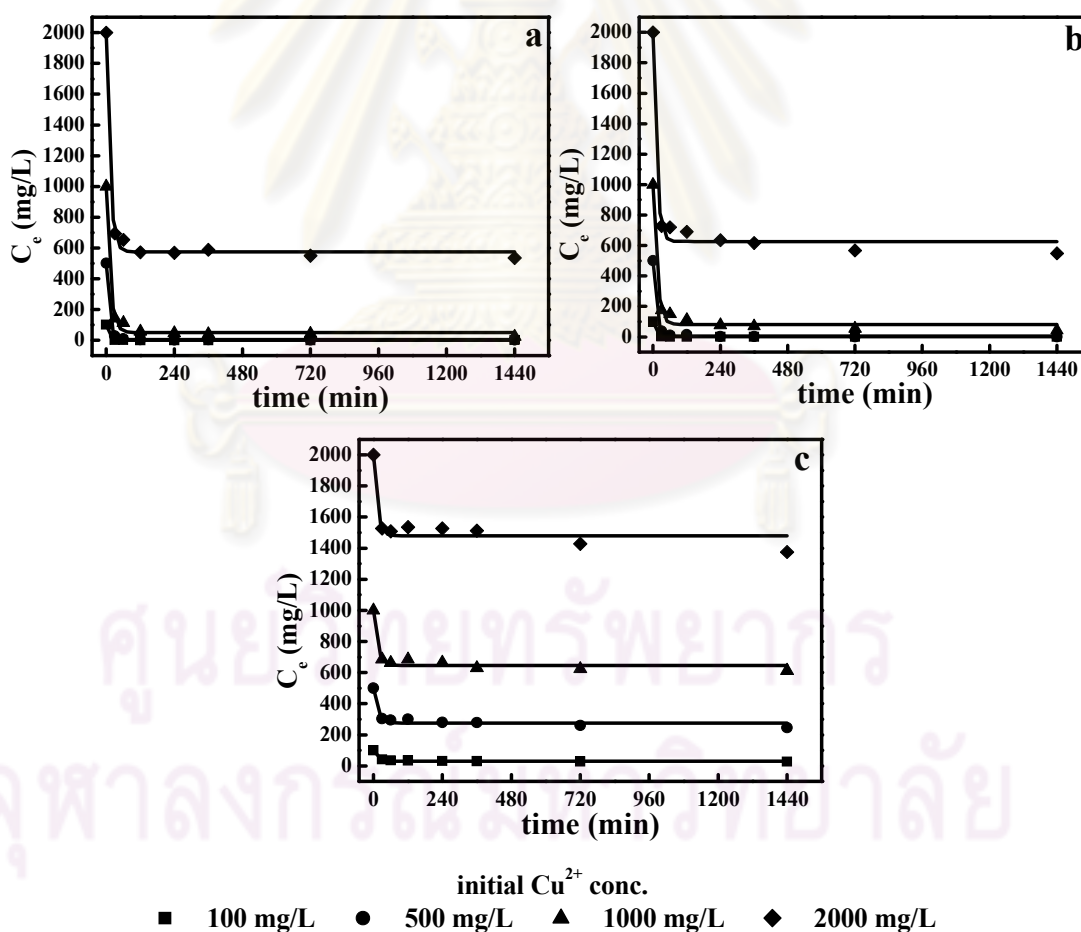


Fig. A-4 Final concentration (C , C_e) of Cu^{2+} using a. CCB-EGDE, b. CCB-ECH, and c. CCB-GLA beads as adsorbents in terms of time and initial Cu^{2+} concentration

Table A-5 Adsorption capacity (q_e) of CCB-EGDE, CCB-ECH, and CCB-GLA beads in terms of time and initial Cu^{2+} concentration

contact time (min)	100 mg/L			500 mg/L			1000 mg/L			2000 mg/L		
	CCB-EGDE	CCB-ECH	CCB-GLA	CCB-EGDE	CCB-ECH	CCB-GLA	CCB-EGDE	CCB-ECH	CCB-GLA	CCB-EGDE	CCB-ECH	CCB-GLA
0	0.00	0.00	0.00	0.00	0.00	0.00	0.00	0.00	0.00	0.00	0.00	0.00
30	1.19	1.18	0.70	5.68	5.54	2.36	10.30	9.89	3.77	15.67	15.26	5.68
60	1.20	1.20	0.78	5.90	5.88	2.47	10.64	10.19	4.05	16.16	15.36	5.90
120	1.20	1.20	0.79	5.95	5.83	2.40	11.31	10.66	3.77	17.14	15.72	5.59
240	1.20	1.20	0.82	5.98	5.98	2.65	11.46	11.08	4.02	17.18	16.36	5.67
360	1.20	1.20	0.83	5.98	5.98	2.66	11.03	11.16	4.45	16.94	16.61	5.84
720	1.20	1.20	0.87	5.99	6.00	2.89	11.37	11.35	4.52	17.41	17.19	6.87
1440	1.20	1.20	0.88	5.98	6.00	3.06	11.72	11.49	4.66	17.59	17.43	7.50

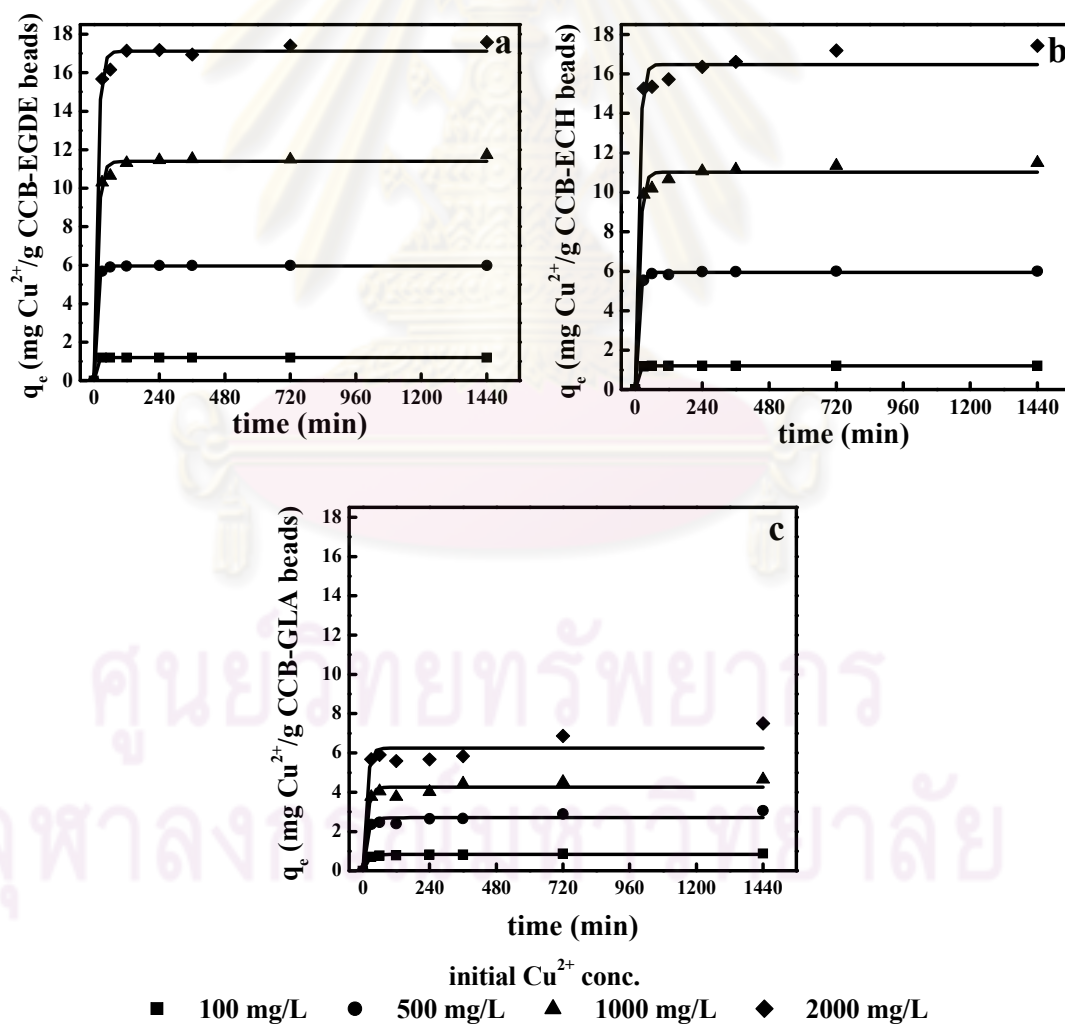


Fig. A-5 Adsorption capacity (q_e) of a. CCB-EGDE, b. CCB-ECH, and c. CCB-GLA beads in terms of time and initial Cu^{2+} concentration

Table A-6 Percent adsorption of CCB-EGDE, CCB-ECH, and CCB-GLA beads in terms of time and initial Cu^{2+} concentration

contact time (min)	100 mg/L			500 mg/L			1000 mg/L			2000 mg/L		
	CCB-EGDE	CCB-ECH	CCB-GLA	CCB-EGDE	CCB-ECH	CCB-GLA	CCB-EGDE	CCB-ECH	CCB-GLA	CCB-EGDE	CCB-ECH	CCB-GLA
0	0.00	0.00	0.00	0.00	0.00	0.00	0.00	0.00	0.00	0.00	0.00	0.00
30	99.32	98.23	58.36	94.59	92.37	39.37	85.87	82.43	31.38	65.31	63.59	23.68
60	99.73	99.73	64.8	98.37	97.96	41.11	88.70	84.94	33.73	67.35	64.02	24.59
120	99.95	99.94	65.57	99.25	97.09	39.93	94.28	88.80	31.42	71.41	65.5	23.29
240	99.95	99.96	68.72	99.69	97.71	44.12	95.47	92.30	33.48	71.60	68.3	23.63
360	99.95	99.96	69.23	99.59	99.68	44.4	95.98	93.04	37.05	70.61	69.21	24.33
720	99.97	99.97	72.29	99.86	99.93	48.11	95.85	94.55	37.65	72.53	71.62	28.61
1440	99.94	99.97	73.06	99.72	99.95	50.99	97.69	95.77	38.8	73.28	72.61	31.23

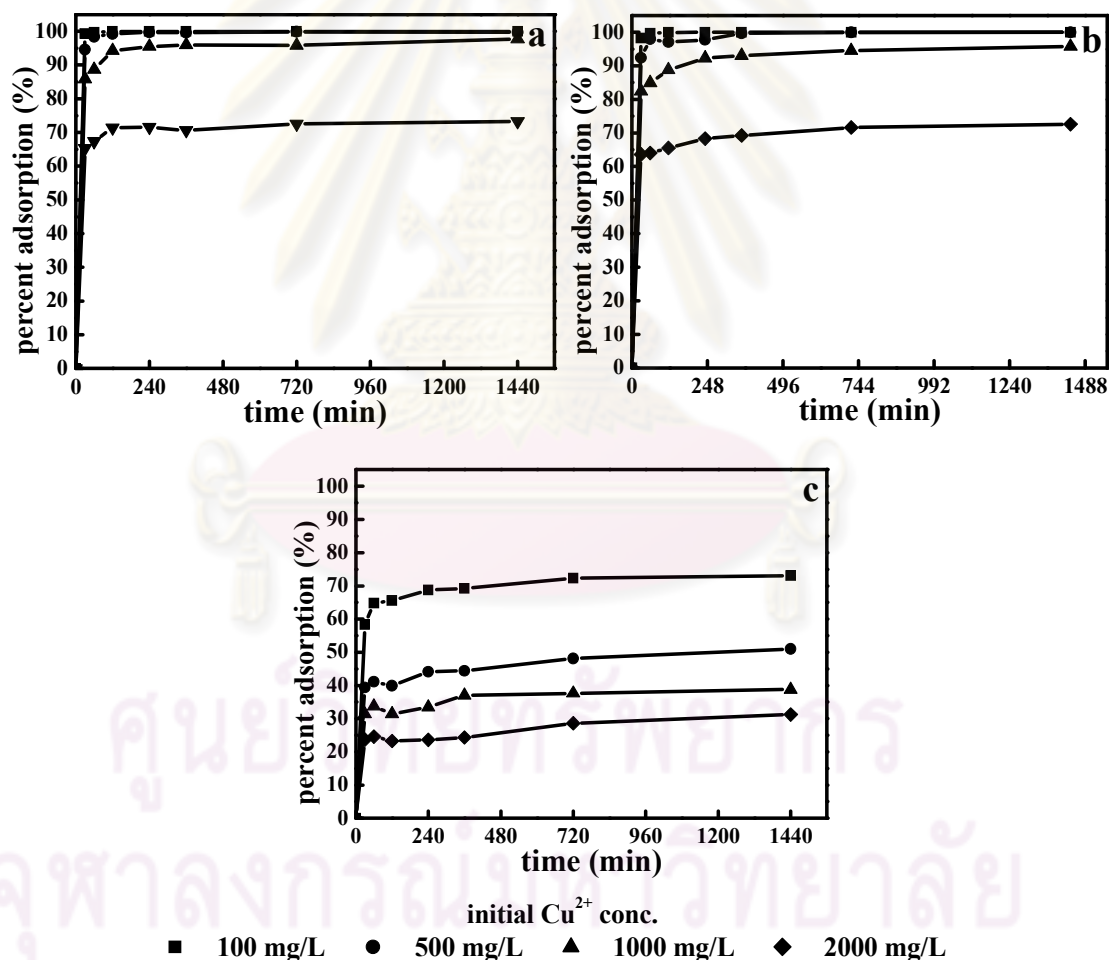


Fig. A-6 Percent adsorption of a. CCB-EGDE, b. CCB-ECH, and c. CCB-GLA beads in terms of time and initial Cu^{2+} concentration

Table A-7 Adsorption isotherm constants and correlation coefficient (R^2) of composite crosslinked chitosan-bentonite

Adsorbents	<i>Langmuir Isotherm</i>				<i>Freundlich Isotherm</i>		
	R^2	K_L (L/g)	b (L/mg)	C_{\max} (mg/g)	R^2	K_F	n
CCB-EGDE	0.996	45.228	4.299	10.52	0.953	4.150	3.89
CCB-ECH	0.998	44.623	3.799	11.75	0.932	4.311	4.13
CCB-GLA	0.984	0.044	0.011	4.17	0.999	0.152	1.89

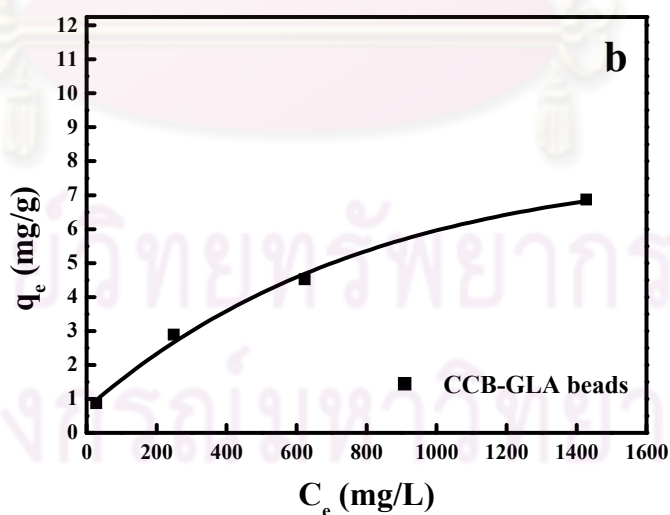
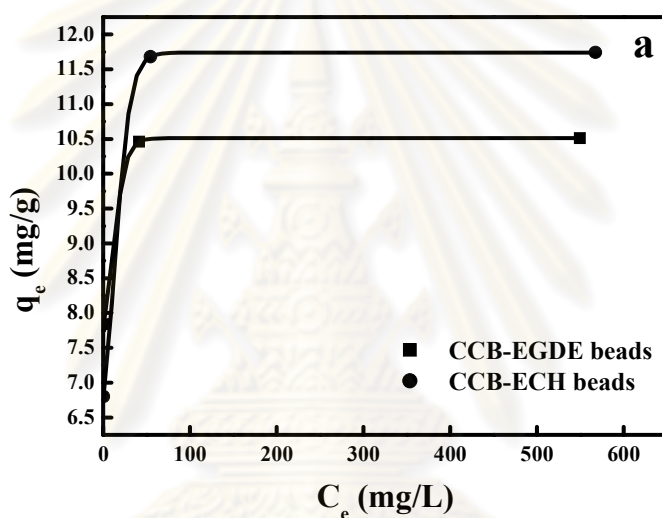
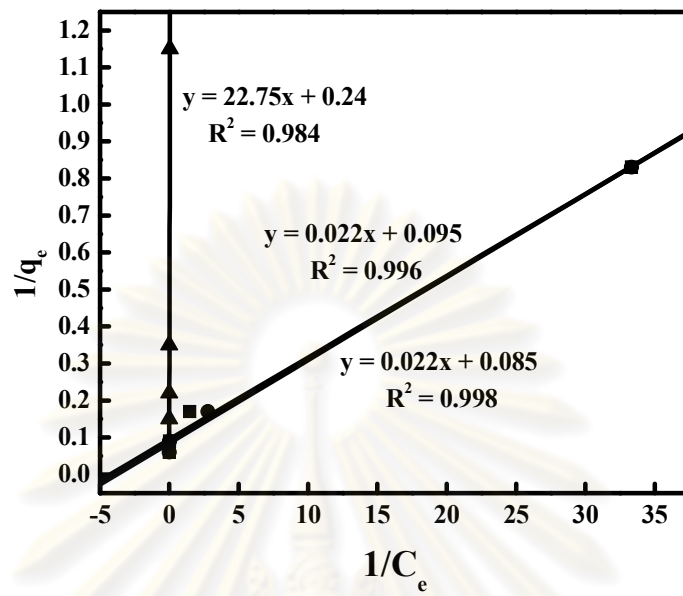
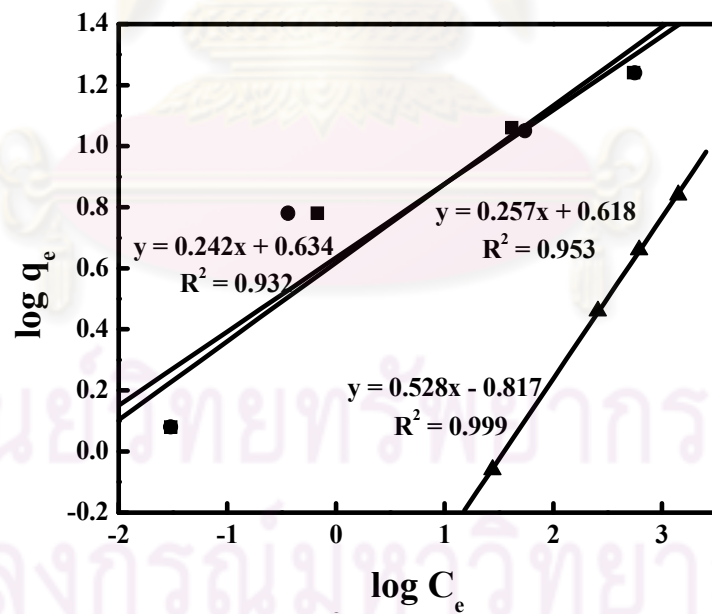


Fig. A-7 Adsorption isotherm of Cu^{2+} adsorbed on a. CCB-EGDE and CCB-ECH beads and b. CCB-GLA beads



■ CCB-EGDE beads ● CCB-ECH beads ▲ CCB-GLA beads

Fig. A-8 Linear plots of Langmuir isotherm of Cu^{2+} adsorbed on a. CCB-EGDE, b. CCB-ECH, and c. CCB-GLA beads



■ CCB-EGDE beads ● CCB-ECH beads ▲ CCB-GLA beads

Fig. A-9 Linear plots of Freundlich isotherm of Cu^{2+} adsorbed on a. CCB-EGDE, b. CCB-ECH, and c. CCB-GLA beads

Table A-8 Pseudo-first- and pseudo-second-order kinetic constants and correlation coefficient (R^2) for adsorption of Cu^{2+} adsorbed on CCB-EGDE, CCB-ECH, and CCB-GLA beads

Adsorbents	Initial Cu^{2+} conc. (mg/L)	Pseudo-first-order kinetic			Pseudo-second-order kinetic		
		R^2	k_1 (L/min)	q_e (mg/g)	R^2	k_2 (g/mg min)	q_e (mg/g)
CCB-EGDE	100	NA	NA	NA	NA	NA	NA
	500	0.910	-0.041	2.208	0.999	0.111	6.020
	1000	0.927	-0.019	3.926	1.000	0.019	11.671
	2000	0.981	-0.048	12.531	0.999	0.016	17.467
CCB-ECH	100	NA	NA	NA	NA	NA	NA
	500	0.778	-0.028	1.941	1.000	0.063	6.034
	1000	0.879	-0.024	5.272	1.000	0.015	11.315
	2000	0.788	-0.023	6.026	0.999	0.014	16.589
CCB-GLA	100	0.880	-0.026	0.403	1.000	0.209	0.838
	500	0.688	-0.016	1.024	0.998	0.052	2.696
	1000	0.595	-0.006	1.415	0.996	0.018	4.463
	2000	0.595	-0.009	1.129	0.999	0.089	5.818

NA: not available

ศูนย์วิทยทรัพยากร
จุฬาลงกรณ์มหาวิทยาลัย

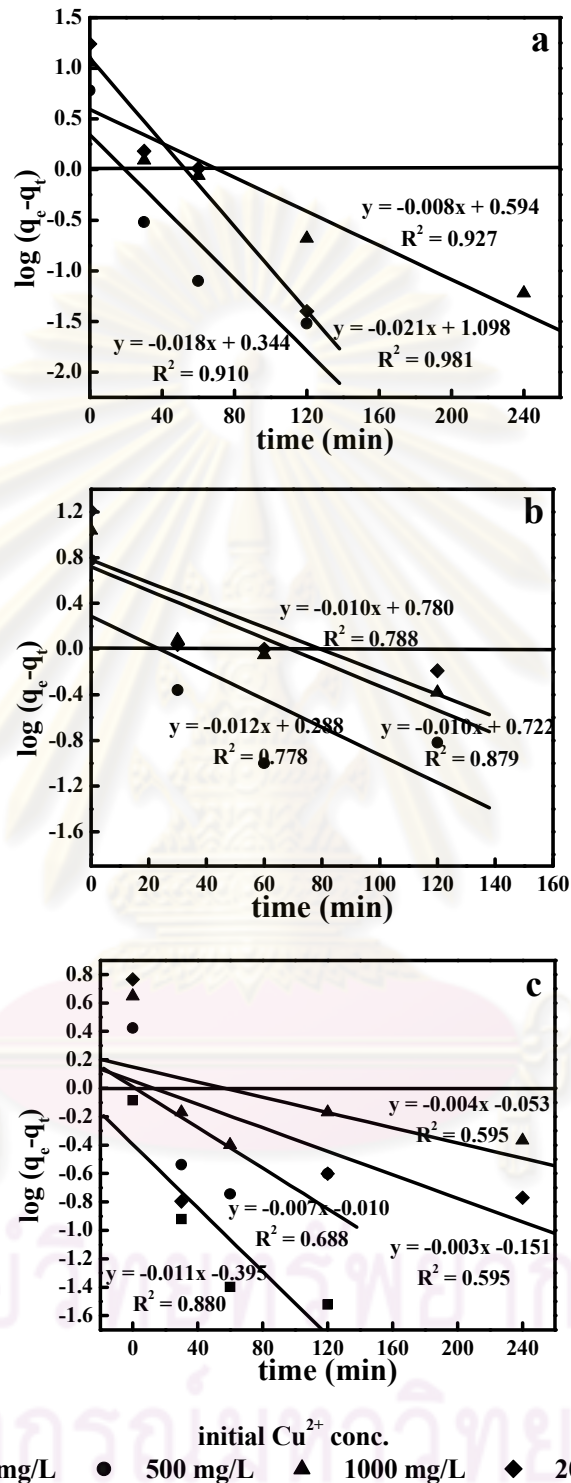
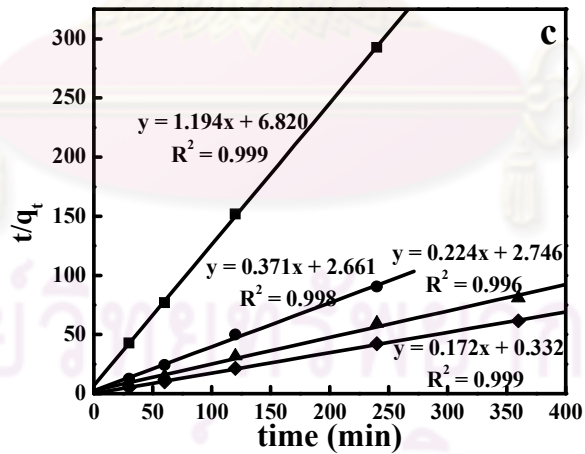
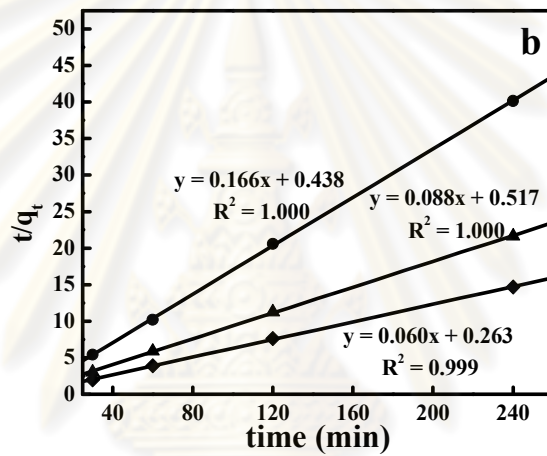
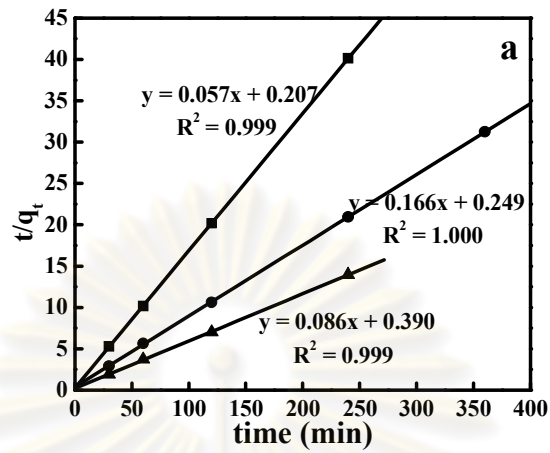


Fig. A-10 Linear plots of pseudo-first-order kinetic adsorption of Cu^{2+} adsorbed on a. CCB-EGDE, b. CCB-ECH, and c. CCB-GLA beads



initial Cu^{2+} conc.
 ■ 100 mg/L ● 500 mg/L ▲ 1000 mg/L ◆ 2000 mg/L

Fig. A-11 Linear plots of pseudo-second-order kinetic adsorption of Cu^{2+} adsorbed on
 a. CCB-EGDE, b. CCB-ECH, and c. CCB-GLA beads

Table A-9 Percent desorption of Cu^{2+} from CCB-EGDE and CCB-ECH beads using deionized water pH 7 and acid solution at pH 1 and pH 3 at equilibrium contact time (240 min)

Adsorbents beads	Initial Cu^{2+} conc. (mg/L)	% desorption		
		pH 1	pH 3	pH 7
CCB-EGDE	100	95.05	0.00	0.00
	500	92.71	0.00	0.00
	1000	99.54	0.66	0.16
	2000	99.12	4.53	0.09
CCB-ECH	100	76.99	0.14	0.03
	500	82.61	0.01	0.15
	1000	85.52	0.20	0.32
	2000	89.39	2.64	3.06

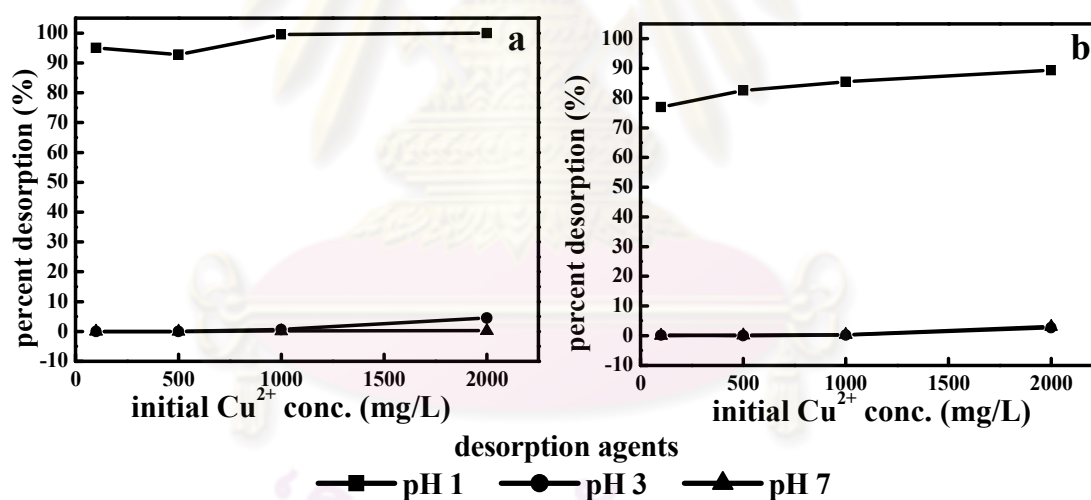


Fig. A-12 Percent desorption of Cu^{2+} from a. CCB-EGDE and b. CCB-ECH beads using desorption agents pH 1, 3, and 7

Table A-10 Regeneration study of Cu^{2+} on CCB-EGDE and CCB-ECH beads after desorbed in deionized water pH 7 and acid solution pH 1 and pH 3 at equilibrium contact time (240 min)

Adsorbent beads	pH of desorption agents	Parameters	Initial Cu^{2+} concentration (mg/L)			
			100	500	1000	2000
CCB-EGDE	1	C_e (mg/L)	93.95	498.75	998.03	2002.67
		q_e (mg/g)	0.07	0.04	0.02	0.00
		Percent adsorption (%)	2.02	0.65	0.20	0.00
	3	C_e (mg/L)	0.01	26.40	390.85	1519.00
		q_e (mg/g)	1.20	5.68	7.31	5.77
		Percent adsorption (%)	99.99	94.72	60.92	24.05
	7	C_e (mg/L)	0.01	16.42	324.57	1430.67
		q_e (mg/g)	1.20	5.80	8.10	6.83
		Percent adsorption (%)	99.99	96.72	67.54	28.47
CCB-ECH	1	C_e (mg/L)	57.11	363.37	806.33	1749.73
		q_e (mg/g)	0.51	1.64	2.32	3.00
		Percent adsorption (%)	42.89	27.33	19.37	12.51
	3	C_e (mg/L)	0.01	19.88	297.95	1334.33
		q_e (mg/g)	1.20	5.76	8.42	7.99
		Percent adsorption (%)	99.99	96.02	70.21	33.28
	7	C_e (mg/L)	0.01	16.15	328.60	1354.20
		q_e (mg/g)	1.20	5.81	8.06	7.75
		Percent adsorption (%)	99.99	96.77	67.14	32.29

ศูนย์วิทยทรัพยากร
จุฬาลงกรณ์มหาวิทยาลัย

Table A-11 Final concentration (C_e) of Cu^{2+} on CCB-EGDE and CCB-ECH beads from effect of pH studied at equilibrium contact time (240 min) and different initial Cu^{2+} concentration

Adsorbent beads	pH of Cu^{2+} solution	C_e (mg/L) from initial Cu^{2+} conc.			
		100 (mg/L)	500 (mg/L)	1000 (mg/L)	2000 (mg/L)
CCB-EGDE	1	84.5900	466.1250	968.7500	1943.6000
	2	0.4590	60.7250	588.0500	1025.9000
	3	0.0000	0.0500	104.4500	650.6000
	4	0.0000	1.9200	89.2500	640.7000
CCB-ECH	1	76.9867	402.3333	838.5000	1637.9333
	2	9.6497	401.2500	537.9000	881.6000
	3	0.0403	161.8000	84.2000	617.7333
	4	0.0370	1.5500	95.7333	641.1333

Table A-12 Adsorption capacity (q_e) of Cu^{2+} on CCB-EGDE and CCB-ECH beads from effect of pH studied at equilibrium contact time (240 min) and different initial Cu^{2+} concentration

Adsorbent beads	pH of Cu^{2+} solution	q_e (mg/g) from initial Cu^{2+} conc.			
		100 (mg/L)	500 (mg/L)	1000 (mg/L)	2000 (mg/L)
CCB-EGDE	1	0.1850	0.4060	0.3750	0.6770
	2	1.1940	5.2710	4.9430	11.6890
	3	1.2000	5.9990	10.7460	16.1920
	4	1.2000	5.9760	10.9280	16.3110
CCB-ECH	1	0.2762	1.1719	1.9378	4.3446
	2	1.0841	1.1849	5.8738	13.4208
	3	1.1995	4.0580	10.9890	16.5865
	4	1.1995	5.9812	10.8506	16.3055

Table A-13 Percent adsorption of Cu^{2+} on CCB-EGDE and CCB-ECH beads from effect of pH studied at equilibrium contact time (240 min) and different initial Cu^{2+} concentration

Adsorbent beads	pH of Cu^{2+} solution	Percent adsorption (%) from initial Cu^{2+} conc.			
		100 (mg/L)	500 (mg/L)	1000 (mg/L)	2000 (mg/L)
CCB-EGDE	1	15.410	6.775	3.125	2.820
	2	99.000	87.855	41.195	48.705
	3	100.000	99.995	89.555	67.470
	4	100.000	99.616	91.075	67.965
CCB-ECH	1	23.013	19.533	16.150	18.103
	2	90.350	19.750	46.210	55.920
	3	99.960	67.640	91.580	69.113
	4	99.963	99.690	90.427	67.943

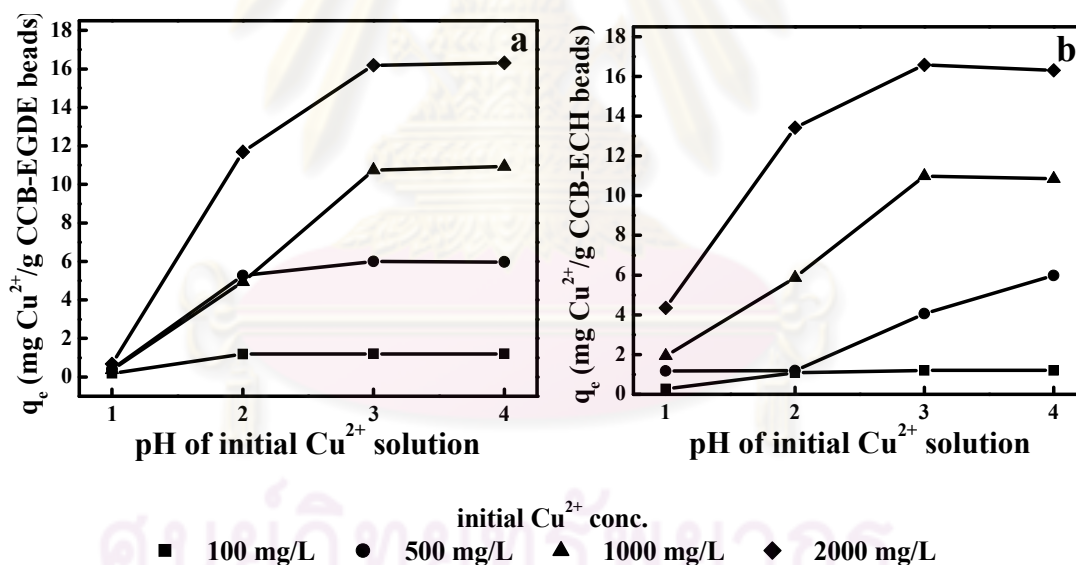
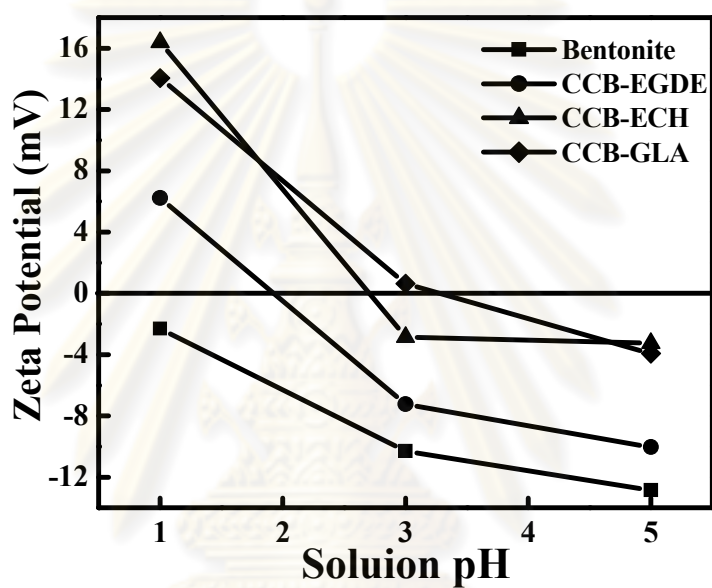


Fig. A-13 Adsorption capacity (q_e) of Cu^{2+} on a. CCB-EGDE and b. CCB-ECH beads from effect of pH studied at equilibrium contact time (240 min) and different initial Cu^{2+} concentration

Table A-14 Zeta-potential (mV) of adsorbents in the different solution pH values

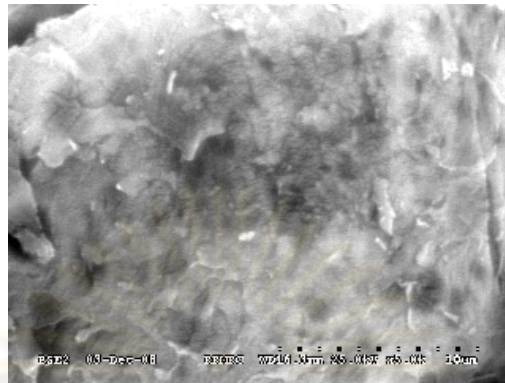
pH of solution	Bentonite	CCB-EGDE beads	CCB-ECH beads	CCB-GLA beads
1	-2.300	6.220	16.400	14.050
3	-10.30	-7.230	-2.850	0.632
5	-12.85	-10.030	-3.200	-3.925

**Fig. A-14** Zeta-potential (mV) of adsorbents in the different solution pH values

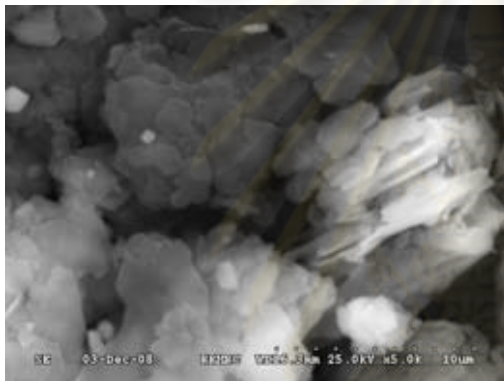
ศูนย์วิทยทรัพยากร
จุฬาลงกรณ์มหาวิทยาลัย

Table A-15 Flow through of Cu^{2+} 500 mg/L on 5 and 10 g of CCB-EGDE beads in packed column

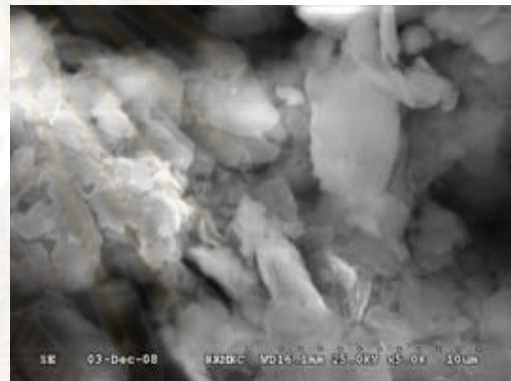
Time (hour)	5 g CCB-EGDE beads			10 g CCB-EGDE beads		
	C_c (mg/L)	C/C_0	q_c (mg/g)	C_c (mg/L)	C/C_0	q_c (mg/g)
1	0.0080	0.0000	3.00	0.0060	0.0000	1.50
2	0.0000	0.0000	3.00	0.0160	0.0000	1.50
3	0.0000	0.0000	3.00	0.0120	0.0000	1.50
4	0.0000	0.0000	3.00	0.0240	0.0000	1.50
5	0.0000	0.0000	3.00	0.0220	0.0000	1.50
6	0.0000	0.0000	3.00	0.0180	0.0000	1.50
7	0.0000	0.0000	3.00	0.0260	0.0001	1.50
8	0.0000	0.0000	3.00	0.0000	0.0000	1.50
9	0.0000	0.0000	3.00	0.0000	0.0000	1.50
10	0.0020	0.0000	3.00	0.0060	0.0000	1.50
11	0.0000	0.0000	3.00	1.4950	0.0030	1.50
12	0.0000	0.0000	3.00	0.0240	0.0000	1.50
13	0.0000	0.0000	3.00	0.1180	0.0002	1.50
14	0.0000	0.0000	3.00	0.0880	0.0002	1.50
15	0.0000	0.0000	3.00	0.0440	0.0001	1.50
16	0.0000	0.0000	3.00	0.0680	0.0001	1.50
17	0.0000	0.0000	3.00	0.0120	0.0000	1.50
18	0.0000	0.0000	3.00	0.0000	0.0000	1.50
19	0.0000	0.0000	3.00	0.0020	0.0000	1.50
20	0.0000	0.0000	3.00	0.0180	0.0000	1.50
21	0.0000	0.0000	3.00	0.0060	0.0000	1.50
22	0.0000	0.0000	3.00	0.0780	0.0002	1.50
23	0.0000	0.0000	3.00	0.3500	0.0007	1.50
24	0.0000	0.0000	3.00	2.3900	0.0048	1.49
25	0.0000	0.0000	3.00	0.0000	0.0000	1.50
26	0.0000	0.0000	3.00	0.0000	0.0000	1.50
27	0.0020	0.0000	3.00	0.0000	0.0000	1.50
28	0.0000	0.0000	3.00	0.0000	0.0000	1.50
29	0.0000	0.0000	3.00	0.0000	0.0000	1.50
30	0.0000	0.0000	3.00	0.0000	0.0000	1.50
31	0.0000	0.0000	3.00	0.0380	0.0001	1.50
32	0.1840	0.0004	3.00	0.0780	0.0002	1.50
33	0.7760	0.0016	3.00	0.0580	0.0001	1.50
34	10.7000	0.0214	2.94	0.3340	0.0007	1.50
35	32.5000	0.0650	2.81	0.0180	0.0000	1.50
36	51.4100	0.1028	2.69	0.0180	0.0000	1.50
37	71.6900	0.1434	2.57	0.0460	0.0001	1.50
38	90.1000	0.1802	2.46	0.1380	0.0003	1.50
39	96.5300	0.1931	2.42	1.3400	0.0027	1.50
40	104.6000	0.2092	2.37	4.2250	0.0085	1.49
41	108.7000	0.2174	2.35	15.1200	0.0302	1.45
42	137.3500	0.2747	2.18	20.0000	0.0400	1.44
43	141.8500	0.2837	2.15	25.0000	0.0500	1.43
44	147.2500	0.2945	2.12	26.8400	0.0537	1.42
45	161.2000	0.3224	2.03	32.8600	0.0657	1.40
46	179.7000	0.3594	1.92	36.2050	0.0724	1.39
47	189.5000	0.3790	1.86	44.4600	0.0889	1.37
48	176.5000	0.3530	1.94	49.7400	0.0995	1.35
49	183.2000	0.3664	1.90	197.6200	0.3952	0.91
50	190.5000	0.3810	1.86	212.9000	0.4258	0.86
51	205.6000	0.4112	1.77	230.1400	0.4603	0.81
52	232.4000	0.4648	1.61	267.2600	0.5345	0.70
53	243.8500	0.4877	1.54	320.9800	0.6420	0.54
54	256.1000	0.5122	1.46	309.9000	0.6198	0.57



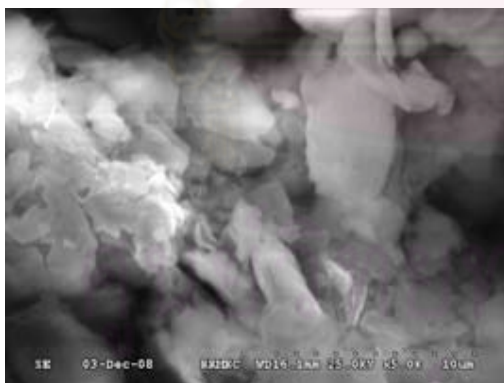
a. Chitosan



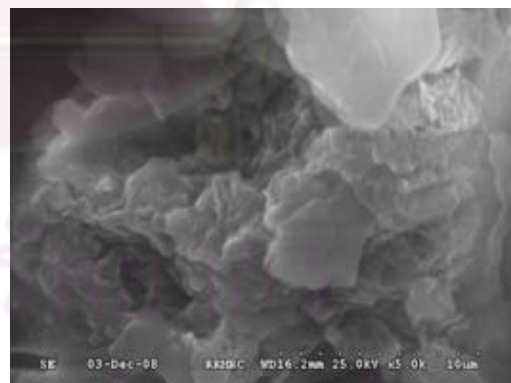
b. Kaolinite



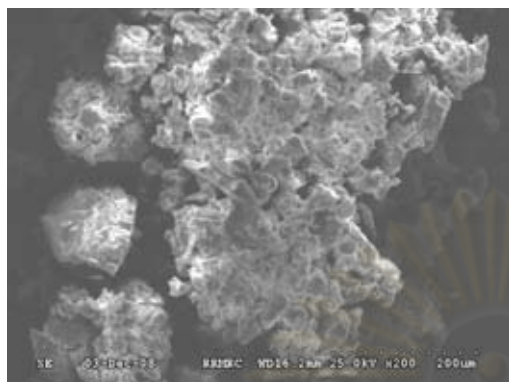
c. Bentonite



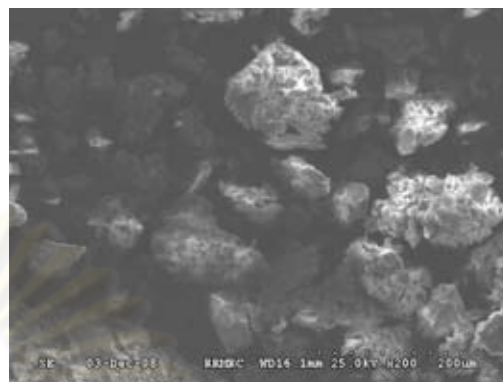
d. CCK beads



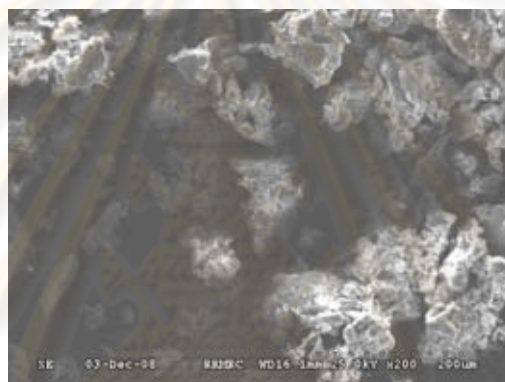
e. CCB beads



f. CCB-EGDE beads



g. CCB-ECH beads



h. CCB-GLA beads

Fig. A-15 Scanning electron microscopy (SEM) images of materials used in the experiment

ศูนย์วิทยทรัพยากร
จุฬาลงกรณ์มหาวิทยาลัย

Table A-16 Intensity at various 2θ of adsorbents from XRD

2θ	Bentonite	Chitosan	CCB	CCB-EGDE	CCB-ECH	CCB-GLA
5	-8.5076	-11.511	-12.877	-12.791	-8.8599	-13.065
5.02	-6.0156	-11	-11.702	-12.711	-9.3778	-10.737
5.04	-4.0742	-11.091	-12.633	-12.64	-5.9118	-6.5028
5.06	-2.4389	-11.106	-12.571	-10.672	-2.2634	-5.4063
5.08	-1.5296	-10.735	-11.998	-10.154	-0.1522	-4.3476
5.1	-0.7068	-10.254	-12.461	-9.6493	2.573	-4.763
5.12	0.9736	-10.715	-10.598	-7.7501	3.065	-2.2623
5.14	4.5367	-10.667	-9.7591	-5.3013	4.0317	0.8599
5.16	6.9219	-9.4823	-7.6462	-1.7053	7.3279	4.4081
5.18	8.0232	-6.5906	-4.1204	1.9449	10.243	8.914
5.2	9.8757	-7.2083	0.5057	2.3831	13.248	8.6317
5.22	10.659	-7.1	-0.7649	5.2688	13.083	11.63
5.24	11.014	-10.126	-0.4368	8.8527	10.226	13.388
5.26	17.556	-8.4795	0.781	8.9181	13.071	13.009
5.28	16.878	-5.8559	5.6594	11.289	13.665	13.853
5.3	22.272	-4.5312	5.5451	15.973	17.354	13.77
5.32	24.653	-3.4402	6.6921	18.62	19.546	15.199
5.34	28.343	-0.9019	7.3139	21.205	17.86	16.515
5.36	30.226	-0.3064	7.6459	23.05	21.342	19.371
5.38	31.706	0.4547	11.456	26.602	20.999	14.191
5.4	34.172	0.917	13.527	26.106	20.595	13.768
5.42	39.052	1.1083	14.578	23.757	20.335	14.337
5.44	45.312	1.5611	17.116	25.887	19.606	21.192
5.46	52.459	2.0124	18.305	25.489	19.934	26.036
5.48	59.951	2.589	19.356	25.256	23.671	31.6
5.5	67.025	1.6005	22.804	26.026	24.079	36.855
5.52	71.221	-1.0459	25.084	28.106	25.509	36.886
5.54	76.571	-2.5918	20.24	31.389	26.613	42.355
5.56	85.124	-4.7833	19.661	32.043	25.13	47.407
5.58	93.88	-6.5676	25.641	33.459	28.01	50.686
5.6	97.588	-6.1679	26.55	40.076	34.997	55.351
5.62	105.13	-8.0515	25.928	46.846	35.907	54.602
5.64	110.63	-7.1193	28.555	52.081	41.581	57.863
5.66	116.06	-3.9999	32.248	54.768	43.079	58.888
5.68	118.98	-3.5818	33.68	57.874	49.316	62.967
5.7	122.99	-3.0229	36.855	61.198	54.25	61.053
5.72	130.25	-3.4717	39.223	59.79	60.365	63.67
5.74	134.92	-2.3185	41.478	60.858	63.42	63.567
5.76	141.05	0.2077	43.023	63.815	65.283	66.245
5.78	148.14	-1.5463	44.905	68.013	67.932	66.792
5.8	156.14	-1.6765	45.068	71.005	69.755	69.278
5.82	159.38	-2.3842	47.402	74.816	70.003	66.709
5.84	163.08	-1.5826	46.437	78.634	69.439	64.975
5.86	167.84	-2.9994	45.6	80.835	67.095	69.081
5.88	175.46	-3.6902	46.656	79.837	65.97	73.74
5.9	180.97	-5.7263	48.555	83.032	64.586	75.319
5.92	186.92	-6.0705	45.415	84.393	68.652	78.113
5.94	193.29	-7.1996	42.43	83.83	66.19	75.438
5.96	204.23	-6.3117	42.37	84.507	71.918	78.616
5.98	207.43	-5.8619	43.822	85.569	75.771	77.507
6	213.01	-7.1011	40.857	88.899	81.501	80.127
6.02	220.55	-6.2242	43.586	91.705	86.221	78.133
6.04	224.74	-5.3768	44.057	90.701	88.573	76.799
6.06	225.37	-3.5619	44.482	96.89	88.757	71.234

Table A-16 Intensity at various 2θ of adsorbents from XRD (cont.)

2θ	Bentonite	Chitosan	CCB	CCB-EGDE	CCB-ECH	CCB-GLA
6.08	224.07	-2.7797	47.206	100.5	91.56	72.138
6.1	226.65	-2.5532	47.3	108.18	93.059	70.397
6.12	222.08	-1.74	50.831	112.02	91.862	65.771
6.14	214.53	-0.7335	54.115	112.22	89.106	60.831
6.16	210.8	0.0145	55.376	112.84	86.231	60.74
6.18	207.32	-1.0595	58.511	114.21	85.598	59.4
6.2	208.33	-2.0547	55.707	111.98	84.859	58.12
6.22	205.46	-3.3363	54.256	109.13	83.944	57.928
6.24	205.01	-4.5482	54.506	104.61	83.687	60.577
6.26	206.18	-3.2324	54.791	103.3	81.536	59.165
6.28	208.97	-4.4724	55.161	99.929	81.415	61.225
6.3	206.44	-5.6428	52.013	100.29	79.096	62.951
6.32	209.72	-5.2946	49.373	100.81	79.315	64.754
6.34	209.76	-1.9852	49.947	100.2	77.788	63.579
6.36	207.62	-1.8384	48.53	101.18	76.91	61.276
6.38	206.45	-0.8697	49.166	101.11	75.959	58.69
6.4	202.87	-0.0016	50.549	102.25	79.174	58.166
6.42	203.15	1.5025	49.395	104.23	76.931	52.009
6.44	195.5	2.355	49.749	103.03	78.074	47.488
6.46	188.68	4.664	49.152	97.217	76.406	43.57
6.48	180.76	6.4049	48.032	95.983	77.093	39.466
6.5	174.96	6.1504	50.554	92.286	77.459	35.736
6.52	165.3	5.9283	47.777	89.213	75.805	33.205
6.54	157.06	6.3703	51.887	83.383	70.967	35.038
6.56	147.5	4.4886	53.199	80.285	68.429	33.33
6.58	137.39	5.2586	52.689	75.161	63.392	34.106
6.6	125.9	4.1478	50.604	69.401	58.505	31.702
6.62	116.16	3.509	47.337	67.088	53.346	34.481
6.64	107.36	5.1225	45.722	64.313	51.325	30.051
6.66	98.069	6.4805	40.867	63.041	47.46	25.718
6.68	91.312	4.6635	37.332	61.337	46.556	22.891
6.7	83.016	4.5539	34.971	56.065	45.811	21.02
6.72	79.712	4.9133	32.354	54.76	48.331	18.189
6.74	76.187	5.2803	25.457	50.343	45.752	14.986
6.76	71.284	6.9956	19.877	47.178	47.739	13.818
6.78	66.599	8.313	20.115	43.977	46.334	11.22
6.8	60.928	9.313	20.014	40.444	44.539	9.9653
6.82	56.879	7.0514	22.332	37.625	46.623	9.0209
6.84	53.209	5.6736	23.422	38.293	43.766	8.2606
6.86	54.386	2.7864	23.894	35.687	41.647	12.146
6.88	50.404	0.5726	23.661	32.606	42.239	11.416
6.9	47.728	0.5986	25.916	28.62	38.067	11.814
6.92	46.827	-1.5998	26.168	29.226	36.798	11.041
6.94	44.164	-0.8742	26.289	27.089	35.777	11.566
6.96	42.688	1.1408	24.631	25.051	34.56	4.9343
6.98	40.961	1.8818	22.175	24.493	30.79	5.1059
7	39.966	2.3766	20.348	23.025	27.504	4.9322
7.02	37.292	4.4302	18.139	18.352	24.717	2.8176
7.04	37.988	8.9403	17.238	13.913	22.79	0.6988
7.06	34.717	10.173	15.536	12.392	20.232	1.7509
7.08	31.835	11.912	15.816	14.739	18.923	0.4589
7.1	31.767	13.297	17.686	14.289	16.972	-1.4569
7.12	29.105	11.634	18.402	12.376	14.053	-3.025
7.14	26.975	9.1667	18.448	13.295	15.497	-3.6019

Table A-16 Intensity at various 2θ of adsorbents from XRD (cont.)

2θ	Bentonite	Chitosan	CCB	CCB-EGDE	CCB-ECH	CCB-GLA
7.16	25.999	7.435	17.325	11.079	13.657	-2.1973
7.18	24.244	5.3302	15.224	9.546	15.154	-1.1548
7.2	21.841	4.7316	16.679	6.2993	14.107	-0.9296
7.22	18.583	1.8836	17.716	6.5805	14.853	-0.4995
7.24	16.497	1.0403	15.486	9.3433	13.79	1.8974
7.26	13.518	1.4894	17.269	6.7981	13.452	1.4322
7.28	11.897	0.9648	15.233	6.4156	11.066	3.1523
7.3	8.4509	2.2002	13.13	6.8303	9.4187	6.3745
7.32	6.9235	0.722	10.682	6.3365	7.8001	7.1653
7.34	3.9739	2.8644	8.5348	3.9836	7.0281	6.1576
7.36	3.8559	3.7575	11.488	4.9977	7.474	7.6343
7.38	4.1857	0.7172	10.61	8.5645	8.2772	10.32
7.4	4.8642	0.1799	9.7229	10.136	7.574	7.2604
7.42	8.3464	-3.5325	9.1254	12	8.2931	5.1993
7.44	11.088	-5.0389	7.3681	11.851	5.5398	3.3037
7.46	13.667	-5.6894	5.0918	10.603	5.8837	2.6787
7.48	14.127	-7.4561	2.1077	8.5375	6.3466	1.4327
7.5	14.755	-9.5587	1.6758	8.207	5.4175	0.4079
7.52	13.157	-10.109	-1.3648	6.8193	4.1214	1.4278
7.54	11.543	-11.311	-1.1999	6.7799	3.4673	1.6874
7.56	12.381	-9.12	-1.6128	4.6246	0.5359	1.6574
7.58	11.782	-9.5626	-1.0338	0.7495	3.9092	3.0682
7.6	9.2243	-10.419	-1.7509	0.3622	5.4231	5.1616
7.62	4.483	-9.3289	-2.0055	-2.5994	8.9599	4.7254
7.64	3.9048	-9.2253	-2.2713	-3.3551	9.1543	3.858
7.66	1.0937	-8.9653	-2.4152	-3.5146	11.331	3.0925
7.68	1.2956	-10.645	0.0737	-4.0564	11.08	2.5362
7.7	1.3053	-9.8776	-1.0153	-2.9558	12.467	3.505
7.72	1.7945	-7.6937	0.3026	-1.5996	13.227	3.3224
7.74	4.0982	-4.403	-0.4094	2.9966	13.638	3.8643
7.76	7.9644	0.7962	-0.0088	1.7338	11.534	3.7635
7.78	8.0704	1.867	1.7335	2.101	10.285	4.2483
7.8	6.1317	1.8835	3.0529	2.2316	8.0346	4.3844
7.82	5.393	2.3751	3.2341	3.178	5.6771	5.0686
7.84	4.8265	2.5122	1.5001	2.2065	5.5778	6.5302
7.86	5.3456	2.3815	3.7084	1.1438	3.3869	6.1702
7.88	6.6591	2.8683	4.0045	-1.6232	2.2468	5.3722
7.9	4.1263	0.9789	3.7725	-1.7229	3.2598	7.7319
7.92	1.2951	-2.2371	2.2134	-2.3876	1.0387	7.8276
7.94	0.0634	-0.2412	1.835	-3.9081	1.1315	5.5424
7.96	-0.6803	0.4281	1.4702	-4.6128	-1.3749	3.8034
7.98	-2.0258	-2.1953	0.6484	-5.7432	-0.5922	2.9078
8	-0.7284	0.1612	-0.0144	-7.1814	-3.0528	2.3294
8.02	-0.2434	1.6925	-1.5367	-6.5686	-0.9084	4.3776
8.04	0.1723	1.1944	-2.674	-6.8302	-0.0165	3.5235
8.06	0.559	2.3076	-3.7172	-7.3565	0.6908	2.3237
8.08	1.9229	0.6422	-2.818	-9.5405	0.8453	-0.9616
8.1	2.651	-2.0868	-1.7288	-7.8304	0.5459	-0.9752
8.12	1.6008	-6.3313	-2.9821	-6.6975	0.6595	-0.7707
8.14	3.0479	-7.8498	-3.6646	-3.5847	2.0252	0.0852
8.16	3.0944	-10.828	-4.1819	-3.591	1.673	1.0237
8.18	2.9727	-11.576	-3.7599	-4.1622	1.1532	0.0217
8.2	1.7878	-10.08	-2.9218	-4.0105	-0.1566	0.0973
8.22	-1.6057	-8.8493	-2.77	-1.6496	-1.745	1.573

Table A-16 Intensity at various 2θ of adsorbents from XRD (cont.)

2θ	Bentonite	Chitosan	CCB	CCB-EGDE	CCB-ECH	CCB-GLA
8.24	-1.2944	-5.8242	-3.9977	-0.055	-3.3946	1.9425
8.26	0.217	-0.6212	-0.0323	1.6373	-4.4197	2.5391
8.28	0.4454	0.2086	1.1138	2.3034	-3.8464	1.3136
8.3	2.3848	0.235	0.001	2.3364	-2.4989	1.9017
8.32	3.7781	-0.0745	-2.2624	1.7178	-3.9688	3.5498
8.34	1.096	-2.1256	-3.636	1.6766	-4.1383	4.592
8.36	3.0752	-4.2558	-4.2468	0.4297	-4.1056	5.1189
8.38	2.8056	-5.2048	-3.5191	1.5993	-2.6249	4.997
8.4	3.4203	-8.5796	-5.1307	0.0244	-0.3137	4.8919
8.42	6.6561	-10.795	-5.7659	0.4758	1.9695	7.1473
8.44	7.1539	-9.9718	-8.4402	-0.0401	4.1439	9.3204
8.46	9.5825	-7.2586	-5.3362	-0.4584	5.1013	10.551
8.48	8.9543	-7.3085	-4.615	-4.1816	6.5512	10.135
8.5	6.5368	-5.0691	-3.9112	-7.3273	6.7919	9.3462
8.52	6.1934	-0.3421	-3.8285	-9.1711	5.0989	8.1284
8.54	5.9811	2.2966	-2.4537	-8.8515	5.2802	9.8624
8.56	6.7134	3.943	-0.4615	-7.9792	3.6052	10.842
8.58	7.3543	4.69	1.4451	-8.3374	2.3308	12.192
8.6	8.6802	2.8812	1.1671	-6.8984	3.9277	10.512
8.62	7.4164	1.3896	-0.7413	-8.2224	2.9129	11.044
8.64	5.5158	-2.0354	-2.8621	-6.9597	1.2461	12.048
8.66	5.5859	-4.4063	-3.2264	-4.7665	-0.1408	10.663
8.68	7.4741	-5.5126	-4.7876	-4.3921	-0.2805	9.7342
8.7	6.2678	-4.961	-5.9328	-4.4898	-1.4278	8.485
8.72	7.1393	-5.4265	-9.1791	-5.5363	-1.0883	9.7171
8.74	7.9777	-4.2528	-9.1672	-5.2004	-0.0334	11.43
8.76	7.0946	-5.6813	-9.5597	-6.03	0.2285	12.157
8.78	6.7968	-4.8575	-6.6407	-5.9911	0.0809	11.019
8.8	3.9005	-6.5059	-7.6122	-8.8175	1.3842	11.699
8.82	2.1702	-6.3943	-8.5268	-8.9797	1.0051	12.377
8.84	3.2282	-2.0057	-4.9387	-8.9667	1.2065	13.673
8.86	2.2479	1.0253	-0.7581	-7.9327	2.6513	16.54
8.88	2.1611	2.4386	1.0336	-7.6772	0.2466	18.455
8.9	2.485	1.0298	2.1608	-7.5532	3.2961	19.912
8.92	3.5322	2.0281	4.2458	-5.1179	6.7942	23.752
8.94	4.7268	2.3189	6.2484	-4.7058	6.4225	33.395
8.96	5.9079	3.1561	7.8343	1.033	7.225	45.312
8.98	11.549	3.4685	10.938	3.1078	7.1932	58.88
9	17.229	6.4727	15.118	6.2338	4.1826	75.484
9.02	26.172	7.6921	20.918	12.16	5.6717	91.213
9.04	36.648	8.235	30.545	20.116	6.5244	105.21
9.06	46.217	7.6276	40.084	27.913	11.217	115.23
9.08	60.989	5.1115	47.027	37.039	17.113	119.99
9.1	76.31	8.7888	52.766	48.597	25.084	120.07
9.12	91.51	7.5544	56.352	56.176	36.387	114.77
9.14	104.72	7.6341	59.853	69.335	47.896	104.41
9.16	114.67	8.5295	60.243	80.542	56.02	91.291
9.18	117.19	8.7763	55.903	89.757	64.717	73.231
9.2	114.94	6.4673	46.521	92.704	69.741	53.691
9.22	108.86	3.2712	36.417	91.043	72.732	35.238
9.24	99.284	4.3336	26.164	86.52	69.17	23.79
9.26	85.5	4.0322	14.452	78.522	63.257	15.825
9.28	66.654	3.1037	5.9323	67.423	55.066	11.055
9.3	51.471	5.217	-1.6695	50.957	44.694	10.093

Table A-16 Intensity at various 2θ of adsorbents from XRD (cont.)

2θ	Bentonite	Chitosan	CCB	CCB-EGDE	CCB-ECH	CCB-GLA
9.32	37.115	10.1	-6.4126	40.367	32.329	10.669
9.34	25.301	10.377	-8.6281	28.239	24.179	10.902
9.36	14.781	15.018	-6.3503	17.976	13.058	13.564
9.38	7.4117	17.131	-5.6162	9.4457	7.264	16.744
9.4	6.4806	21.744	-4.9211	1.335	3.7247	18.437
9.42	7.4957	23.823	-2.4107	-4.0031	2.9608	17.757
9.44	9.7263	24.253	-0.0167	-8.0331	4.8049	17.478
9.46	10.522	23.945	2.0131	-4.0151	6.5079	15.534
9.48	11.893	24.27	2.4713	-0.2864	6.5403	12.621
9.5	9.9438	24.367	2.9988	0.3139	9.2272	7.9305
9.52	8.6497	22.512	-0.4818	-1.6477	9.9248	5.0461
9.54	10.664	23.396	-1.3668	-2.2454	8.6731	3.1761
9.56	10.108	25.42	-2.1238	-2.665	9.045	3.4689
9.58	8.8595	26.164	-1.5421	-4.1789	9.6176	2.4589
9.6	6.9911	25.006	0.1336	-7.3971	7.8203	1.9925
9.62	4.7593	28.536	-0.2328	-8.3877	6.4129	3.3918
9.64	3.9784	30.154	0.0954	-6.507	5.0614	3.9379
9.66	4.1467	28.697	0.9573	-7.5102	5.1059	5.3226
9.68	4.0663	29.938	0.6563	-5.9575	2.9041	7.7819
9.7	4.7184	27.279	0.2295	-5.524	1.4691	9.2905
9.72	6.3662	27.6	0.5624	-6.0052	1.9028	10.374
9.74	7.3071	23.56	-0.0169	-6.0514	1.4519	9.803
9.76	6.9526	24.491	-0.0718	-4.8669	2.1639	12.178
9.78	8.0056	25.86	-1.5341	-2.0057	3.3517	9.9817
9.8	8.2625	23.766	-3.1966	-0.2854	3.5965	8.7494
9.82	5.2697	24.088	-5.9941	-2.0278	5.9556	8.3266
9.84	6.4955	25.291	-8.3973	-1.2671	6.3737	7.5708
9.86	8.6324	27.224	-7.7025	-0.0588	8.3397	7.2404
9.88	7.5422	26.108	-7.2759	-0.6415	9.0596	7.2241
9.9	6.2156	27.838	-4.6407	-0.9564	9.4414	5.4475
9.92	4.688	26.67	-5.8836	-1.895	9.5552	4.8115
9.94	0.3811	26.212	-5.2647	-3.5966	7.8963	3.6537
9.96	0.4114	25.801	-5.013	-4.1759	8.2634	2.0885
9.98	1.8511	28.541	-4.045	-5.6978	7.1612	1.0077
10	2.189	29.496	-4.0417	-5.5958	6.2274	0.6897
10.02	3.1666	29.542	-2.2633	-7.1609	5.1374	-0.2058
10.04	3.6694	31.225	-0.6571	-6.4953	4.3631	1.6709
10.06	2.7738	34.667	-1.0715	-6.9487	3.554	4.4096
10.08	4.9759	35.368	-1.5558	-6.8618	1.9851	6.1992
10.1	5.9161	35.148	-3.6056	-5.3244	0.9447	5.9252
10.12	5.8403	31.378	-4.713	-5.7018	-0.7179	6.8258
10.14	5.4753	33.519	-6.2836	-7.932	-0.6669	7.9321
10.16	8.9668	33.626	-6.7076	-6.6108	-1.7112	7.6218
10.18	8.5562	34.13	-4.6846	-4.3654	-1.6871	9.3995
10.2	7.9401	33.016	-4.9205	-4.394	-1.455	7.9154
10.22	7.004	34.557	-4.9694	-2.7397	1.0729	7.2437
10.24	5.7509	32.124	-6.6055	-3.3223	2.3686	6.1121
10.26	4.7041	32.346	-5.2682	-4.2127	2.685	4.6165
10.28	5.5632	33.238	-6.1681	-3.1047	4.6907	3.4319
10.3	5.2974	36.996	-6.9369	-1.6606	5.4973	1.9204
10.32	5.566	40.637	-6.4661	-2.3729	7.2885	1.6177
10.34	4.6508	41.481	-7.2046	-2.5509	6.4064	0.7404
10.36	3.8458	40.296	-7.5179	-0.2939	6.9837	2.88
10.38	3.0583	39.542	-7.1303	-0.4068	6.3332	4.219

Table A-16 Intensity at various 2θ of adsorbents from XRD (cont.)

2θ	Bentonite	Chitosan	CCB	CCB-EGDE	CCB-ECH	CCB-GLA
10.4	4.4182	35.155	-6.1842	0.0175	5.78	2.1693
10.42	3.4488	36.138	-5.4413	-0.5503	5.937	3.4708
10.44	3.986	32.745	-4.0657	-0.8904	4.1758	3.0925
10.46	4.5189	34.521	-3.5805	-2.0185	3.2703	3.0437
10.48	5.3386	37.224	-2.506	-0.6124	2.4652	2.3771
10.5	5.6959	39.863	1.0496	0.4363	1.3735	3.2505
10.52	4.0829	39.612	1.0119	-1.7085	1.5307	0.5648
10.54	3.8558	38.747	1.9042	-1.2665	1.036	1.1746
10.56	4.0919	37.331	2.2466	-2.8415	1.4898	1.3895
10.58	4.5497	38.494	2.1227	-3.6037	0.1184	1.3518
10.6	3.9786	38.041	0.3064	-4.0237	0.1878	1.1266
10.62	5.1679	36.742	-1.227	-1.9281	1.5651	2.2278
10.64	5.8297	40.41	-2.6416	-1.7999	1.2965	3.6276
10.66	6.6977	39.715	-4.0117	-1.119	3.0695	1.9172
10.68	8.2922	36.519	-3.8264	0.5356	6.5929	3.5581
10.7	8.7091	32.597	-4.126	1.5944	6.9815	4.869
10.72	9.7749	33.179	-3.991	1.596	9.7707	4.6239
10.74	9.7003	33.663	-3.8239	1.432	9.6819	5.3926
10.76	10.485	32.86	-4.1138	2.5948	9.9782	4.884
10.78	11.012	34.994	-5.6658	0.5393	10.629	4.2002
10.8	11.002	35.72	-6.6778	1.501	9.5532	5.0906
10.82	10.929	38.17	-6.0324	0.0154	7.3209	4.3661
10.84	8.9753	39.453	-7.6427	-2.7874	7.0465	2.6988
10.86	8.6708	39.002	-7.6389	-3.7589	5.7765	3.1009
10.88	9.1887	40.769	-6.1879	-5.4997	5.2602	3.4609
10.9	7.0521	43.877	-4.5592	-6.6351	2.6274	1.875
10.92	6.6822	44.412	-4.8148	-7.255	2.2931	2.6154
10.94	5.7649	42.746	-4.4407	-6.7985	1.8239	3.4625
10.96	3.5577	46.896	-4.0686	-6.3001	0.5077	3.2222
10.98	2.9742	46.992	-2.2216	-6.7692	2.2361	1.301
11	0.9864	43.979	-1.9431	-5.0539	3.3744	3.3045
11.02	0.5228	40.536	-1.5211	-3.1977	3.4552	2.8573
11.04	0.815	42.934	-0.2093	-1.3306	5.1998	2.4083
11.06	-0.0108	41.203	0.1129	0.1233	5.0386	0.4535
11.08	0.9606	38.062	-0.282	1.4891	4.1666	0.6693
11.1	1.6008	36.39	-0.6106	0.7543	3.3051	-0.478
11.12	3.0939	31.961	-1.7493	2.0924	2.1477	0.9525
11.14	4.6268	31.855	-1.8094	-0.2088	2.9637	-0.9273
11.16	5.7113	30.28	-2.9613	-0.5826	4.7067	-0.4818
11.18	7.3138	30.459	-2.5485	-0.2954	4.4448	-0.8764
11.2	9.2364	32.113	-2.6391	-0.3657	4.4906	-0.8301
11.22	9.8571	31.596	-3.3416	-0.9049	2.9588	-1.7392
11.24	11.646	29.244	-3.7365	-1.7613	1.9236	-1.3614
11.26	11.278	26.624	-3.4955	-2.0249	1.5244	0.1127
11.28	11.549	27.779	-6.1109	-2.2341	2.0955	-0.1631
11.3	10.475	29.667	-4.784	-1.7637	3.3335	0.5438
11.32	9.8219	30.067	-4.1804	-0.3628	4.8731	2.6545
11.34	10.353	30.202	-3.4951	-0.2049	4.609	3.6644
11.36	8.6815	31.441	-3.4154	0.6233	4.1109	4.8304
11.38	8.1328	31.1	-4.1922	0.6173	3.9546	3.4808
11.4	8.5055	29.853	-4.5313	1.2414	3.1618	4.3085
11.42	7.2239	28.774	-4.3119	-0.3991	3.5035	3.0602
11.44	8.0835	28.285	-5.822	-0.6727	5.3634	5.5668
11.46	8.9976	32.677	-6.0523	0.3712	6.3268	4.8059

Table A-16 Intensity at various 2θ of adsorbents from XRD (cont.)

2θ	Bentonite	Chitosan	CCB	CCB-EGDE	CCB-ECH	CCB-GLA
11.48	8.4493	31.494	-6.6344	0.7882	7.598	5.5977
11.5	8.8286	29.75	-6.9213	2.1201	7.1676	4.2436
11.52	9.3275	28.787	-7.6156	3.1534	7.1194	3.8722
11.54	9.6085	25.956	-6.3386	3.5784	5.93	1.545
11.56	9.2568	21.232	-5.8098	3.5964	5.1103	-0.5208
11.58	7.8018	18.967	-5.4191	2.4984	4.3383	-0.358
11.6	7.553	16.886	-3.8136	3.1357	5.2023	-1.6579
11.62	4.557	13.903	-1.1791	3.205	5.696	-2.5287
11.64	3.1604	8.5528	-0.9428	2.18	4.4762	-1.0347
11.66	1.9577	4.3342	-1.3678	-1.2645	3.2816	-0.301
11.68	1.2708	2.1016	-1.2716	-1.3327	2.113	-0.3527
11.7	0.9513	3.3132	-2.3476	-1.811	1.6477	-1.0161
11.72	0.5376	3.2106	-2.3976	-3.4363	0.3079	-1.4862
11.74	0.7049	3.9701	-2.6602	-4.7813	0.1029	-2.1686
11.76	1.6202	9.2822	-2.7884	-5.5272	1.0282	-0.6577
11.78	3.8626	11.651	-4.064	-5.7978	0.0098	-0.4365
11.8	4.1347	12.047	-4.5893	-7.3267	1.1397	1.4022
11.82	5.1271	12.206	-4.9245	-6.1833	0.6912	1.2298
11.84	6.8613	14.332	-5.9397	-5.577	0.6052	2.5015
11.86	7.3746	14.103	-7.4987	-5.0371	1.1865	0.8952
11.88	6.8278	11.412	-7.5858	-5.347	2.7602	0.7082
11.9	7.5153	11.868	-6.5122	-5.4912	2.8484	1.3709
11.92	7.1303	8.851	-4.5675	-3.4046	6.3464	1.23
11.94	6.9671	3.7585	-4.9312	-3.6879	7.687	1.4619
11.96	6.3073	1.8409	-4.399	-4.66	9.6453	3.045
11.98	6.018	0.1229	-2.4168	-5.2342	11.026	3.6201
12	5.6439	1.3538	-1.5974	-2.3114	10.916	4.3699
12.02	4.7918	1.7689	-1.9843	-1.6129	12.587	4.7372
12.04	5.0624	0.0368	-0.8499	-2.0026	12.665	2.5114
12.06	5.6662	-0.0591	0.1494	-1.3195	12.369	2.9526
12.08	4.8571	0.8403	0.9982	-1.6409	11.119	3.0886
12.1	5.7187	2.0074	1.1608	-0.9514	11.16	2.6779
12.12	3.35	4.1482	2.2101	0.3466	10.844	2.3274
12.14	2.8842	2.0149	1.3255	0.9	9.9221	0.7368
12.16	5.0519	1.0162	-0.1523	1.3746	8.2864	0.1784
12.18	6.7076	-0.7705	-1.0314	2.7766	8.7232	-0.3817
12.2	7.5603	2.6363	-0.0023	3.6817	8.6906	-1.4822
12.22	8.7957	5.9982	0.347	2.6256	7.3621	0.8891
12.24	7.8813	5.4389	0.3351	4.7166	9.843	2.6302
12.26	9.3126	4.8749	-0.9109	4.8867	9.644	6.1931
12.28	9.4702	6.8759	0.1446	5.6652	9.5423	7.2496
12.3	8.2861	7.448	-0.1362	7.1605	8.3489	10.4
12.32	8.491	6.5851	-1.131	8.2457	7.9773	12.007
12.34	9.4903	3.7237	-2.1773	8.0817	7.4614	12.687
12.36	9.3647	1.2786	-1.1884	7.6036	7.7363	11.857
12.38	9.8045	1.0331	-1.4428	7.0745	6.415	13.66
12.4	7.9335	-0.2944	-1.5816	7.5471	6.324	13.065
12.42	6.5381	-4.0787	-0.9266	7.2008	6.3427	12.082
12.44	5.5564	-6.3042	-1.3912	8.3639	5.7651	12.558
12.46	7.9977	-9.3548	-0.9475	6.7144	6.0525	10.942
12.48	11.042	-10.909	1.3518	6.3637	6.4465	10.937
12.5	12.524	-11.56	3.1415	5.2283	7.4951	12.439
12.52	13.321	-7.4791	5.6103	4.0605	6.9226	11.502
12.54	14.996	-10.694	6.2785	3.0151	7.7539	13.087

Table A-16 Intensity at various 2θ of adsorbents from XRD (cont.)

2θ	Bentonite	Chitosan	CCB	CCB-EGDE	CCB-ECH	CCB-GLA
12.56	16.788	-10.31	6.759	4.9589	8.1251	14.447
12.58	17.206	-9.2836	8.3335	6.2511	7.5968	16.604
12.6	18.352	-8.5405	10.572	7.2229	8.243	17.121
12.62	17.381	-11.876	11.635	6.8125	9.7419	19.761
12.64	18.729	-13.195	12.076	5.9517	10.347	19.888
12.66	18.719	-12.842	12.594	5.9872	10.991	20.673
12.68	17.234	-12.989	12.663	5.913	12.897	20.781
12.7	16.798	-11.479	9.0342	7.9116	14.472	20.373
12.72	15.499	-11.202	8.3537	10.351	15.219	19.202
12.74	14.618	-9.9017	7.2533	11.338	14.632	17.611
12.76	14.311	-7.7487	8.021	13.691	16.893	15.439
12.78	13.031	-5.232	8.1706	12.442	17.882	11.149
12.8	13.14	-5.494	7.1759	12.595	17.494	10.206
12.82	12.282	-4.9031	5.8232	12.179	16.096	7.7441
12.84	11.596	-2.9082	5.8123	12.725	14.723	3.095
12.86	10.773	-4.1255	4.2576	13.002	14.011	0.0509
12.88	9.2113	-0.8954	2.9208	12.945	11.363	-0.7101
12.9	7.85	-0.6329	2.675	12.427	11.592	-2.3986
12.92	7.749	-3.4525	1.8111	10.019	10.878	-1.0796
12.94	5.9649	-6.9735	3.1032	6.6784	9.7221	-0.4527
12.96	4.0409	-5.8148	0.9723	4.2462	6.9238	0.4078
12.98	2.8429	-6.5124	-0.4484	0.6052	5.3807	1.9785
13	0.0921	-7.1	-3.0569	1.0214	2.9535	2.2379
13.02	0.1297	-6.7914	-4.048	0.9254	4.2117	3.3345
13.04	-0.0369	-7.5464	-2.3569	-0.2463	1.6198	3.5099
13.06	-0.2757	-5.1791	-2.4015	-0.98	2.1252	2.7268
13.08	-2.0513	-4.8165	-1.3056	-1.3249	3.9414	2.7965
13.1	-2.605	-3.0406	-2.4593	-2.0367	5.341	1.4929
13.12	-1.1895	-6.2571	-3.584	-2.3567	4.9585	1.2774
13.14	-1.0321	-4.6423	-3.6641	-2.0312	4.469	0.7814
13.16	-1.2324	-3.3729	-3.2168	-0.9888	5.7176	-1.0538
13.18	0.2965	-2.2846	-2.7931	0.7301	7.0665	-0.2561
13.2	0.9733	-1.1576	-4.3155	1.7076	7.4632	-0.7852
13.22	2.6512	-1.3821	-3.7935	1.1202	9.6784	-1.7402
13.24	2.9021	-4.2924	-5.6295	-0.9795	8.4554	-0.0592
13.26	2.3778	-3.3127	-5.876	-3.4894	8.2367	-1.7484
13.28	1.4438	-4.0343	-6.9139	-4.6168	6.5951	-0.3557
13.3	1.0286	-3.5562	-7.8671	-7.4174	7.7845	1.5924
13.32	0.4173	-4.151	-7.8736	-4.5523	7.2198	1.8424
13.34	1.455	-3.5059	-6.724	-4.1593	8.7028	2.1783
13.36	3.0643	-3.9769	-7.115	-3.4767	8.9672	1.7745
13.38	3.1058	-1.4465	-5.8361	-3.0308	8.2206	1.8243
13.4	2.4806	-0.7009	-4.3239	-2.6793	8.2926	2.7473
13.42	2.3619	-0.9631	-4.3522	-3.4717	9.4587	1.6199
13.44	2.9541	-1.5334	-3.9986	-3.12	6.4706	0.9398
13.46	2.5452	0.2878	-1.8265	-1.4199	4.6317	2.3349
13.48	1.8596	-2.5303	-1.5263	0.3932	3.8254	1.7958
13.5	3.2441	-3.9693	-1.5593	1.5888	3.0903	0.8644
13.52	3.7357	-7.4996	-2.9751	0.7613	1.1876	0.9407
13.54	3.2602	-9.3999	-2.3463	-1.0058	-0.5513	1.725
13.56	4.4709	-10.841	-2.6173	-3.2325	-2.763	1.2712
13.58	3.9095	-9.2054	-2.1565	-2.4267	-2.0185	1.596
13.6	3.1024	-9.3181	-2.6697	-2.9598	-1.4791	3.6393
13.62	3.1239	-7.0515	-4.0796	-3.1321	1.7317	4.3568

Table A-16 Intensity at various 2θ of adsorbents from XRD (cont.)

2θ	Bentonite	Chitosan	CCB	CCB-EGDE	CCB-ECH	CCB-GLA
13.64	4.2927	-6.9846	-4.0085	-1.2563	1.8442	3.0231
13.66	3.8134	-6.8419	-4.6142	0.0979	3.1114	2.1243
13.68	4.3577	-4.8309	-5.7079	0.7199	3.5049	1.2298
13.7	3.7305	-2.9763	-3.494	1.6006	3.7624	0.9992
13.72	3.6069	-2.1852	-3.4027	1.421	6.9161	0.9651
13.74	3.4944	-0.7735	-3.3505	-0.1347	7.9033	0.635
13.76	4.0805	-0.7875	-2.3529	0.2679	6.5319	-0.8981
13.78	4.3496	-3.0322	-0.1962	0.9322	7.4931	-0.2936
13.8	4.3638	-6.876	-0.3696	-0.9437	7.8982	-1.6413
13.82	5.069	-10.142	-2.1239	-1.1461	10.345	-2.8763
13.84	4.774	-10.336	-1.1619	-2.545	11.536	-0.243
13.86	3.9927	-12.637	-1.0779	-3.8835	11.898	-0.1471
13.88	4.7625	-12.685	-2.064	-5.1924	13.916	1.6158
13.9	4.8678	-11.822	-2.3833	-3.8837	14.891	4.0333
13.92	3.1523	-11.137	-3.881	-3.6754	15.362	5.0589
13.94	2.1229	-8.9763	-3.7986	-2.7628	15.442	4.5162
13.96	0.7482	-11.554	-3.3806	-1.9816	13.65	4.2534
13.98	-0.6927	-11.877	-2.8655	-1.1462	11.284	4.0973
14	-1.3941	-10.006	-2.6001	-0.7054	8.9445	4.5586
14.02	-2.2058	-12.416	-1.643	-1.5633	7.751	4.1172
14.04	-2.2248	-13.418	-0.5145	-3.3514	3.7662	5.1013
14.06	-0.8293	-10.465	-0.1465	-4.4073	0.9671	6.127
14.08	0.7518	-8.0369	1.4797	-3.285	-0.9633	4.9311
14.1	2.445	-4.9013	1.621	-3.2974	-0.3478	6.4331
14.12	2.0628	-4.7209	0.9492	-5.7446	0.6954	5.9241
14.14	1.3048	-4.282	-0.4211	-5.537	4.1754	5.0078
14.16	0.8831	-1.207	-1.1742	-6.3835	5.9625	6.1485
14.18	1.6151	-1.3131	-2.0778	-6.0766	5.9982	8.1605
14.2	1.1044	-0.1422	-3.2093	-3.8331	8.85	9.3132
14.22	2.1993	1.6989	-2.061	-1.1545	9.2125	7.4177
14.24	0.1384	2.9192	-5.215	0.8012	11.038	6.3904
14.26	-0.0198	1.4506	-4.5536	2.5264	9.9775	3.8443
14.28	-0.6497	-3.2827	-4.7269	2.3028	10.307	3.6617
14.3	0.0599	-4.897	-3.93	2.3532	8.8232	2.561
14.32	-0.2411	-7.1506	-4.3239	2.173	8.0129	1.8425
14.34	-0.0973	-9.7247	-4.6825	0.0719	6.2503	1.438
14.36	1.8409	-9.9474	-5.1081	-1.5105	4.362	3.3722
14.38	3.5829	-7.5526	-5.0001	-2.7724	5.6762	4.4874
14.4	5.8842	-5.6207	-4.2964	-4.299	5.9731	5.0126
14.42	7.4536	-6.1981	-4.8888	-4.9322	6.1661	5.7527
14.44	7.5792	-6.4241	-4.7215	-7.6351	7.6204	4.4181
14.46	6.8862	-6.1193	-2.7048	-7.0759	9.1503	4.1075
14.48	6.4986	-2.3455	-3.0181	-6.6823	9.6783	5.3206
14.5	7.7941	-2.1616	-2.1755	-6.2096	8.1086	6.5647
14.52	6.3361	-4.0597	-2.954	-4.3979	8.6206	4.751
14.54	6.0255	-1.526	-2.072	-4.0582	8.9234	4.297
14.56	5.3639	-2.4026	-4.3002	-2.3329	8.8714	2.7546
14.58	3.5154	-5.9898	-3.2857	0.5518	9.1829	2.6587
14.6	1.836	-6.4516	-2.8831	0.8004	8.2666	1.8614
14.62	1.4619	-4.011	-0.9994	2.9485	8.6086	2.3742
14.64	0.9722	-3.7795	-0.3251	3.4853	8.4688	3.1697
14.66	0.6949	-1.9087	-0.3184	3.7852	8.962	3.9715
14.68	0.7539	-1.1881	-0.0845	3.7494	10.472	4.1794
14.7	0.2266	0.2863	1.4633	2.0557	11.311	2.8045

Table A-16 Intensity at various 2θ of adsorbents from XRD (cont.)

2θ	Bentonite	Chitosan	CCB	CCB-EGDE	CCB-ECH	CCB-GLA
14.72	-0.082	0.6012	0.2846	-0.4258	11.136	2.5066
14.74	0.4874	2.1715	-0.5554	-0.237	9.4983	2.0273
14.76	-0.0712	3.2015	0.0237	-2.0589	9.4745	2.0973
14.78	0.0563	3.914	1.9105	-2.0246	9.9351	2.2894
14.8	1.2601	5.2101	-0.217	-2.7504	9.8705	2.3962
14.82	3.6515	1.3003	-0.7861	-3.9513	8.0086	2.8108
14.84	3.5712	1.4198	-2.1032	-4.7759	7.1974	3.7902
14.86	4.9201	0.8566	-0.8557	-5.8992	8.7156	4.4153
14.88	5.9521	-2.9435	-0.8857	-7.8166	7.4178	3.4859
14.9	5.3482	-3.6183	0.8502	-7.4343	8.3814	4.173
14.92	6.0403	-2.4557	1.7606	-7.3197	8.306	3.1792
14.94	7.4062	-0.6259	3.3966	-6.1167	10.625	3.5192
14.96	8.802	0.0846	5.6438	-5.5623	12.249	1.9255
14.98	8.4225	0.4281	7.4029	-5.1394	13.177	-0.065
15	8.1534	-0.2485	8.1229	-4.3805	13.772	-1.981

ศูนย์วิทยทรัพยากร
จุฬาลงกรณ์มหาวิทยาลัย

Table A-17 N₂ adsorption-desorption analysis data of bentonite

N ₂ adsorption		N ₂ desorption	
relative pressure	volume adsorbed (cm ³ /g)	relative pressure	volume adsorbed (cm ³ /g)
0.005576803	15.6672	0.994244809	88.9664
0.006798229	16.3439	0.9500416	79.7371
0.008735181	17.2277	0.891551554	74.5935
0.010125891	17.643	0.838732113	70.7862
0.014549222	18.6626	0.801670811	68.1865
0.020396582	19.5269	0.750459249	64.661
0.024687242	20.0018	0.700266185	61.283
0.030067154	20.5123	0.650394356	57.9818
0.035282406	20.9253	0.600230531	54.7975
0.040257019	21.2866	0.550302531	51.8121
0.045148551	21.6209	0.502798388	47.8487
0.050260818	21.9407	0.447572446	34.1088
0.055025742	22.2146	0.398326659	32.3561
0.060161855	22.5052	0.33411257	30.7382
0.06525541	22.7767	0.301706635	29.9397
0.070224384	23.0302	0.250466027	28.6542
0.075216604	23.2632	0.200350732	27.3658
0.080208098	23.4794	0.150649237	25.9086
0.085195705	23.7032	0.100464317	24.1805
0.090202135	23.9143	0.090249335	23.7632
0.095221851	24.1042	0.080253491	23.34
0.100270513	24.2941	0.070335826	22.8693
0.147487561	25.9266	0.060229548	22.3566
0.20109512	27.5421	0.050375736	21.7899
0.25163561	28.9098	0.040209995	21.1403
0.302418663	30.1788	0.030316873	20.3587
0.350248996	31.3102	0.020440861	19.3251
0.400058208	32.5169	0.010001246	17.3183
0.45037823	33.7154		
0.500333408	34.9039		
0.550314747	36.0854		
0.600240341	37.3132		
0.650150761	38.6374		
0.700175859	40.1444		
0.750030336	41.9462		
0.79995293	44.213		
0.84958992	47.3156		
0.89858703	52.2253		
0.945668847	61.6224		
0.994244809	88.9664		

Analysis Bath: 77.24 K

Sample Weight: 0.2034 g

Table A-18 N₂ adsorption-desorption analysis data of CCB beads

N ₂ adsorption		N ₂ desorption	
relative pressure	volume adsorbed (cm ³ /g)	relative pressure	volume adsorbed (cm ³ /g)
0.006341615	8.5379	0.984975161	40.1652
0.007641984	8.8171	0.938698485	36.3666
0.009837473	9.1626	0.884818465	34.3448
0.011319906	9.3459	0.833080799	33.1416
0.01517137	9.708	0.801051126	32.5217
0.020092779	10.067	0.749894872	31.6912
0.025214425	10.3629	0.699978654	30.9915
0.030187308	10.6011	0.649981924	30.3281
0.035142071	10.8082	0.599824428	29.7048
0.040223892	11.0017	0.549896532	29.099
0.045308877	11.1935	0.501429749	27.7744
0.050341026	11.3616	0.451715889	17.5044
0.055116333	11.5132	0.400436479	16.5077
0.060326144	11.6688	0.331937008	15.7102
0.065271425	11.8084	0.281466423	15.1229
0.070291657	11.9424	0.249988077	14.7318
0.075220067	12.064	0.199818046	14.1606
0.08027304	12.1815	0.150363172	13.4949
0.085358116	12.2957	0.100210594	12.7053
0.09031529	12.4056	0.09007965	12.5069
0.09521631	12.5146	0.080174534	12.2987
0.100350447	12.6228	0.070237187	12.0775
0.148766669	13.4668	0.060290886	11.8377
0.200633533	14.2666	0.050303502	11.5751
0.251048763	14.9439	0.040266625	11.2673
0.301254216	15.5856	0.030379867	10.8909
0.350062396	16.1789	0.020267037	10.3732
0.400106707	16.7523	0.010407152	9.5586
0.449920998	17.3059		
0.499925146	17.8491		
0.549755358	18.3976		
0.599707711	18.9788		
0.649689997	19.6158		
0.699532712	20.3451		
0.749444047	21.2128		
0.799226703	22.3091		
0.848848178	23.88		
0.898203635	26.4074		
0.9464574	31.2085		
0.984975161	40.1652		

Analysis Bath: 77.24 K

Sample Weight: 0.2081 g

Table A-19 N₂ adsorption-desorption analysis data of CCB-ECH beads

N ₂ adsorption		N ₂ desorption	
relative pressure	volume adsorbed (cm ³ /g)	relative pressure	volume adsorbed (cm ³ /g)
0.010876662	7.1455	0.983886875	39.114
0.016608105	7.5793	0.939426276	34.9742
0.022640196	7.8901	0.885321222	32.7383
0.028552465	8.1238	0.833561244	31.3307
0.034412251	8.3286	0.800975416	30.5814
0.040131847	8.5089	0.749930649	29.5865
0.045317302	8.6671	0.700339506	28.7856
0.050276223	8.8058	0.650642489	27.9676
0.05517953	8.9368	0.600200516	27.1647
0.060320982	9.0645	0.550365135	26.3855
0.065285056	9.1815	0.501261416	25.1765
0.070212113	9.2939	0.452510232	14.9456
0.075264749	9.4011	0.39868753	13.8456
0.080350133	9.5047	0.332487004	13.0111
0.085321788	9.6032	0.282045799	12.4058
0.090364952	9.7018	0.250384935	12.0173
0.09535212	9.7886	0.200198049	11.4682
0.100320672	9.8791	0.150694424	10.8342
0.149080918	10.5888	0.100291143	10.1105
0.200565852	11.2852	0.090262062	9.9248
0.250819658	11.8879	0.080308871	9.7378
0.301054653	12.4871	0.0703636	9.5417
0.350899767	13.0729	0.060289058	9.3322
0.400210848	13.6449	0.050288597	9.102
0.450174015	14.2138	0.040239117	8.8408
0.500171265	14.7953	0.030286191	8.5391
0.550105058	15.3843	0.020402009	8.1043
0.60001692	16.017	0.010302401	7.399
0.650080656	16.71		
0.699928341	17.4997		
0.749869285	18.4537		
0.799748353	19.6849		
0.849480833	21.3993		
0.89887839	24.0924		
0.946949148	29.2336		
0.983886875	39.114		

Analysis Bath: 77.24 K

Sample Weight: 0.2110 g

Table A-20 N₂ adsorption-desorption analysis data of CCB-EGDE beads

N ₂ adsorption		N ₂ desorption	
relative pressure	volume adsorbed (cm ³ /g)	relative pressure	volume adsorbed (cm ³ /g)
0.022626861	3.584	0.985843582	23.9029
0.028874324	3.7219	0.93945335	20.2936
0.034574835	3.8731	0.885441075	18.655
0.03543766	3.8987	0.83418958	17.6237
0.040542729	3.9948	0.802118906	17.0795
0.045330528	4.0765	0.751359906	16.3391
0.050406648	4.1564	0.701285824	15.7444
0.055426257	4.2343	0.651590648	15.0692
0.060560425	4.3075	0.600750386	14.489
0.065610825	4.3786	0.551359743	13.9452
0.070635443	4.4449	0.500599188	13.2879
0.075530034	4.5083	0.448306585	8.2728
0.080641523	4.5723	0.398747384	7.6076
0.085705289	4.629	0.331823909	7.0437
0.090740482	4.6885	0.281423067	6.6296
0.09575482	4.7506	0.250339096	6.3589
0.100668475	4.8316	0.200034473	6.0142
0.149746686	5.2538	0.150636027	5.606
0.200484572	5.6859	0.100047836	5.1794
0.250522132	6.055	0.090409791	5.0341
0.30067051	6.4331	0.080068948	4.9086
0.350768039	6.8086	0.070392277	4.7862
0.400396162	7.2277	0.060351362	4.6549
0.450748836	7.565	0.050185377	4.5117
0.500212394	7.959	0.040241221	4.3514
0.550713023	8.3574	0.030265457	4.1602
0.600491393	8.7821	0.020294921	3.8925
0.650587591	9.2571	0.010263213	3.4659
0.700709065	9.7736		
0.750658844	10.3726		
0.800727939	11.1126		
0.850648111	12.1255		
0.900458985	13.7031		
0.949168736	16.8574		
0.985843582	23.9029		

Analysis Bath: 77.24 K

Sample Weight: 0.2047 g

Table A-21 N₂ adsorption-desorption analysis data of CCB-GLA beads

N ₂ adsorption		N ₂ desorption	
relative pressure	volume adsorbed (cm ³ /g)	relative pressure	volume adsorbed (cm ³ /g)
0.035286984	2.631	0.98632333	18.1045
0.046186988	2.7288	0.937311192	15.1402
0.057738461	2.8235	0.884247903	13.6972
0.0604525	2.8227	0.83325555	12.7836
0.074874467	2.9159	0.801313278	12.2906
0.086525041	2.9854	0.75062963	11.6232
0.090396864	3.0091	0.700681419	11.0237
0.095463969	3.0617	0.650676035	10.4544
0.100439817	3.0752	0.600452333	9.9749
0.150088614	3.4076	0.550942678	9.4054
0.200560793	3.7417	0.500453336	8.7662
0.250773144	4.0139	0.455814567	5.4783
0.301092179	4.3049	0.400141511	4.8591
0.351077498	4.6114	0.331654394	4.3534
0.400317058	4.9003	0.281389718	3.9808
0.450218556	5.2048	0.250374583	3.7562
0.500272888	5.5139	0.200267855	3.4463
0.550319952	5.835	0.150451629	3.0775
0.600274945	6.1701	0.093941202	2.6086
0.650384409	6.5209	0.07707128	2.4435
0.7002669	6.9293	0.060135576	2.264
0.750327354	7.4101	0.051469412	2.1545
0.800214107	8.0244	0.042948921	2.0498
0.85019602	8.8663	0.034467553	1.948
0.899922115	10.1449	0.030297229	1.8696
0.948894242	12.6468	0.019884812	1.6642
0.98632333	18.1045	0.010062763	1.3266

Analysis Bath: 77.24 K

Sample Weight: 0.2134 g

ศูนย์วิทยทรัพยากร
จุฬาลงกรณ์มหาวิทยาลัย

Table A-22 N₂ adsorption-desorption analysis data of chitosan

N ₂ adsorption		N ₂ desorption	
relative pressure	volume adsorbed (cm ³ /g)	relative pressure	volume adsorbed (cm ³ /g)
0.03255068	0.3496	0.988504847	3.5265
0.040506162	0.389	0.935162705	1.8346
0.052014594	0.4357	0.882490508	1.5174
0.054841164	0.4568	0.832162798	1.3861
0.060417121	0.4847	0.78190658	1.3172
0.065429127	0.5095	0.731856813	1.2648
0.07041786	0.534	0.681817492	1.2337
0.075394194	0.5575	0.631695751	1.2129
0.080485709	0.5776	0.581600155	1.2019
0.085352289	0.6005	0.531568369	1.1865
0.090409746	0.6179	0.481495151	1.1772
0.095506412	0.638	0.431412865	1.1606
0.100480552	0.6572	0.381313482	1.142
0.150510205	0.757	0.331185566	1.1186
0.200671919	0.8676	0.281211565	1.0828
0.250745664	0.9277	0.230977743	1.0568
0.300878294	0.9881	0.180892179	1.0153
0.350892071	1.0419	0.150668567	0.9783
0.400984298	1.0914	0.100453102	0.9137
0.451110846	1.1357	0.090482667	0.912
0.52064136	1.1661	0.068413418	0.8744
0.569731905	1.1938	0.060197501	0.8534
0.619769248	1.2078	0.050270419	0.8312
0.669681332	1.225	0.040229396	0.807
0.719742376	1.2463	0.030242519	0.7786
0.769738375	1.2737	0.020160663	0.731
0.819673787	1.3214	0.010112757	0.673
0.850634182	1.3748		
0.900667032	1.4881		
0.950462928	1.817		
0.988504847	3.5265		

Analysis Bath: 77.24 K

Sample Weight: 0.2014 g

ศูนย์วิทยทรัพยากร
จุฬาลงกรณ์มหาวิทยาลัย

Table A-23 Summary characteristics of adsorbents by N₂ adsorption-desorption analysis

Characteristics	Bentonite	CCB	CCB-ECH	CCB-EGDE	CCB-GLA	Chitosan
AREA						
BET surface area, m ² /g	94.2834	48.8102	38.9610	20.1799	13.4493	3.4052
Langmuir surface area, m ² /g	131.0743	67.8313	55.6219	29.6267	20.5144	5.6443
Micropore area, m ² /g	22.9400	12.3473	7.5967	0.5733	0.8528	-1.2141
BJH adsorption cumulative surface area of pores between 17.000000 and 3000.000000 A diameter, m ² /g	52.1062	25.6921	24.3469	15.5014	12.0161	2.4659
BJH desorption cumulative surface area of pores between 17.000000 and 3000.000000 A diameter, m ² /g	87.2026	45.7160	46.5520	25.1927	18.6102	1.3582
VOLUME						
Micropore volume, cm ³ /g	0.011298	0.006066	0.003706	0.000197	-0.000493	-0.000706
BJH adsorption cumulative surface area of pores between 17.000000 and 3000.000000 A diameter, cm ³ /g	0.116089	0.050426	0.052867	0.034424	0.027070	0.005134
BJH desorption cumulative surface area of pores between 17.000000 and 3000.000000 A diameter, cm ³ /g	0.131154	0.057841	0.060482	0.036432	0.027482	0.004422
PORE SIZE						
Average pore diameter (4V/A by BET), nm	5.83828	5.09136	6.21149	7.32869	8.32878	6.40757
BJH adsorption average pore diameter (4V/A), nm	8.91175	7.85076	8.68556	8.88294	9.01110	8.32838
BJH desorption average pore diameter (4V/A), nm	6.01607	5.06053	5.19695	5.78454	5.90696	13.02190

Appendix B

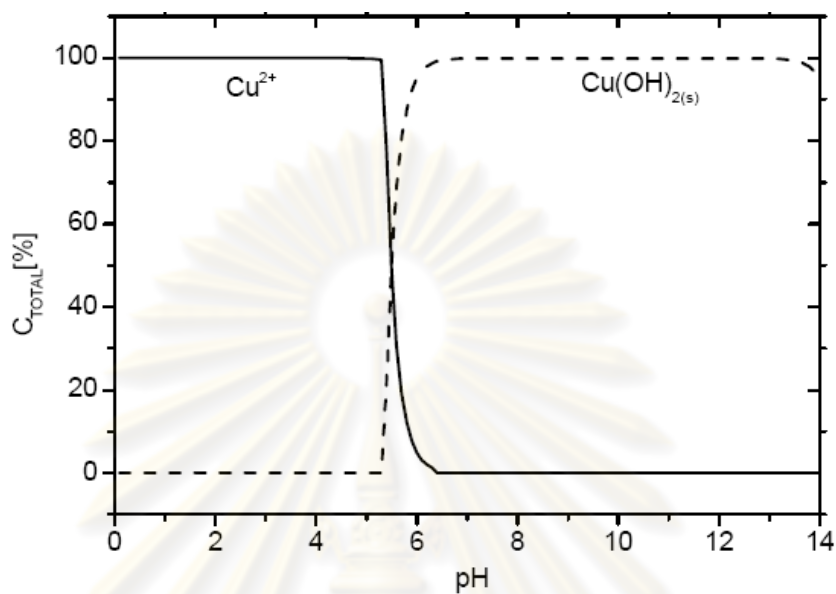


Fig. B-1 Thermodynamic equilibrium diagram of Cu (Ayres, Davis, and Gietka, 1994; Václavíková and Gallios, 2006)

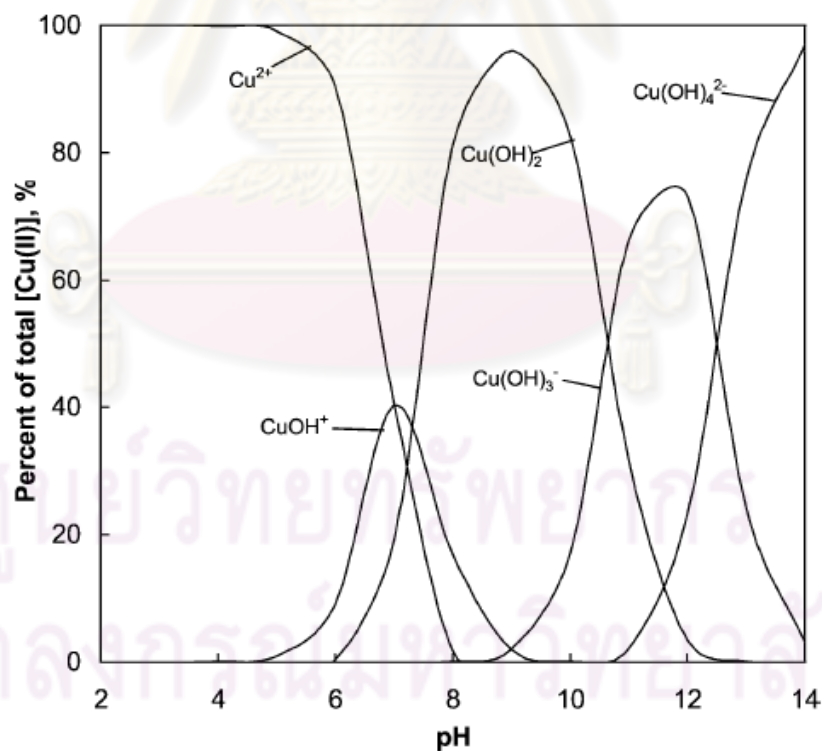


Fig. B-2 Speciation diagram for the Cu(II)-H₂O system (Doyle, and Liu, 2003; Wang, Li, and Sun, 2009)

Table B-1 pH of Cu²⁺ solution before and after adsorption by adsorbent beads at different contact time

Contact time (min)	100 mg/L	pH-solution	pH-Diagram	500 mg/L	pH-solution	pH-Diagram	1000 mg/L	pH-solution	pH-Diagram	2000 mg/L	pH-solution	pH-Diagram
CCB-EGDE												
0	100	4.81	5.30	500	4.63	4.9	1000	4.55	4.7	2000	4.46	4.55
30	0.68	6.04	6.35	27.05	4.80	5.55	141.33	4.32	5.15	693.80	4.44	4.83
60	0.27	5.92	6.50	8.13	4.96	5.85	113.03	4.36	5.30	652.93	4.40	4.83
120	0.05	6.13	7.20	3.77	4.86	6.00	57.20	4.35	5.35	571.80	4.33	4.85
240	0.05	6.47	7.20	1.53	5.80	5.99	45.33	4.48	5.43	567.93	4.36	4.86
360	0.05	6.26	7.20	2.03	4.89	6.10	40.20	4.33	5.44	587.87	4.31	4.86
720	0.03	6.55	7.25	0.68	5.82	6.45	41.50	4.21	5.45	549.40	4.07	4.86
1440	0.06	6.79	7.18	1.40	6.31	6.35	23.13	4.33	5.68	534.40	4.14	4.86
CCB-ECH												
0	100	4.81	5.30	500	4.63	4.9	1000	4.55	4.7	2000	4.46	4.55
30	1.77	5.9	6.50	38.13	4.5	5.45	175.72	4.1	5.20	728.27	4.2	4.82
60	0.27	6.1	7.20	10.19	5.0	5.85	150.57	4.3	5.22	719.60	4.3	4.82
120	0.06	6.1	7.45	14.54	5.2	5.80	112.02	4.5	5.30	690.00	4.4	4.83
240	0.04	6.1	7.46	1.43	4.7	6.35	77.03	4.8	5.40	633.93	4.4	4.85
360	0.04	6.1	7.46	1.62	5.9	6.34	69.60	4.6	5.40	615.87	4.3	4.85
720	0.03	6.2	7.46	0.36	6.0	6.50	54.48	4.3	5.40	567.53	4.5	4.86
1440	0.03	6.3	7.46	0.26	5.9	6.50	42.32	4.5	4.25	547.80	4.5	4.86
CCB-GLA												
0	100	4.81	5.30	500	4.63	4.9	1000	4.55	4.7	2000	4.46	4.55
30	41.64	4.21	5.45	303.17	4.07	5.00	686.17	4.06	4.83	1526.40	4.01	4.60
60	35.20	4.31	5.50	294.47	4.14	5.00	662.67	4.09	4.84	1508.20	4.10	4.60
120	34.43	4.35	5.50	300.33	4.14	5.00	685.83	4.10	4.83	1534.20	4.05	4.60
240	31.28	4.38	5.60	279.40	4.16	5.05	665.17	4.09	4.84	1527.33	4.08	4.60
360	30.77	4.40	5.60	278.00	4.25	5.05	629.50	4.15	4.85	1513.33	4.11	4.60
720	27.71	4.43	5.61	259.43	4.22	5.05	623.50	4.14	4.85	1427.80	4.11	4.63
1440	26.94	4.48	5.60	245.07	4.24	5.05	612.00	4.19	4.85	1375.33	4.18	4.64

Table B-2 pH of Cu²⁺ solution after adsorption by CCB-EGDE beads packed column

Contact time (min)	Flow through Cu ²⁺ conc. (mg/L)	pH
0	0.0000	8.27
2	0.0000	8.29
4	0.0000	7.68
6	0.0000	7.87
8	0.0000	7.54
10	0.0020	7.35
12	0.0000	7.54
14	0.0000	7.54
16	0.0000	7.37
18	0.0000	7.53
20	0.0000	7.40
22	0.0000	6.71
24	0.0000	6.70
26	0.0000	6.69
28	0.0000	6.78
30	0.0000	6.81
32	0.1840	6.65
34	10.7000	6.68
36	51.4100	6.60
38	90.1000	6.50
40	104.6000	6.01
42	137.3500	5.28
44	147.2500	5.23
46	179.7000	4.87
48	176.5000	4.74
50	190.5000	4.59
52	232.4000	4.57
54	256.1000	4.94

ศูนย์วิทยทรัพยากร
จุฬาลงกรณ์มหาวิทยาลัย

Appendix C

U.S. Environmental Protection Agency Ground Water & Drinking Water Consumer Factsheet on: COPPER

Copper is a metal found in natural deposits on ores containing other elements. It is widely used in household plumbing materials.

In 1974, Congress passed the Safe Drinking Water Act. This law requires EPA to determine safe levels of chemicals in drinking water which do or may cause health problems. These non-enforceable levels, based solely on possible health risks and exposure, are called Maximum Contaminant Level Goals.

The MCLG for copper has been set at 1.3 parts per million (ppm) because EPA believes this level of protection would not cause any of the potential health problems described below.

Since copper contamination generally occurs from corrosion of household copper pipes, it cannot be directly detected or removed by the water system. Instead, EPA is requiring water systems to control the corrosiveness of their water if the level of copper at home taps exceeds an Action Level.

The Action Level for copper has also been set at 1.3 ppm because EPA believes, given present technology and resources, this is the lowest level to which water systems can reasonably be required to control this contaminant should it occur in drinking water at their customers home taps.

These drinking water standards and the regulation for ensuring these standards are met, are call National Primary Drinking Water Regulations. All public water supplies must abide by these regulations.

Short- and long-term effects: Copper is an essential nutrient, required by the body in very small amounts. However, EPA has found copper to potentially cause the following health effects when people are exposed to it at levels above the Action Level. Short periods of exposure can cause gastrointestinal disturbance, including nausea and vomiting. Use of water that exceeds the Action Level over many years could cause liver or kidney damage. People with Wilsons disease may be

more sensitive than others to the effect of copper contamination and should consult their health care provide.

Drinking Water Standards:

MCLG: 1.3 ppm

Action level: 1.3 ppm



ศูนย์วิทยทรัพยากร
จุฬาลงกรณ์มหาวิทยาลัย

Pollution Control Department (PCD)**Water Quality Standards: Copper*****Drinking Water Quality Standard***

Maximum Acceptable Concentration: 1.0 mg/dm³

Maximum Allowable Concentration: 1.5 mg/dm³

Source: Notification of the Ministry of Industry, No. 322, B.E. 2521 (1978), issue under the Industrial Products Standards Act B.E. 2511 (1968), published in the Royal Gazette, Vol. 95, Part 68 dated July 4, B.E. 2521 (1978)

Bottled Drinking Water Quality Standard

Maximum Allowable Concentration: 1.0 mg/L

Source: Notification of the Ministry of Public Health, No. 61 B.E. 2524 (1981), issued under the Food Act B.E. 2522 (1979), published in the Royal Gazette, Vol. 98, Part 157 (Special Issue), dated September 24, B.E. 2524 (1981).

Ground Water Quality Standards for Drinking Purposes

Suitable Allowance: ≤ 1.0 mg/L

Maximum Allowable: 1.5 mg/L

Source: Notification of the Ministry of Industry, No. 4, B.E. 2521 (1978), issued under the Ground Water Act B.E. 2520 (1977), published in the Royal Gazette, Vol. 95, Part 66, dated June 27, B.E. 2521 (1978).

ศูนย์วิทยทรัพยากร
จุฬาลงกรณ์มหาวิทยาลัย

BIOGRAPHY

- Name:** Miss Siriporn Akewaranugulsiri
- Date of Birth:** November 11, 1983
- Nationality:** Thai
- University Education:** 2003-2006 Bachelor Degree of Science in
Environmental Science and Technology,
Faculty of Environment and Resource Studies, Mahidol
University, Bangkok, Thailand
- Presentation:**
- Chi-Chuan Kan, Meng-Wei Wan, Siriporn Akewaranugulsiri, Nurak Grisdanurak, and Chih-Hsiang Liao. *Removal of Cu²⁺ from Aqueous Solution on Crosslinked Chitosan Intercalated Clay*. 20th The Proceedings of 中華民國環境工程學會第二十屆年會暨各專門學術研討會 The Chinese Institute of Environmental Engineering Wastewater Treatment Conference 2008, Taipei, Taiwan, November 7-8, Organized by National Taiwan University, Graduate of Environmental Engineering
- Siriporn Akewaranugulsiri, Nurak Grisdanurak, Meng-Wei Wan, Chi-Chuan Kan, Chih-Hsiang Liao. *Removal of copper(II) ions from aqueous onto chitosan intercalated clay*. 1st the proceeding of International Symposium on Environmental Management: Hazardous-Environmental Management Toward Sustainability 2008, Royal Hill Resort & Spa, Nakorn Nayok, Thailand, September 22-23, Organized by National Center of Excellence for Environmental and Hazardous Waste Management, Thammasart University